EXPERIMENTAL AND NUMERICAL STUDIES ON FIRE IN TUNNELS

A THESIS SUBMITTED TO
THE GRADUATE SCHOOL OF NATURAL AND APPLIED SCIENCES
OF
MIDDLE EAST TECHNICAL UNIVERSITY

BY

ALPER ÇELİK

IN PARTIAL FULFILLMENT OF THE REQUIREMENTS
FOR
THE DEGREE OF MASTER OF SCIENCE
IN
MECHANICAL ENGINEERING

SEPTEMBER 2011

Approval of the thesis:

EXPERIMENTAL AND NUMERICAL STUDIES ON FIRE IN TUNNELS

submitted by **ALPER ÇELİK** in partial fulfillment of the requirements for the degree of **Master of Science in Mechanical Engineering Department, Middle East Technical University** by,

Prof. Dr. Canan Özgen _____
Dean, Graduate School of **Natural and Applied Sciences**

Prof. Dr. Suha Oral _____
Head of Department, **Mechanical Engineering**

Asst. Prof. Dr. Ahmet Yozgatlıgil _____
Supervisor, **Mechanical Engineering Dept., METU**

Examining Committee Members:

Prof. Dr. Kahraman Albayrak _____
Mechanical Engineering Dept., METU

Assist. Prof. Dr. Ahmet Yozgatlıgil _____
Mechanical Engineering Dept., METU

Assoc. Prof. Dr. Almıla Yazıcıoğlu _____
Mechanical Engineering Dept., METU

Dr. Serkan Kayılı _____
Mechanical Engineering Dept., METU

Dr. Ekin Özgirgin _____
Mechanical Engineering Dept., Atılım University

Date: 16.09.2011

I hereby declare that all information in this document has been obtained and presented in accordance with academic rules and ethical conduct. I also declare that, as required by these rules and conduct, I have fully cited and referenced all material and results that are not original to this work.

Alper ÇELİK

Signature:

ABSTRACT

EXPERIMENTAL AND NUMERICAL STUDIES ON FIRE IN TUNNELS

ÇELİK, Alper
M.Sc., Department of Mechanical Engineering
Supervisor: Assist. Prof. Dr. Ahmet Yozgatlıgil

September 2011, 112 Pages

Fire is a complex phenomenon including many parameters. The nature of fire makes it a very dangerous and hazardous. For many reasons the number of tunnels are increasing on earth and fire safety is one of the major problem related to tunnels. This makes important to predict and understand the behavior of fire, i.e., heat release rate, smoke movement, ventilation effect etc. The literature includes many experimental and numerical analyses for different conditions for tunnel fires. This study investigates pool fire of three different fuel sources: ethanol, gasoline and their mixture for different ventilation conditions, different geometries and different amounts. Combustion gases and the burning rates of the fuel sources are measured and analyzed. The numerical simulation of the cases is done with Fire Dynamics Simulator (FDS), a CFD code developed by NIST.

Keyword: Fire Safety, Pool Fire, Tunnel Ventilation, Fire Dynamics Simulator (FDS), Heat Release Rate

ÖZ

TÜNEL YANGINLARI ÜZERİNE DENEYSEL VE NUMERİK ÇALIŞMALAR

ÇELİK, Alper
Yüksek Lisans, Makina Mühendisliği Bölümü
Tez Yöneticisi: Yrd. Doç. Dr. Ahmet Yozgatlıgil

Eylül 2011, 112 Sayfa

Yangın birçok parametre içeren karmaşık bir olgudur. Yangının doğası tehlikeli ve yıkıcıdır. Birçok farklı nedenden ötürü yeryüzündeki tünel sayısı artmakta ve yangın güvenliği de bu tünellerdeki en önemli parametrelerden biri haline gelmektedir. Bu sebeple yangınlarda ortaya çıkacak ısı yükünün, duman hareketinin, havalandırma etkisinin vs. tahmini ve anlaşılmasını önemli kılmaktadır. Literatürde birçok farklı durum için deneysel ve nümerik incelemeler bulunmaktadır. Bu çalışma etanol, benzin ve etanol ve benzin karışımı olmak üzere üç farklı sıvı yakıt türünün farklı miktarlarda, farklı geometrilerde ve farklı havalandırma şartları altındaki yangın durumunu incelemektedir. Yanma sonucu ortay çıkan gazlar ve yanma miktarları ölçülmüş ve analiz edilmiştir. Bu deneylerin nümerik çalışmaları NIST tarafından geliştirilmiş bir CFD kodu olan Fire Dynamics Simulator (FDS) ile yapılmıştır.

Anahtar Kelimeler: Yangın güvenliği, Havuz Yangını, Tünel havalandırması, Fire Dynamics Simulator (FDS), Yangın Yükü

To those who appreciates and enjoys each

and every second of life

ACKNOWLEDGMENTS

It was an honor for me to study with Prof. Dr. O. Cahit Eralp for two years. It was a privilege to share his knowledge and vision.

I would like to express my gratitude to my supervisor Asst. Prof. Dr. Ahmet Yozgatlıgil for their guidance, criticism and insight throughout this work.

I would also like to thank Dr. Serkan Kayılı for his contributions, advices, suggestions and comments throughout my works. I would like to show my gratitude to specially Mehmet Özçiftçi for his help and Rahmi Ercan.

I am grateful to my friends Tolga Köktürk, Ertan Hataysal, Gençer Koç , Özgür Cem Ceylan for their friendship I n this three year time.

I would like to extend my gratitude to Ersin Yorgun, Osman Akdağ , Eren Demircan for their help in both experimental and numeric parts of the thesis.

Finally, I owe my deepest gratitude to my parents Ayşe and Ferudun ÇELİK, my sisters Derya and Eda, my uncle Şenol, and my friends for their love, patience, support, understanding, encouragement and every way of support all through my education life.

TABLE OF CONTENTS

LIST OF TABLES

TABLES

LIST OF FIGURES

FIGURES

NOMENCLATURE

ρ	: Density
$\vec{u}, u, U$	: Velocity
P	: Pressure
$\vec{g}$	: Gravitational acceleration vector
$\vec{f}_b$	: Body forces
τ_{ij}	: Viscous stres tensor
h_s	: Sensible enthalpy
$\dot{q}'''$	: Heat release rate per unit volume
$\dot{\vec{q}}''$	: Heat flux vector
$\dot{\vec{q}}_r''$	: Radiative flux vector to a solid surface
$\dot{\vec{q}}_c''$	: Convective flux vector to a solid surface
ε	: Dissipation rate
R	: Universal gas constant
T	: Temperature
W_α	: Molecular weight of the gas species α
v_α	: Stociometric coefficient, species α
Z	: Mixture fraction
Y_α	: Mass fraction of species α
$Y_{O_2}^{\infty}$	: Mass fraction of oxygen in ambient
Y_F^l	: Mass fraction of fuel in fuel stream
x	: Number of carbon atoms in fuel molecule
s	: Unit vector in direction of radiation intensity

I	: Radiation intensity
I_b	: Radiation blackbody intensity
λ	: Wavelength
σ_s	: Scattering coefficient
B	: Emission source term
Φ	: In-scattering from other directions
κ	: Absorption coefficient
χ_r	: Radiative loss fraction
$\dot{m}''_p$	: Pyrolysis rate
$\dot{m}_\alpha$	: Mass burning rate of species α
A	: Pre-exponential factor - Area of geometry
E_A	: Activation energy
D	: Diameter
c_p	: Specific heat
k	: Conductivity
H_c	: Heat of combustion
H_R	: Heat of reaction
MLR	: Mass loss rate
HRR	: Heat release rate
FDS	: Fire dynamics simulation

CHAPTER 1

INTRODUCTION

Fire is a complex physical phenomenon that includes some major aspects of engineering science, i.e.; heat transfer, fluid mechanics, combustion processes. From very early time of existence, mankind tried to understand and solve the mechanisms of fire. Yet there are still a number of issues to be understood. For the last 500 years, science has progressed at an accelerating pace to understand universe, however one of the oldest tools of mankind, needed the last 50 years to give it mathematical expression [1].

Today scientific research on understanding fire behavior is one of the major concepts in public safety. Although developing technology enables us a great easiness in life, it introduces a great risk of fire at every level which may result in loss of life or property. The current US defense spending is at 3.59% of GPD [1]

The focus of this thesis, which is tunnel fire, differs from open fires since they occur in a confined space, which changes the dominant physical phenomenon. Over the past few years, fires in transport tunnels became an important concern. By technology, tunnels of length up to 50 km are possible. The fires in Mont Blanc Tunnel which joins France to Italy [2] Tauren tunnel in Austria [3] and Channel Tunnel joining UK to France [4] reminds the devastating of power of fire not only in terms of property but also in terms of loss of life.

This part of the thesis includes the basic information on tunnel fires and the aim of the thesis.

1.1.Tunnel Fire

Tunnel fire is a type of enclosure or compartment fire. The compartment or enclosure here stands for any confined space that may limit or control the air supply and thermal environment. The complex interaction for an enclosure fire can be seen in Figure 1-1.

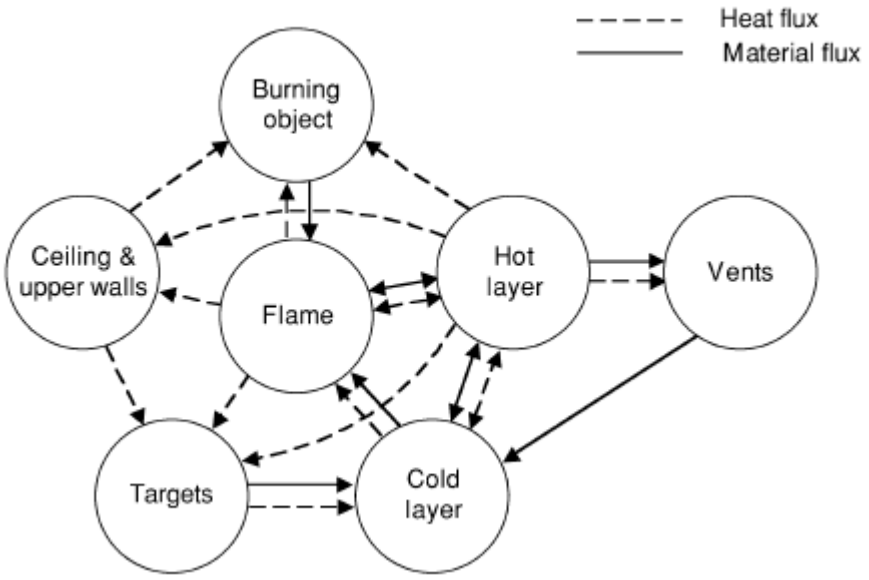

Figure 1-1 Schematic of mass fluxes and heat fluxes occurring in an enclosure fire [5]

There are two major effects that differs an enclosure or a tunnel fire from an open fire. The first one is the possible limitation of oxygen due to no or under ventilation and the second one is the increased burning rate of fuel source due to back radiation from the hot gas layer accumulated at the ceiling and back radiation from hot walls

[5].Enclosure fires are discussed under different stages characterized by the temperature. These stages are ignition, growth, flashover, fully-developed fire and decay as can be seen from Figure 1-2.

Figure 1-2 Phases of fire [5]

Ignition can be defined as triggering an exothermic reaction by increasing temperature above ambient by chemical, electrical or mechanical term. Growth stage is where the flame spreads over the fuel source. When the total fuel source surface involves in the combustion process it is called the flashover. After flashover, the heat release rate reaches its peak values and this period is called the fully developed fire. After the fuel is consumed the energy release rate starts to decrease which is called the decay period.

1.2.Literature Survey on Tunnel Fire

1.2.1. Experimental Studies on Tunnel Fire

When the subject is fire, the main aim is generally to identify how devastating the results are going to be and how the risk can be kept minimum. Fire tests are carried out with many different reasons with the main two as to gain understanding of fire dynamics and related phenomenon in tunnels and to test commission tunnel installations [6]. For this purposes the major areas of the experimental studies focuses on; the maximum heat release rate which gives an insight about the power of fire, smoke movement and critical air velocity to avoid back layering which is one of the key issues in evacuations and safety. Ventilation conditions, temperature distributions, flame lengths etc are the other subjects to experimental studies. The experiments investigating the enclosure fire are based on Froude number scaling if not to full scale.

Full scale experiments are expensive and time consuming however most reliable data can be collected by this way. There are numerous studies in the literature. This part consists of studies for both wood crib fire and liquid pool and spill fire.

In 1965 [6], in Switzerland researchers tired to find out what would happen if there were a fuel tanker fire in one of their tunnel. The recorded data was visibility, air temperature, CO and O_2 concentration, air velocity for different pool sizes of 6.6m^2, 47.5m^2, 95m^2 of aircraft quality petrol. It was seen that due to lack of oxygen natural or semi-transversely ventilated fires burn slower than their equivalent in the open air, maximum temperatures observed within the first two minutes and there is no chance of survival for a 30-40m pool fire with any kind of ventilation.

In 1970 [6] five tests are conducted in Glasgow. The tests are carried out in a 620m long, 5.2m high, and 7.6m wide railway tunnel. Collected data were smoke

movements and temperature. The fire load was 2MW. The main outcome was that the smoke layer thickened as the fire size grows.

In 1980 [6], sixteen full scale tests were conducted by Japanese Public Works Research Institute (PWRI) in a 700m long fire gallery and eight full-scale tests in a 3.3 km road tunnel. The fire sources were $4m^2$ and $6m^2$ pools of petrol. The collected data was temperature, smoke, gas concentration under longitudinal and natural ventilation. It was observed that for petrol pool fires heat release rate of a fire increases for higher ventilation velocities.

In 1985 [6] two fire tests are conducted in Finland. The fire source was wood crib. Tests were conducted in a tunnel in Lappeenranta. The main aim was to observe the effect of linings on fire. It was observed that using identical wood cribs at different ends of the tunnel did not result in same burning characteristics. "The crib at the windward end of the line burned with almost twice HRR of that of the other end."
Without any doubt the fire experiments in largest scale is conducted between 1990-1992 in Hammerfest , Norway, Germany and Finland with majority in Norway, using fire sources of wooden cribs, train carriages, heptane pools, heavy goods vehicle under EUREKA EU-499 Firetun series. The researchers tires to gather information on many different aspects of fire phenomenon. Some of the important results were maximum temperature during most of the vehicle fires reached to 800 to 900^oC whereas with HGV the temperatures reached near 1300C. It is observed that burning rate can be accelerated by a free supply air [6].

Pool fire tests are carried out in France in 1992 to compare the results with EUREKA EU-499 in INERIS (Institut National de l'Environnement Industiel et des Risques). It is observed that heat release rate of a pool fire in a fire gallery was considerably greater than its equivalent in open air. This difference was attributed to re-radiation [6].

Another test series was conducted in Australia in 1990 at Londonberry Occupational Safety Centre. The ventilation velocity changed from 0.5 m/s to 2m/s whereas two pool diameters are used 0.57 and 2m. These experiments are carried out to compare with numerical studies. It was observed that increasing velocity for 1m pool fire decreases the heat release rate and the mass loss rate of larger pools are greater of smaller proportionally [7].

R.O. Carvel *et al* [8] investigated the influence of forces longitudinal ventilation on car fires, pool fires and heavy goods vehicle fires in tunnels. For pool fires the results rare presented for three different pool sizes i.e., small, medium large pools. Large pool fires are probably ventilation controlled which means that increasing the velocity will increase the heat release rate, however for smaller pool fires it will probably be fuel-controlled and increasing the ventilation will tend to decrease heat release rate. For car fires ventilation velocity at 1.5m/s will not affect the heat release rate of the car fire. For heavy good vehicle, the ventilation will greatly increase the heat release rate. At 3m/s the fire will probably be four or five times larger than if natural ventilation is [8] used.

Roh, J. S. *et al* investigated the effect of ventilation velocity on burning rate in tunnel fires for n-heptane pool fire case. A model tunnel is used with a scaling ratio 1/20 to the full scale tunnel. The scaling is done according to Froude scaling. The results are compared with the empirical relationships proposed by Burgess [9] for burning rate with constant value. It is found that for n-heptane fuel, the burning rate increases as the ventilation velocity increases since the effect of supplying oxygen is more dominant than cooling effect of the ventilation. They also note that non-dimensional critical velocity is proportional to one-third power of the dimensional heat release rate. Hence, the ventilation system designed for the constant heat release rate may enhance the effect of fire [10].

Lee and Ryou [11] investigated the effect of aspect ratio i.e., height/width of the tunnel of the tunnel cross section on the critical velocity. Ethanol pool is used as fire source with Froude Scaling. The used aspect ratios are 0.5, 0.667, 1.0, 1.5 and 2.0. It is seen that as the aspect ratio increased for the tunnel with same hydraulic diameter, the critical velocity increased. Another consequence to note was that critical velocity varies with one-third power of the heat release rate. Yet one another result is that the smoke –font velocity increases as the aspect ratio increase [11].

Bing, Chen *et al* [12] investigated the effect of initial fuel temperature on burning rate of n-heptane pool fire. As seen in Figure 1-3, four different initial fuel temperatures were considered where $T_{f,o}$ stands for initial fuel temperature. The burning rate during the steady burning stage was observed to be relatively independent of the initial fuel temperature. However, the burning rate of the bulk boiling burning stage increases with increased initial fuel temperature.

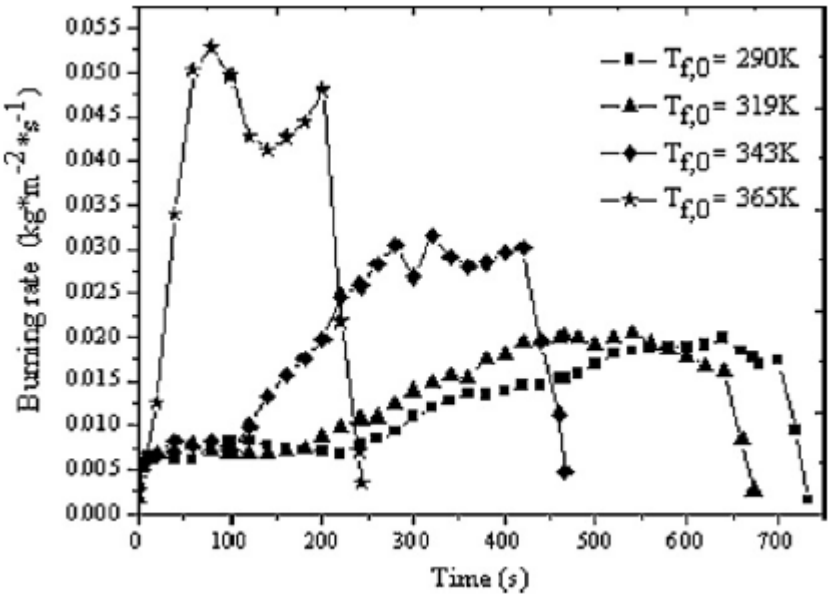

Figure 1-3 Burning rates for 100mm n-heptane pool fire [12]

Another result is that, increased initial fuel temperature decreases the duration of steady burning stage. One of the important outcomes of the experiment is as the initial temperature approaches the boiling point, the steady burning stage nearly disappears and the burning rate moves directly from the initial development stage to the transition stage as can be seen in Figure 1-4.

Hamis *et al* [13] studied on characteristics of pool fire burning. The radiative power of different liquid source is given with respect to pool diameter as seen in Figure 1-5.

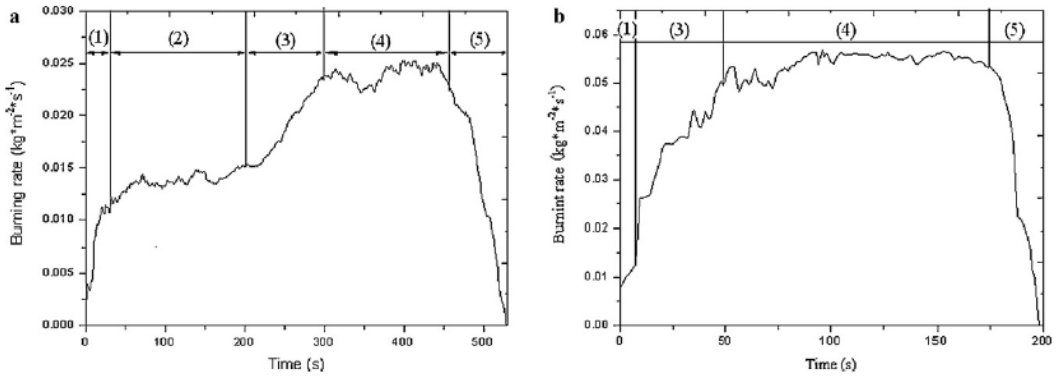

Figure 1-4 Temporal evolution of n-heptane pool fire burning rate of the same diameter but different initial temperatures, a)$T_{f,0}$=290K, b) $T_{f,0}$=365K [12]

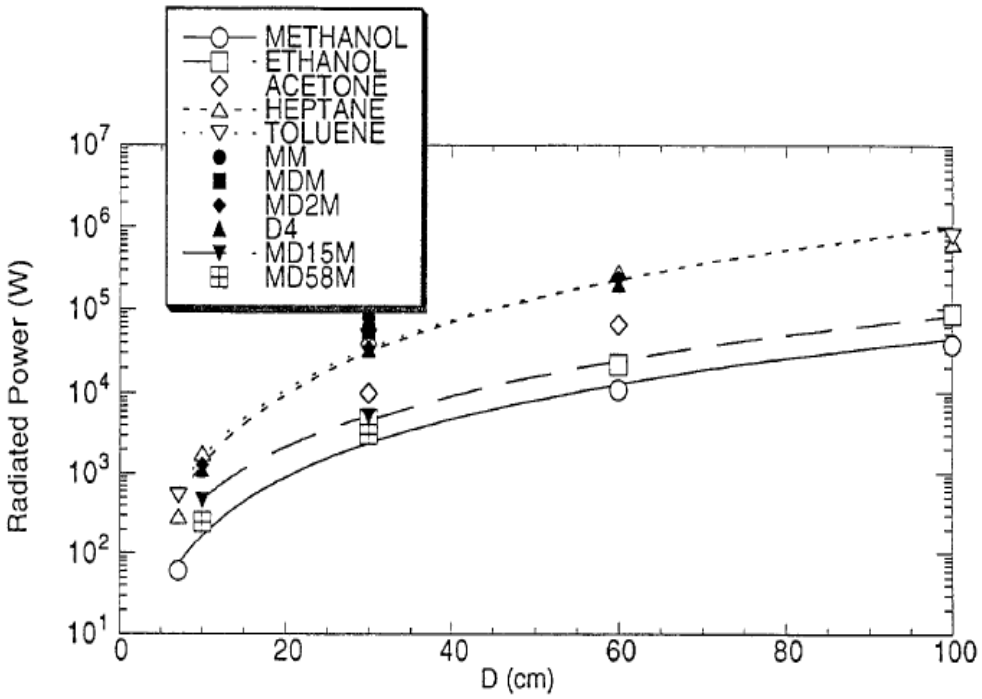

Figure 1-5 Measurements of radiative power as a function of pool diameter for fires [13]

It is noted that although it is expected for the heat feedback to fuel source to increase as the radiative power increases, it would be difficult to judge the real physics this way due to complexity of radiation blockage by fuel vapor, pyrolysis intermediates and soot particles play an important role.

Sugawa *et al* [14] studied on a full scale semi-enclosed gasoline station and 1/15 scaled gasoline pool fire experimentally. It was seen that the re-radiation effect enhances the burn rate about 20-24% in a semi enclosed compartment. Wind effect enhanced the burning rate at about 50-75%.

Woods *et al* [15] investigated the effects of transverse airflow on burning rates of rectangular methanol pool fires. The parameters subject to change were size and

shape of the pool and the air velocity. The flame luminosity images were also collected to make more realistic comments on burning rate. In the study it is noted from the past studies that for all fuels, except for the heavy fuel oil, the burning rates monotonically increased with air speed, but eventually approached an asymptotic limit. However, circular pools, ranging in diameter from 0.9 to 15 m and those from 0.6 to 2 m burning aviation fuel, showed the opposite behavior in that burning rates diminished with increasing transverse air speeds [15].

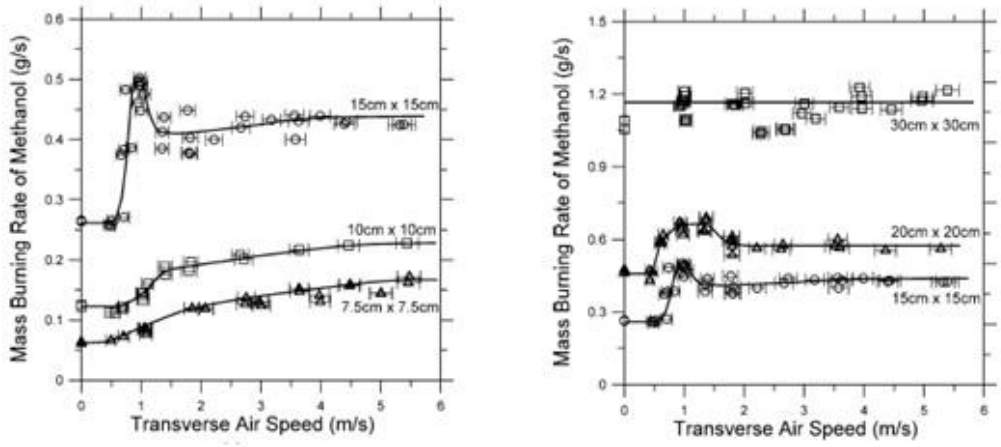

Figure 1-6 Burning rates of square methanol pools when exposed to a uniform low-turbulence transverse air flow (a) Smaller pools tested (b) Larger pools tested [15]

The transitional drops that can be seen in the Figure 1-6 in burning rate corresponded to the observation that the flame separated from the trailing edge of the pool. The study includes a discussion of how altering the air speed affects the various paths that energy flows from the flame and combustion products to the pool to support the evaporation of the fuel was used to explain the observed results.

Parag and Raghavan [16] investigated burning rates of pure ethanol and ethanol blended fuels. It is found that fuel mass burning rate increases with sphere size and air velocity. Moreover it is stated that when water is added to ethanol, the mass burning rate, flame luminosity and flame standoff distances decrease. For ethanol blended with diesel, the mass burning rate does not vary significantly. Yet another important result to be noted is that ethanol blended with gasoline, the mass burning rate increases with increasing gasoline content due to higher volatility of gasoline [16].

Kang *et al* [17]experimentally investigated the burning rate of a small scale heptane pool fire. It is stated that the flame height and burning rate of boiling burning phase are greater than those of quasi-steady state burning phase. It is also observed that the steady and boiling burning rates both increase with the diameter [17].

Chatris *et al* [18] studied on burning rate of hydrocarbon pool fires. They used diesel and gasoline as fuel. They both studied the effect of diameter and the effect of wind speed on burning rate. Since the wind changed in every test, and its effect on mass burning rate is shown in Figure 1-7. There is not a net effect of wind velocity up to 2m/s. The velocities over 2 m / s tend to increase the burn rate [18].

Hua *et al* [19] studied the burning rates of methanol and gasoline in square and rectangular pans for different ventilation velocities. It is revealed that the burning rate of methanol and gasoline pool fire showed different response to the longitudinal air flow. The main difference between the two fuel sources is methanol pool fire produces a translucent blue diffusive flame with low thermal radiation. Gasoline, on the other hand, produces a yellow diffuse flame with high thermal radiation [19].

As seen in Figure 1-8 burning rates for methanol is higher when convection is dominant heat transfer mechanism, however with the increase of pool size, radiation becomes the dominant character and gasoline burn rate overwhelms methanol [19].

The square pool results show that except for 5 cm square pool size, methanol burning rate firstly decreases then increases with increased ventilation velocity. For gasoline, the burning rate trend is always in increasing as can be seen from Figure1-9 and Figure 1-10.

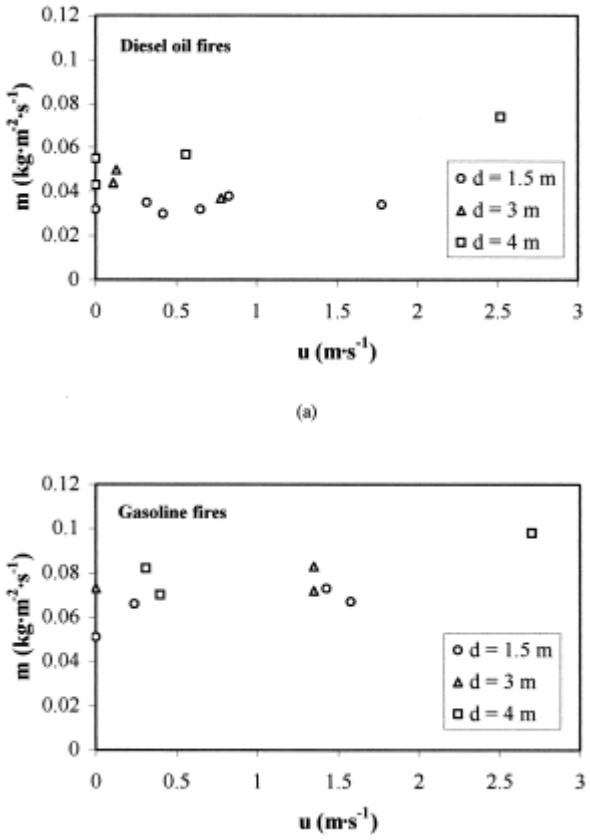

Figure 1-7 Mass burning rate as a function of average wind speed measured during stationary period [18]

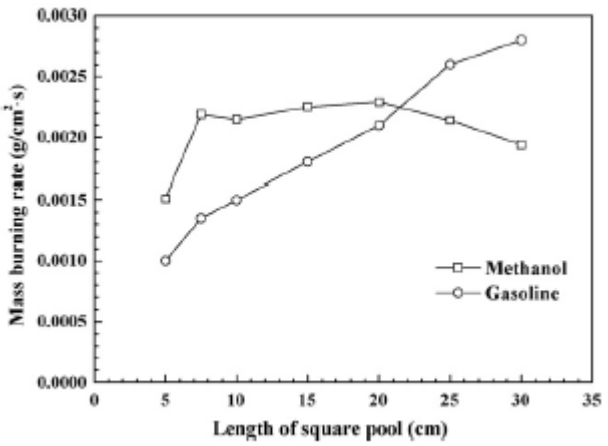

Figure 1-8 Variation of burn rate with pool size in quiescent condition [19]

Garo *et al* investigated spill fire burning rate.One of the investigation topic was the effect of initial fuel layer thickness on regression rate for crude oil.It is observed that the regression rate increased for increasing pan diameter up to certain limits for different pan diameters then become constant as can be seen from Figure 1-11 [20].

Hayasaka [21] studied experimentally and theoretically showed that for unsteady pan fires, the lower initial burning rates are due to heat loss to heat the pan and the fuel [21].

Benfer [39] conducted experiments about spill depths of various flammable and non-flammable liquids. Moreover burning rates of spills are investigated. Figure 1-12 shows the average burning rate, which is calculated by dividing mass burned to the burning time, with respect to volume data of spill.

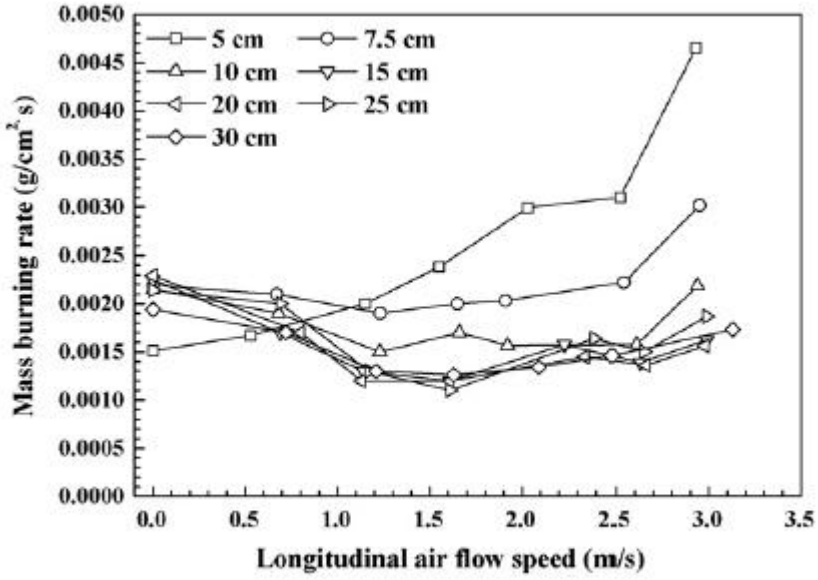

(a) Methanol pool

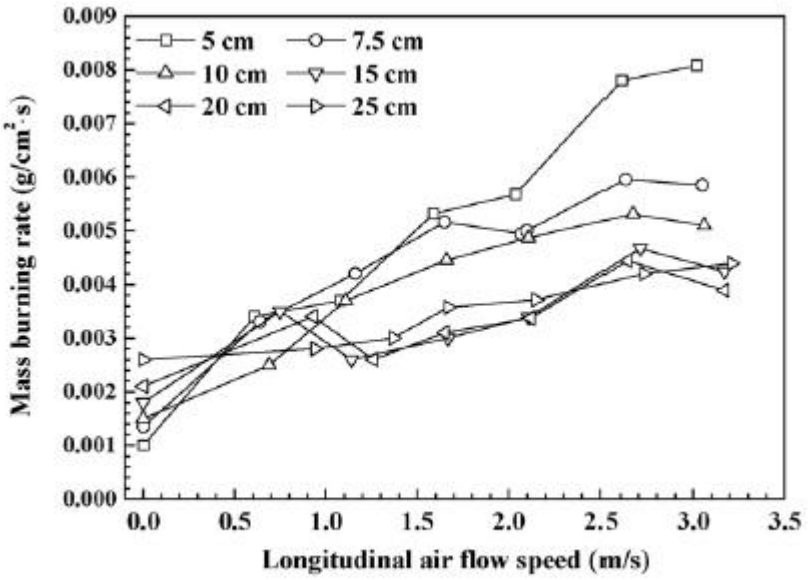

(b) Gasoline pool

Figure 1-9 Burning rates of square pool fires for increasing ventilation velocity [19]

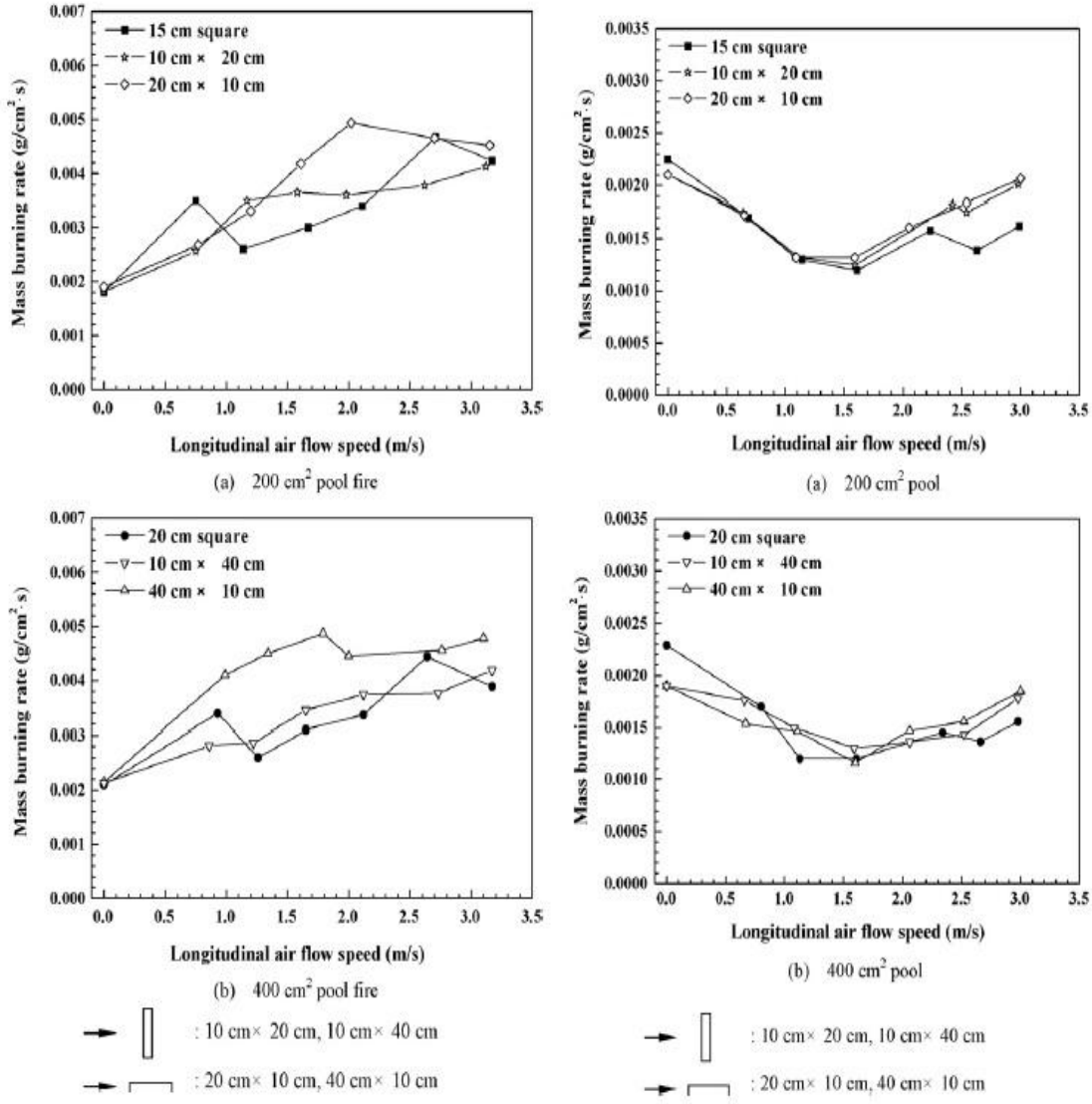

(a) **(b)**

Figure 1-10 Burning rates of rectengular pool fires for increasing ventilation velocity of (a) gasoline and (b) methanol [19]

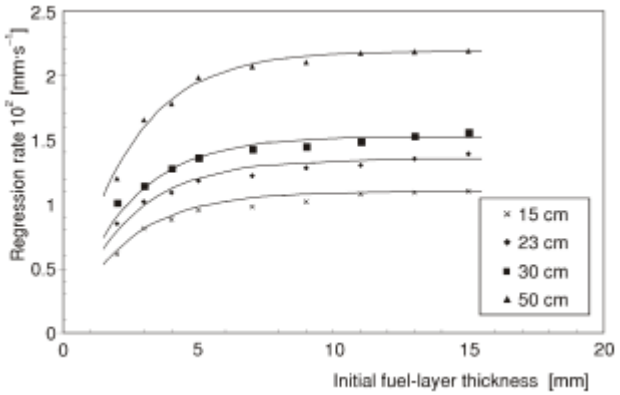

Figure 1-11 Surface Regression rate as a function of initial fuel layer thickness for different pool diameters for crude oil [20]

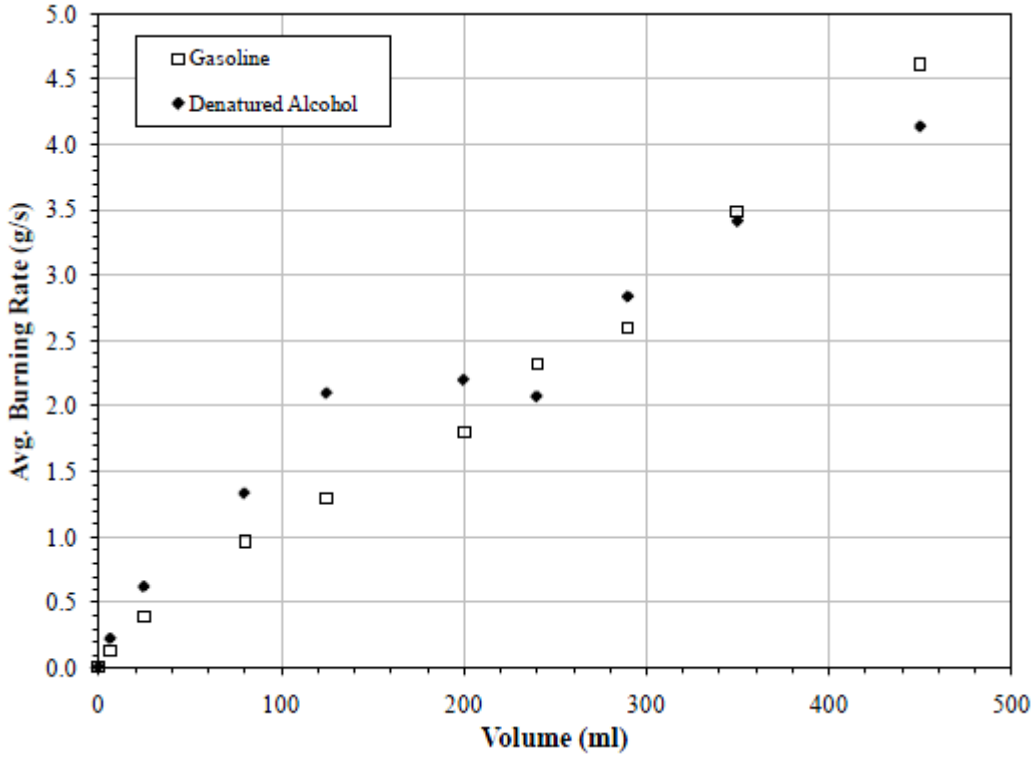

Figure 1-12 Average Burning Rate for different volume of fuel source

1.2.2. Numerical Studies with FDS

Cheong et al [22] developed a simplified representation of burning wood and plastic pallets and illustrates that an FDS simulation is able to reproduce a reasonable estimate of fire growth characteristics. It is noted that FDS is limited in ability to model the effects of wood. In the domain sensitivity analysis, it is seen that it is important to create a suitable domain to capture all the flames. In the simulations it was possible to obtain same HRR with the experimental data used however FDS couldn't reproduce the fuel package collapse [22].

M.K. Cheong et al studied the difference of statistical and numerical approach for a tunnel fire of light goods vehicle carrying wood pallets and then compare the results of two methods against the Runehamar's fire experiment [23].

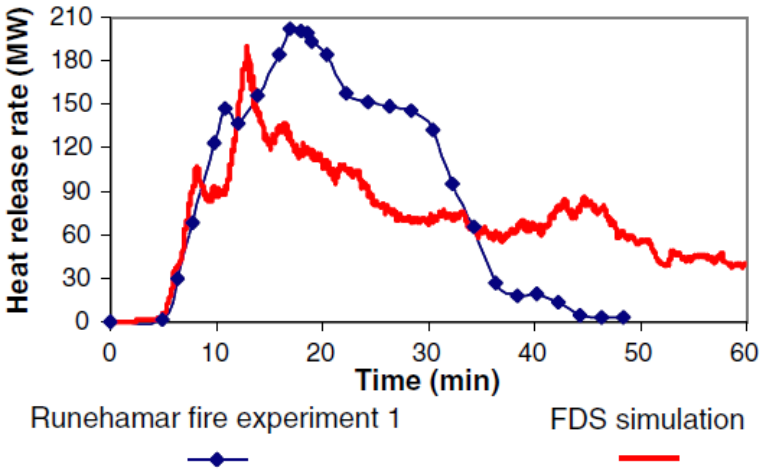

Figure 1-13 Comparison of Runehamar experiment and FDS [22]

It was observed that the results from the FDS simulations consistently fall within the range of values obtained from the statistical approach.

It is noted that although for low velocities both method gives approximate results, for higher velocities FDS would provide more accurate results.

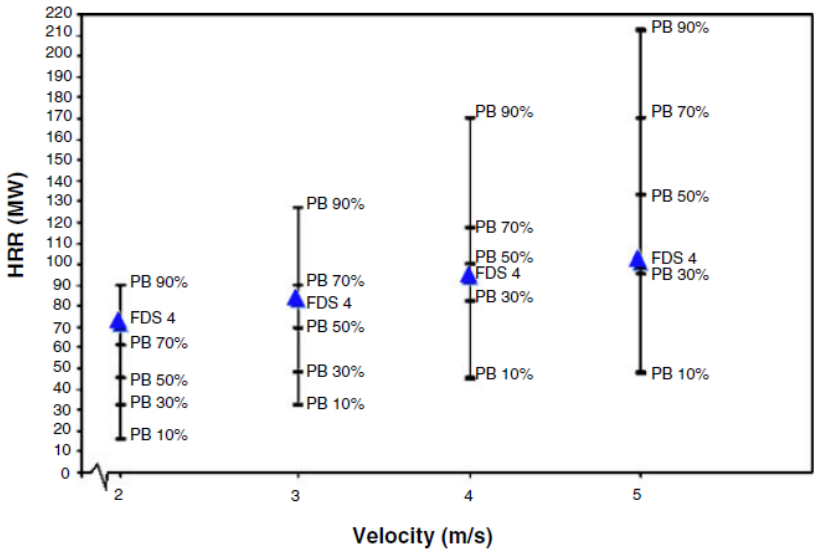

Figure 1-14 Comparison of Statistical and FDS results [23]

Saberand coworkers [24] presents the results of numerical simulations of fire development in a medium-size residential room. The work was part of the process of designing fire experiments in a project concerning the characteristics of fires in various rooms in low-rise residential dwellings of light-frame construction for several ventilation scenarios.

Hwang and Edwards [25] studied whether it is possible to observe leveling of critical velocity in FDS or not. These results are also compared with experimental results.

The CFD results clearly show the leveling-off of the critical ventilation velocity as the fire heat generation increases. It is also observed that the ambient temperature and fuel type do not have a significant effect on critical ventilation velocity. Moreover it is seen that FDS is capable of predicting the critical ventilation, the results compare well with experimental data [25].

Y. Xin et *al* investigated 1m methane pool fire in FDS and compared the results with experiments. The results show that FDS can qualitatively and quantitatively simulate the velocity field of a 1m methane pool fire as seen in Figure 1-15 [26].

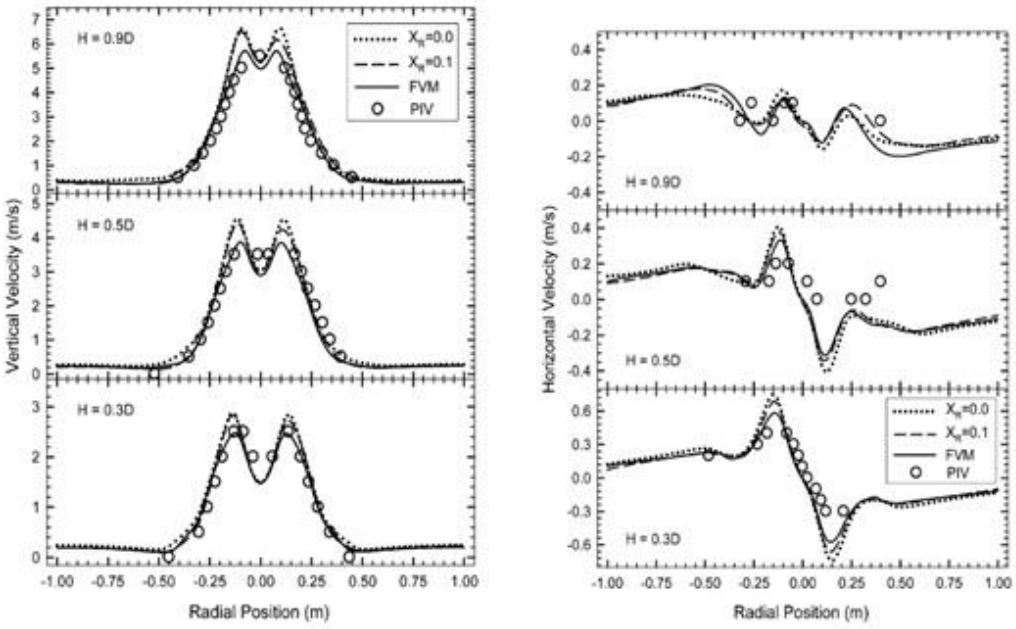

Figure 1-15 Comparison of measured and predicted vertical and horizontal velocities at different elevations above the burner exit of the 1-m methane pool fire the burner size *D* =1 m [26]

J.X. Wen *et al* studied on validation of FDS for medium scale pool fires. In this study pool fire is chosen to be representative of much other fire source. The results have shown that FDS with its existing features can deliver accurate predictions for most important parameters of pool fires that are of significance in the fire safety context [27].

McKeever studied on simulating fuel mass loss rate in fire dynamics simulator. In the study it is stated that the FDS is incapable of calculating enclosure effects on the fuel source. The study is on semi-empirical modeling strategies of the fuel mass loss rate based on furniture calorimeter data and theoretical correction proposed to account for enclosure effects. The modified FDS implementations worked satisfactorily with heptanes fuel case; however the results with upholstered chairs are less satisfactory. Both cases are compared with relevant experimental data as seen in Figure 1-16 and Figure1-17 [28].

McGill simulated a large cryogenic hydrocarbon fuel tanker. The main motivation was to identify how the spill, pool vaporization, turbulent dispersion and fuel-vapor mixing are coupled. A low aspect-ratio obstacle is placed on the vaporizing methane pool under varying wind conditions. The results are presented in the study [29].

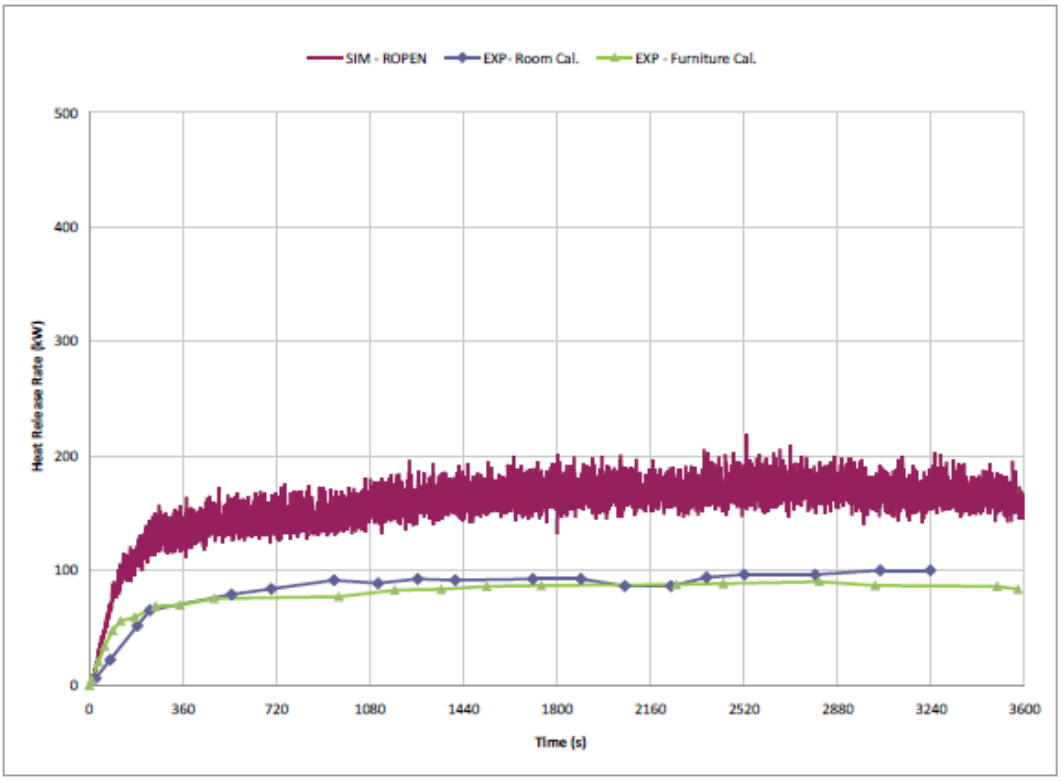

Figure 1-16 Comparison of simulation and experiment for heptane fuel case [28]

Overholt. [30] simulated ethanol pan fire experiments in FDS. It is noted that FDS is not able to simulate mass loss rate with the default properties. In this study the best combination of parameters are searched to simulate open ethanol pool fire. As seen in the Figure 1-18 FDS case 1 represents the FDS default simulation.

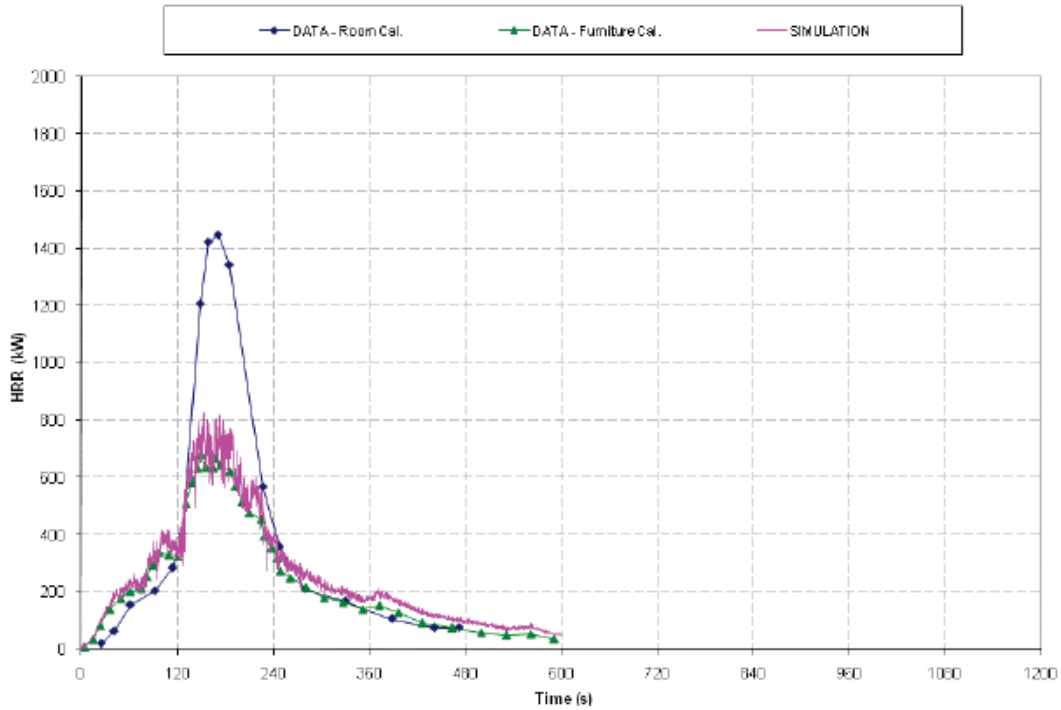

Figure 1-17 Comparison of simulation and experiment for upholstered chairs case [28]

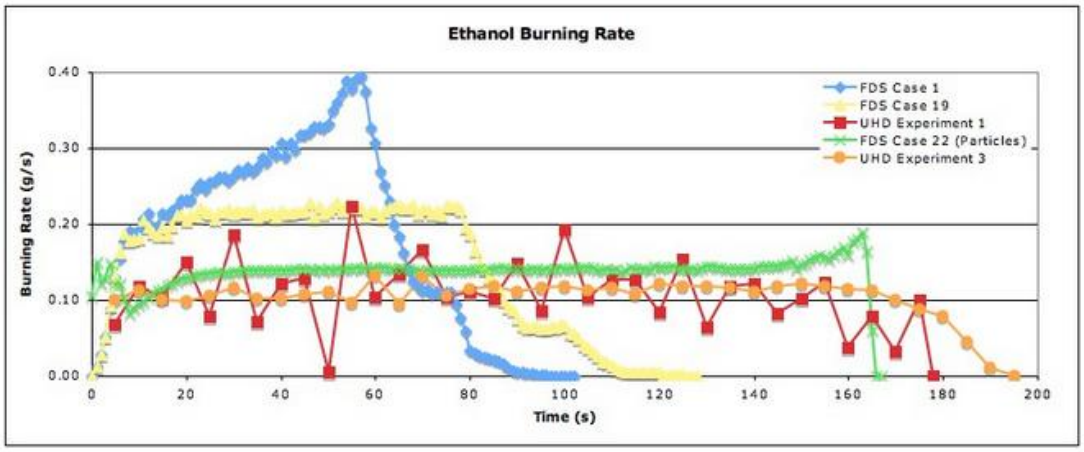

Figure 1-18 Comparison of FDS and experimental burning rate of ethanol [30]

1.3.Aim of the thesis

Fire safely is still an important research subject. In this thesis the main investigation field is tunnel fires. Ethanol is being investigated as an alternative fuel source in recent years due to its renewable characteristics. Hence learning burning behavior of ethanol and ethanol blended gasoline in tunnels will be important for fire safety

The thesis has both experimental and numerical parts. Pool fires are investigated experimentally. Three different fuels are used which are ethanol, gasoline and a mixture of both. Burning behavior of these fuels is observed under several parameters. These parameters are ventilation velocity, pan geometries and initial fuel layer thickness. The results of these experimental studies are simulated by Fire Dynamics Simulator (FDS), a non-commercial CFD program.

CHAPTER 2

EXPERIMENTAL SET-UP & INSTRUMANTATION and PROCEDURE

2.1.Experimental Set-Up

The set-up is constructed as 1/13 scale down of Istanbul Metro System tunnels. The original tunnel has a cross sectional area of 20.75 m^2 with a diameter of 520cm.The scaled tunnel model and the full scale tunnel drawings are given Figure 2-1.

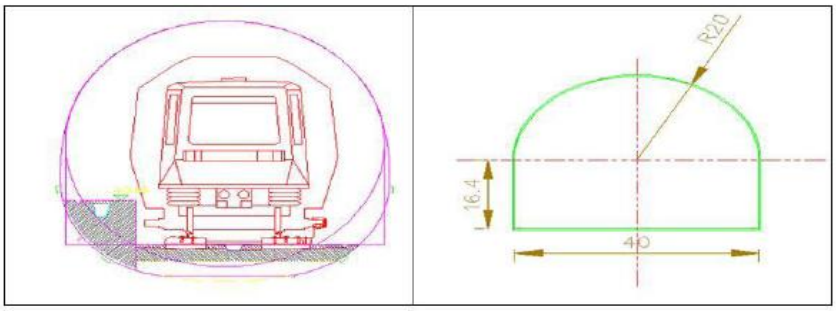

Figure 2-1 Drawing of the original tunnel and model [31]

The total tunnel length is 6 m. There are four portable model tunnels with a length of 150 cm that can be assembled. The model dimensions are represented in Figure 2-2.

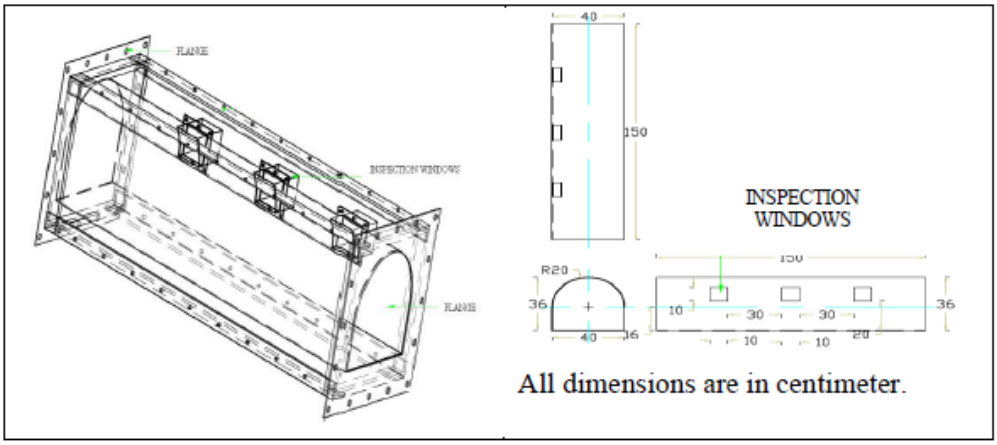

Figure 2-2 Tunnel Model Dimensions [31]

The ventilation of the system is done by an axial compressor as seen in Figure 2-3. The air used for ventilation is sucked from laboratory environment. After passing the compressor, it enters a settling chamber then moves through a 20cmx20cm connection duct to the tunnel. The ventilation velocity can be adjusted with a controller. Since the exit of the duct is higher than the height of the model tunnel, a connection duct is also used. After the auxiliary duct, the flow straigthener (Figure 2-4), whose main aim is to breakdown the large eddies created by turbulence is assembled.

Figure 2-3 Compressor

Figure 2-4 Flow Straightener [31]

After the flow straighteners the burning chamber is set (Figure 2-5). One side of the combustor can be removed in order to place the burning material into the tunnel. To see inside of the tunnel, there are windows on the set-up. To avoid heat transfer between the hot tunnel and atmosphere, the tunnel (Figure 2-6) is insulated with rock wool.

Figure 2-5 Burning Chamber

Figure 2-6 Tunnel

2.2.Experimental Instrumentation

2.2.1. Mass Loss Measurement

A&D GF 20 K High Precision Industrial Balance (Figure 2-7) is used to measure the transient mass of the burning object. The balance is capable of measuring up to 20kg. The precision of the device is 0.1gr. The mass of the burning object is measured each second and the data transferred to computer by a RS232 cable.

Figure 2-7 A&D GF20K Balance

To calculate the mass loss rate from the discrete data, numerical differentiation is used. The centered finite-divided difference formula is used.

$$-\left[\frac{dm}{dt}\right]_i = \frac{-m_{i-2} + 8m_{i-1} - 8m_{i+1} + m_{i+2}}{12\Delta t} \tag{2.1}$$

Where "m" is the mass of the burning substance in grams, "Δt" is the time step in seconds and "i" stands for the data scan number.

2.2.2. Velocity Measurement

Velocity measurement is done with Barnant Tri-sense (Figure 2-8) measurement device and with a differential pressure measuring device shown in Figure 2-9. The measurements are done at the end of the 6m tunnel before experiment with tri-sense device and the entrance duct with a pitot-tube rake for second data set. Tri-sense

device measures velocity directly from pitot tube rake system, whereas the dynamic pressure is read and the velocity is calculated.

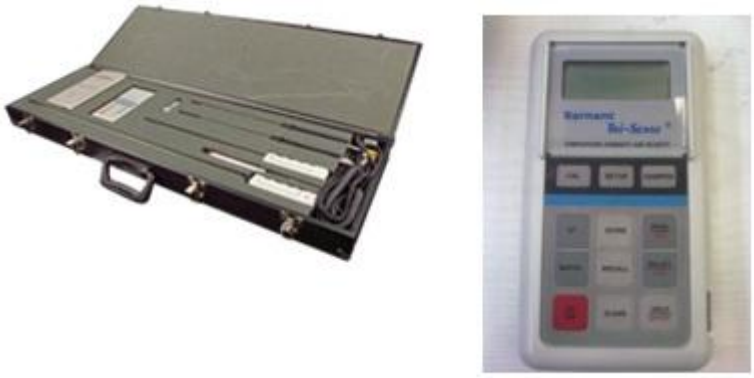

Figure 2-8 Barnant Tri-Sense

Figure 2-9 Differential Pressure Measurement

2.2.3. Gas Concentration Measurement

Gas concentration measurement is done by TESTO 350S gas analyzer which can be seen in Figure 2-10. For heat release rate measurement, oxygen consumption method is used. The detailed information is in experimental results chapter.

Figure 2-10 Gas Concentration Measuring Device

2.3.Experimental Procedure

2.3.1. Experimental Design Parameters

The main of the experiments is to see the effect of ventilation velocity on different fuel sources in different geometries for pool fires in enclosures. Two different pans are used for pool fires; one of them is a square pan of 30cm X 30cm and the second one is a rectangular pan of 30cm X 48cm. The fuels used are gasoline, ethanol and a blend of ethanol and gasoline (70%Gasoline+30%Ethanol). The ventilation velocities are 0m/s, 0.5m/s, 1.5m/s and 2.5m/s. Experiments were also performed to investigate the effect of depth (amount of liquid) of liquid fuel sources.

2.3.2. Steps of Experimental Procedure

The experiments are performed as follows:

1. The atmospheric conditions, i.e., relative humidity, temperature, pressure are measured.
2. The devices are initialized.
3. The fuel source is poured on the scale platform and the model tunnel ventilation is adjusted according to the weather conditions.
4. Fuel source is ignited
5. At every second, the weight of the platform and the gas concentration data are gathered and stored by the computer.
6. The data gathering is stopped when there is no significant change in the data.

Table 2-1 Experiment Matrix

Velocity (m/s)	Fuel Source	Fuel Amount	Pan Geometry
Open Fire	Ethanol	100ml	S
0	Ethanol	100ml	S
0,5	Ethanol	100ml	S
0,5	Ethanol	100ml	S
0,5	Ethanol	100ml	S
0,5	Ethanol	200ml	S
0,5	Ethanol	300ml	S
1,5	Ethanol	100ml	S
1,5	Ethanol	100ml	S
1,5	Ethanol	100ml	S
1,5	Ethanol	200ml	S
1,5	Ethanol	300ml	S
2,5	Ethanol	100ml	S
2,5	Ethanol	100ml	S
2,5	Ethanol	100ml	S
2,5	Ethanol	200ml	S
2,5	Ethanol	300ml	S

Table 2-1 Cont'd Experiment Matrix

Velocity (m/s)	Fuel Source	Fuel Amount	Pan Geometry
Open Fire	Ethanol	100ml	R
0	Ethanol	100ml	R
0	Ethanol	200ml	R
0,5	Ethanol	100ml	R
0,5	Ethanol	100ml	R
0,5	Ethanol	100ml	R
0,5	Ethanol	200ml	R
0,5	Ethanol	200ml	R
0,5	Ethanol	300ml	R
1,5	Ethanol	100ml	R
1,5	Ethanol	100ml	R
1,5	Ethanol	100ml	R
1,5	Ethanol	200ml	R
1,5	Ethanol	200ml	R
1,5	Ethanol	300ml	R
2,5	Ethanol	100ml	R
2,5	Ethanol	100ml	R
2,5	Ethanol	100ml	R
2,5	Ethanol	200ml	R
2,5	Ethanol	200ml	R
2,5	Ethanol	300ml	R

Table 2-1 Cont'd Experiment Matrix

Velocity (m/s)	Fuel Source	Fuel Amount	Pan Geometry
Open Fire	Mixture	100ml	S
0	Mixture	100ml	S
0,5	Mixture	100ml	S
0,5	Mixture	100ml	S
0,5	Mixture	100ml	S
0,5	Mixture	200ml	S
0,5	Mixture	300ml	S
1,5	Mixture	100ml	S
1,5	Mixture	100ml	S
1,5	Mixture	100ml	S
1,5	Mixture	200ml	S
1,5	Mixture	300ml	S
2,5	Mixture	100ml	S
2,5	Mixture	100ml	S
2,5	Mixture	100ml	S
2,5	Mixture	200ml	S
2,5	Mixture	300ml	S

Table 2-1 Cont'd Experiment Matrix

Velocity (m/s)	Fuel Source	Fuel Amount	Pan Geometry
Open Fire	Mixture	100ml	R
0	Mixture	100ml	R
0	Mixture	200ml	R
0,5	Mixture	100ml	R
0,5	Mixture	100ml	R
0,5	Mixture	100ml	R
0,5	Mixture	200ml	R
0,5	Mixture	200ml	R
0,5	Mixture	300ml	R
1,5	Mixture	100ml	R
1,5	Mixture	100ml	R
1,5	Mixture	100ml	R
1,5	Mixture	200ml	R
1,5	Mixture	200ml	R
1,5	Mixture	300ml	R
2,5	Mixture	100ml	R
2,5	Mixture	100ml	R
2,5	Mixture	100ml	R
2,5	Mixture	200ml	R
2,5	Mixture	200ml	R
2,5	Mixture	300ml	R

Table 2-1 Cont'd Experiment Matrix

Velocity (m/s)	Fuel Source	Fuel Amount	Pan Geometry
Open Fire	Gasoline	100ml	S
0	Gasoline	100ml	S
0,5	Gasoline	100ml	S
0,5	Gasoline	100ml	S
0,5	Gasoline	100ml	S
0,5	Gasoline	200ml	S
0,5	Gasoline	300ml	S
1,5	Gasoline	100ml	S
1,5	Gasoline	100ml	S
1,5	Gasoline	100ml	S
1,5	Gasoline	200ml	S
1,5	Gasoline	300ml	S
2,5	Gasoline	100ml	S
2,5	Gasoline	100ml	S
2,5	Gasoline	100ml	S
2,5	Gasoline	200ml	S
2,5	Gasoline	300ml	S

Table 2-1 Cont'd Experiment Matrix

Velocity (m/s)	Fuel Source	Fuel Amount	Pan Geometry
Open Fire	Gasoline	100ml	R
0	Gasoline	100ml	R
0	Gasoline	200ml	R
0	Gasoline	300ml	R
0,5	Gasoline	100ml	R
0,5	Gasoline	100ml	R
0,5	Gasoline	100ml	R
0,5	Gasoline	200ml	R
0,5	Gasoline	200ml	R
0,5	Gasoline	300ml	R
0,5	Gasoline	300ml	R
1,5	Gasoline	100ml	R
1,5	Gasoline	100ml	R
1,5	Gasoline	100ml	R
1,5	Gasoline	200ml	R
1,5	Gasoline	200ml	R
1,5	Gasoline	300ml	R
1,5	Gasoline	300ml	R
2,5	Gasoline	100ml	R
2,5	Gasoline	100ml	R
2,5	Gasoline	100ml	R
2,5	Gasoline	200ml	R
2,5	Gasoline	200ml	R
2,5	Gasoline	300ml	R
2,5	Gasoline	300ml	R

CHAPTER 3

FIRE DYNAMICS SIMULATOR

3.1.Introduction

Fire Dynamics Simulator is a Fortran 90 computer program written by National Institution of Standards and Technology (NIST) that solves the equations of fluid dynamics, i.e. Navier-Stokes and continuity equations; and heat transfer for fire driven flows numerically. FDS is validated for low-speed flows. The partial differential equations of conservation equations are solved as finite differences whereas the thermal radiation problems are solved for finite volume on the same grids. FDS is also capable of simulating smoke motion, nozzles, fuel sprays and discharges by using Lagrangian particles.

FDS is developed to solve engineering problems including complex processes of fire and combustion.FDS can be used to simulate thermal degradation and pyrolysis processes, problems including flame spread and height, sprinkler sprays, transport problems including combustion and heat transfer as long as the flow is defined in low mach number region.

Turbulence management is one of the key points that distincts CFD (Computational Fluid Dynamics) programs from each other. FDS uses LES (Large Eddy Simulation) to handle turbulence. In this method unsteady flow of a large 3-D domain can be directly represented whereas for smaller length scales the fluid motion is modeled.

FDS solves the domain in rectilinear meshes. Hence the problems including non-rectilinear geometries have difficulties in modeling. Those curved surfaces should be treated as linear surfaces.

Like most of the CFD programs FDS has its own limitations. FDS is not applicable to the high speed flows i.e; Mach number >0.3, which makes it useless for detonations, explosions etc. As mentioned earlier, FDS solves rectilinear grids. In some complex geometry this feature may create deficiencies. Fire scenarios may be simulated in two ways in FDS. If the heat release rate is defined and the motion of the gas, temperature distribution or etc is the aim of the simulation, FDS solves these problems with an accuracy of 10-20%. The second type is more complex in which the material properties are defined and the heat release rate is predicted. In these simulations, the results are sensitive to all parameters and the accuracy is lower [32].

3.2.Governing Equations

3.2.1. Conservation Equations and Equation of State

Like in all fluid mechanics problem the solution involves results of solving the continuity, momentum and energy equation in the flow domain.

Conservation of mass or the continuity equation in terms of density ρ can be written as:

$$\frac{\Delta\rho}{\Delta t} + \nabla.\rho\vec{u} = 0 \tag{3.1}$$

In the conservation of mass equation $\vec{u}$ stands for the velocity vector in three dimensions i.e.; $\vec{u} = (u, v, w)$. This expression is the overall mass conservation

requirement which must hold at every point of the low domain. This equation can be used for a single species or for a multi-species problem.

Conservation of momentum energy requires that the total force acting on the flow domain must be equal to the increase in the fluid momentum and the rate of the momentum leaving the flow domain. In mathematical representation it is;

$$\frac{\partial(\rho\vec{u})}{\partial t} + \nabla.\rho\vec{u}\vec{u} + \nabla p = \rho\vec{g} + \vec{f}_b + \nabla.\tau_{ij} \tag{3.2}$$

From point of fire dynamics the buoyant forces which are classified under body forces are the most dominant forces in solution.

Conservation of energy equation is the third fundamental equation that must be satisfied in the flow domain to have satisfactory solution. The conservation of energy equation is the control for first law of thermodynamics which states that the rate of change in the system is equal to the sum of energy gain and loss rate for the system. It is represented mathematically in terms of sensible enthalpy h_s as in Equation

$$\frac{\partial(\rho h_s)}{\partial t} + \nabla.\rho h_s\vec{u} = \frac{Dp}{Dt} + \dot{q}''' - \nabla\cdot\dot{\vec{q}}'' + \varepsilon \tag{3.3}$$

The last equation to be used is the equation of state. FDS assumes that the gases in the simulations obey the perfect gas relationship given by:

$$p = \frac{\rho RT}{W} \tag{3.4}$$

3.2.2. Combustion Modeling

FDS has two modes of for combustion modeling which are mixture fraction modeling and Arrhenius reaction modeling. Arrhenius reaction modeling is more often used directly simulating the motion of oxygen and fuel which is called Direct Numerical Simulation technique which needs a higher grid resolution.
When using grids in lower resolution as in LES, mixture-fraction combustion model is more suitable.

Mixture fraction corresponds to the ratio of the mass of a species to the total mass of the volume. Mixture fraction is conserved in combustion. For illustration, at the surface of a burner the mixture fraction is 1 whereas in the fresh air its 0. Mixing controlled burning in FDS means that when the fuel and the oxygen mix, the reaction occurs immediately and this allows defining all the species in terms of mixture fraction. However there are scenarios that the mixing of the fuel and oxygen do not result in reaction such as under ventilated enclosure fires. Mixture fraction model can directly solve the radiative transport and convective transport for large scales; however for smaller lengths the process can just be approximated.
The general form of a reaction between a fuel and oxygen can be written in the form of:

$$C_x H_y O_z N_a M_b + v_{o_2} O_2 \rightarrow \sum_i v_{P,i}\, products \tag{3.5}$$

The mixture fraction is defined as:

$$Z = \frac{sY_F - (Y_{O_2} - Y_{O_2}{}^{\infty})}{sY_F^l + Y_{O_2}^{\infty}} \tag{3.6}$$

This equation is called to be more traditional and treats Z as a linear combination of oxygen and fuel.

If the combustion takes place in an under-ventilated place it is more appropriate to define Z in terms of carbon carrying products as:

$$Z = \frac{1}{Y_F^l}(Y_F + \frac{W_F}{xW_{CO_2}}Y_{CO_2} + \frac{W_F}{xW_{CO}}Y_{CO} + \frac{W_F}{xW_S}Y_S) \tag{3.7}$$

These equations must satisfy the conservation equation for mixture fraction:

$$\rho\frac{DZ}{Dt} = \nabla\cdot\rho D\nabla Z \tag{3.8}$$

3.2.3. Thermal Radiation Modeling

Recall the Equation 3.9 which handles the energy balance for the system. In this equation $\dot{q}''$ stands for the conductive and radiative heat transfer fluxes;

$$\dot{q}'' = \dot{q}_r'' + \dot{q}_c'' \tag{3.9}$$

The radiative heat transfer equation for a participating medium is an integro-differential equation:

$$s.\nabla I_\lambda(x,s) = -[\kappa(x,\lambda)+\sigma_s(x,\lambda)]I_\lambda(x,s) + B(x,\lambda) + \frac{\sigma_s(x,\lambda)}{4\pi}\int_{4\pi}\Phi(s,s')I_\lambda(x,s')ds' \tag{3.10}$$

The left hand side of the equation represents the intensity change for a certain direction. There are three components in the right hand side of the equation. The first terms represents the absorption and the in-scattering that is inflow of radiation intensity. The second term represents the emission of the particles and the third term

is the out-scattering terms. The second and third term altogether represents the extinguishing terms for the radiation.

The solution of this equation is not possible analytically however it is possible to obtain solutions numerically with some simplifications.

FDS assumes that the medium is non-scattering hence the governing equation for the thermal radiation turns into:

$$s \cdot \nabla I_{\lambda}(x,s) = \kappa(x,\lambda)[I_b(x) - I_{\lambda}(x,s)] \tag{3.11}$$

In this equation I_b refers to source term in terms of Planck function. I_b can be written for each band. For fire scenarios most of the radiation is dominated by the soot which has a continuous spectrum. Hence media including fire and combustion products can be assumed as gray medium.
The default thermal radiation is as black body radiation which leads the intensity to be in the form of:

$$I_b(x) = \sigma T(x)^4 / \pi \tag{3.12}$$

Since the temperature is spread to the grid cell the intensity would be lower than that of the expected diffusion flame. For flame sheets;

$$\kappa I_b = \begin{cases} \kappa\sigma T^4/\pi & \text{Outside the flame zone} \\ \max(\chi_r \dot{q}'''/4\pi, \kappa\sigma T^4/\pi) & \text{Inside the flame zone} \end{cases} \tag{3.13}$$

χ_r is the radiative fraction and defined as the ratio of heat release rate as thermal radiation to the total heat release rate and $\dot{q}'''$ is the chemical heat release rate per unit volume.

Mentioned earlier, the analytical solution of an absorbing-emitting scattering media is only possible for very simple cases with some further simplifications.

Hence, numerical methods should be applied to find the solution. In FDS Finite Volume Methods are applied for the solution of the radiative transport equation.

3.2.4. Pyrolysis Modeling

Pyrolysis modeling is the modeling of reactive processes, charring, evaporating and internal heating. In most of the analysis the heat release rate per unit area is prescribed and the prediction of the heat release rate is not the main concern. In these cases the surfaces are defined as burners and the pre-described heat releases from the intended surface by mass flux. The other method is defining the material properties and reactions and predicting the heat release rate. In both models the mixture fraction combustion model is used.

Solid fuels may undergo reactions by some assumptions [33]:

- instantaneous release of volatiles from solid to the gas phase,
- local thermal equilibrium between the solid and the volatiles,
- no condensation of gaseous products, and
- no porosity effects

Fuel pyrolysis is estimated using a single-step Arrhenius rate law of the first order. The main assumption is incoming energy flux is the source of energy to vaporize the fuel source.

The pyrolysis rate is written as:

$$\dot{m}_p'' = A\rho_s e^{-E_A/RT} \tag{3.14}$$

where R is the universal gas constant, A is the pre-exponential factor and E_A is the activation energy. These parameters cannot be obtained easily. This equation is generally used to obtain a similar behavior of mass loss rate for a material of unknown pyrolysis properties. Defining mass flux and ignition temperature will force FDS to define appropriate A and E_A values if those properties are not known.

CHAPTER 4

EXPERIMENTAL RESULTS

4.1.Background on Pool Fires

Liquid fires are a very likely hazard. However the characterization of the liquid fires is not established for different cases except liquid pan fires of deep pools. The burning behaviors of spill fires are not modeled accurately. Generally the pool fire correlations are used which results in over shot in heat release rates. The differentiation of a spill fire and a pool fire can be done according to SFPE (Society of Fire Protection Engineers) Handbook of Fire Protection Engineering [34]. The fire is a pool fire if the thickness of the fuel source is over 1cm with a confined area whereas the spill fire is generally of unconfined space and the thickness of the fuel layer is in the order of 0.1cm.

There are numerous factors that affect the liquid fire characteristics either a pool fire or a spill fire is of concern. The spread of the liquid, the orientation and properties of the surface, evaporation of the liquid fuel, the initial temperature of the liquid or the depth of the liquid. However since the main focus is the burning rate and heat release rate for liquid pool fire in this thesis, the detailed information is not given.

The burning rate information in the literature is mostly on pool fires of steady depth. The study of Blinov & Khudyakov, Diffusion Burning of Liquids in 1961 for US Army [35] is a widely used reference for liquid pool fire studies.

Wide ranges of studies were conducted in this study. Figure 4-1 shows the regression rate and flame height of common fuels with respect to pan diameter. It is seen that the burning behavior of these fuels are similar.

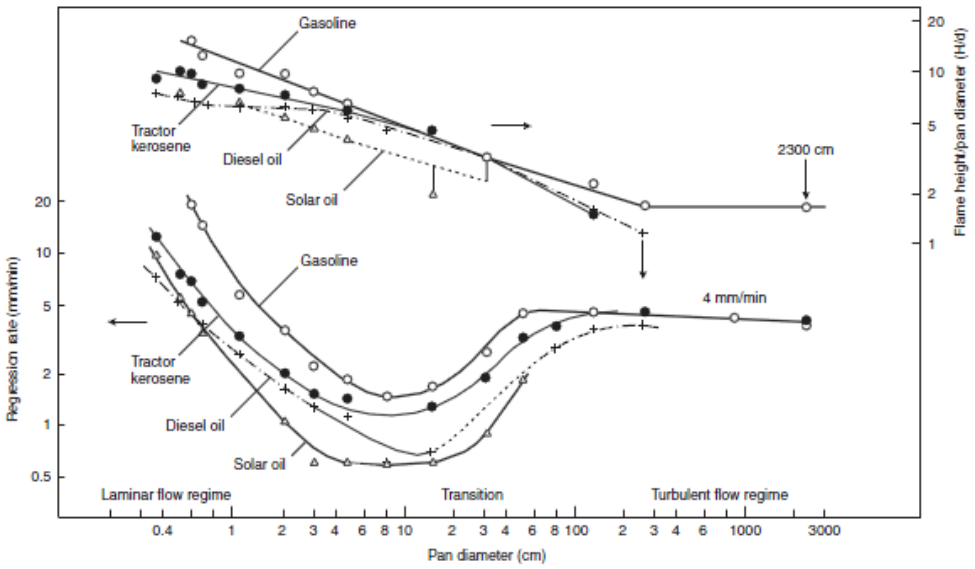

Figure 4-1 Regression Rate and Flame Height for different liquid pools [35]

The heat transfer mechanism which is directly related to the burning behavior of the pool fire is either radiation dominated or convection dominated depending on its diameter. The burning rate of a pool fire was found to fall into four basic different regimes based on the flame mechanisms [19]: "convective heat transfer from the pool rim dominated and laminar flame for D< 0.05 m, convection from the flame dominated and turbulent for 0.05m<D< 0.2 m, radiation from the flame dominated and optically thin for 0.2m<D< 1m, radiation from the flame dominated and optically thick for D> 1m". It is found that mass loss rate is not affected by the pool diameter if it is not flame dominated, i.e., the fire is in convection dominated regime. In the

radiation dominated regime, the mass loss rate increases with increasing diameter to a constant value.

However, SPFE Hand book of Fire Protection Engineers gives different ranges for this categorization. For SPFE the fire diameter above 1m leads to a radiation dominated heat transfer, i.e., radiation from flume to liquid source. For smaller sizes, the fire is dominated by heat conduction and convection. Conduction is due to pan (walls) or the substrate [34].

Zebatakis [34] developed a relationship for mass burning rate for the pool fires of radiation dominated.

$$\dot{m}_f = \dot{m}_{\max}(1-e^{-k\beta D}) \tag{4.1}$$

In this equation D stands for pool diameter, $\kappa\beta$ stand for an empirical constant and $\dot{m}_{\max}$ is the empirically determined mass burning rate for an infinite diameter pool. $\kappa\beta$ values for many common fuel source are supplied in the study of Babrauskas [34] However the above equation is inappropriate for alcohols and the following equation should be used [36]:

$$\dot{m}_f = \dot{m}_{\max} \quad \text{D>0.2m} \tag{4.2}$$

Figures 4- 2 and 4-3 illustrate the behavior of gasoline and alcohol burning rates with respect to pan diameter.

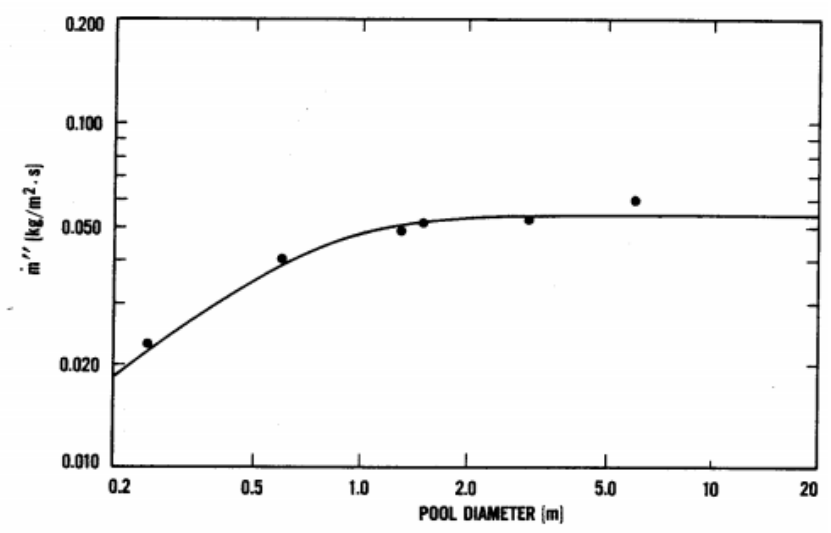

Figure 4-2 Gasoline Pool Burning Rates [36]

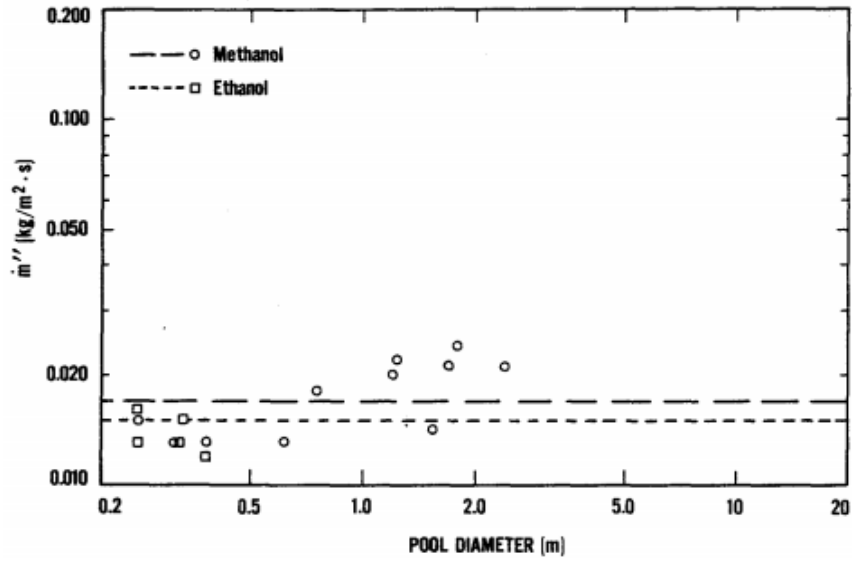

Figure 4-3 Alcohol Pool Burning Rates [36]

As mentioned, systematic data for burning rates are just available for steady-burning rate. The layer thickness of the pool has effect on the burning rate if the fire does not have enough source or time to reach steady-state burning.

In these cases the radiative behavior of the pool substrate and the heat transfer to the pool substrate has importance. There is not enough information on the spill fire burn rate. Gottuk *et al* showed that burning rates of spills are in the order of 1/5-1/4 of pool fires [37].

Effect of the winds on pool fire cannot be directly judged. For small diameter fires it enhances the convective heat transfer. However for larger diameters the flame shape changes and the radiation interactions change.

For windy conditions Blinov and Khudyakov present a formulation [35]:

$$\frac{\dot{m}_{windy}}{\dot{m}_{still}} = 1 + 0.15\frac{u}{D} \tag{4.3}$$

where u stands for wind velocity and D for the pool diameter. It should be noted that this equation is not valid for alcohol fires.7

4.2. Heat Release Rate and Oxygen Consumption Calorimetry

In these experiments all the combinations of ventilation velocity, fuel source, pan shape and fuel amount is used. As mentioned before, the main idea in tunnel fire protection engineering is to predict or know the maximum (peak) heat release rate. Hence, in this analysis the main aim is to investigate the maximum heat release rate for these combinations. The heat release rate is calculated by oxygen consumption method.

4.2.1. Oxygen Consumption Calorimetry

Oxygen consumption calorimetry is developed to create a standard way to calculate the heat release rate in fires of different materials. By this method it is enough to know the oxygen rate in exhaust gas and the amount of air flowing into the system to calculate heat release rate up to a certain approximation and it yields enough accuracy for most of the engineering problems. It is stated that the energy produced for unit mass of the oxygen consumed is nearly 13MJ/kg. The theory can be applied to many fields. One of the most important parameter that the accuracy depends on is how accurate the exhaust gas is measured.

The equation used is:

$$\dot{Q} = \left[\phi - \left(\frac{E'' - E'}{E'} \right) \left(\frac{1-\phi}{2} \right) \frac{X_{CO}^{A}}{X_{O_2}^{A}} \right] E' X_{O_2}^{0} \dot{V}_A \tag{4.6}$$

where the terms of the equation are ;

$\dot{Q}$: Heat release rate (kW)

ϕ : Oxygen depletion factor

E' : Net heat of combustion per unit volume of oxygen consumed (17.2 MJ/m^3)

E'' : Net heat of combustion per unit volume of carbon monoxide consumed (23.1 MJ/m^3)

X_{CO}^{A} : Mole fraction of the carbon monoxide in exhaust flow

$X_{O_2}^{A}$: Mole fraction of the oxygen in exhaust flow

$X_{O_2}^{0}$: Mole fraction of oxygen into the system

$\dot{V}_A$: Volumetric mass flow into system

Figure 4-4 and Figure 4-5 is an example of both time history for mass-mass loss rate and mass loss rate- heat release rate of a chosen experiment.

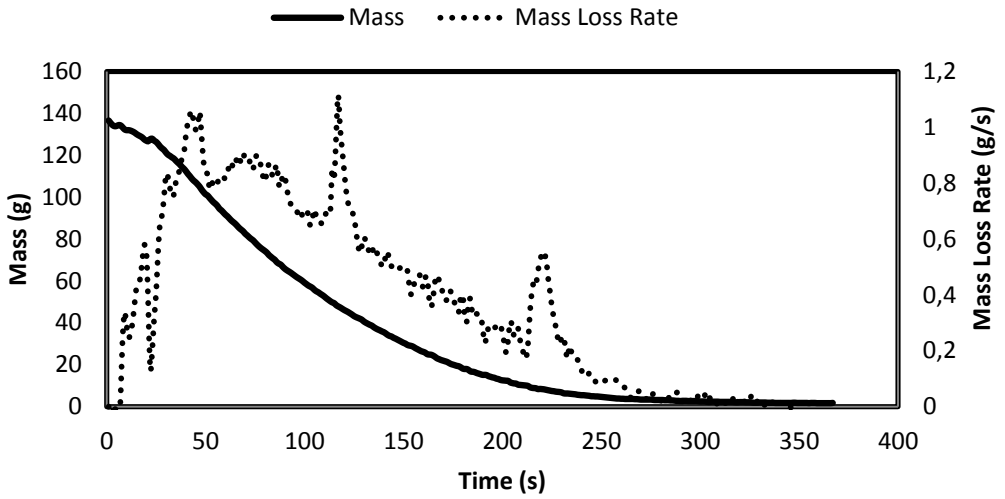

Figure 4-4 Time history for Mass and Mass Loss Rate for 200ml Gasoline with 1.5 m/s ventilation velocity

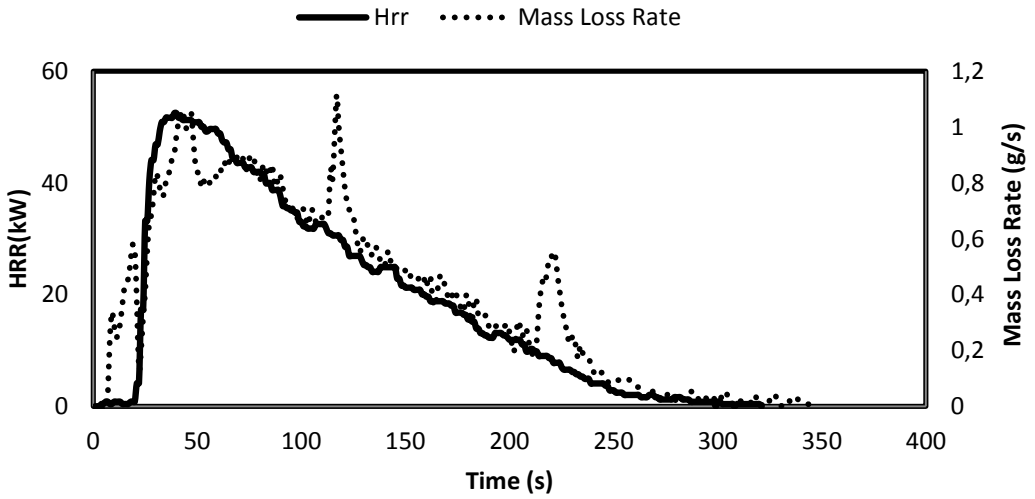

Figure 4-5 Time history for Mass Loss Rate and HRR for 200ml Gasoline with 1.5 m/s ventilation velocity

4.3. Experimental Results

In these experiments the main concern was to investigate effects of different parameters on mass loss rate and heat release rate for pool fires. Various aspects were investigated for a pool fire in an enclosure.

The parameters subject to change are;

I. Ventilation velocity
II. Fuel Type
III. Amount of initial fuel (or initial depth)
IV. Pan geometry

Heat feedback from the flame to the fuel surface occurs through radiative, convective and conductive heat transfer. The relative contributions of these modes to the feedback may depend on a large number of factors including pool diameter, flame shape, flame luminosity etc. [38] In this study there are more factors to effect burning rate such as back radiation from enclosure walls and the effects of ventilation.

It should be noted that these experiments results would be as unique as those of previous studies. There exist three main differences between these experiments and previous works:

1- First reason is that the scale of fire diameter to the tunnel height and width exceeds (nearly 1) far more than those of the previously studied cases.

2- Secondly the velocity of the ventilation for this scaled experiments were 0 m/s, 0.5 m/s, 1.5m/s and 2.5m/s which would be 1.8m/s, 5.4m/s, 9m/s respectively due to Froude scaling there is no previous work for this range of velocity for full scale.

3- Although the experiments are classified as pool fire with the pan being a confined geometry, since the depth of the pool is in the order of 1mm, it behaves like a spill fire. Since in literature the pool fire is generally used for continuously fed pools with steady burning rate, these experiments are likely to be consistent with spill fires.

4.3.1. Open Fire Burn Rates

The open fire results are checked with Equation 4.1. The results are for pool fires and as mentioned earlier, the expected results for spill fire is in the order of 1/5-1/4 of the pool fires.

Table 4-1 Properties of Gasoline and Ethanol

	Gasoline	Ethanol	Unit
$\kappa\beta$	2.1	2.5	(m^{-1})
$\dot{m}''_{\max}$	0.055	0.015	$(kg/s.m^2)$

The pan used are square or rectangle. Hence the diameter is converted to equivalent circular diameter using:

$$D = \sqrt{\frac{4A}{\pi}} \tag{4.4}$$

where A is the area of the non-circular geometry.

Table 4-2 Analytical and experimental results for mass loss rate

	$\dot{m}_{f,s}$ (g/s)	$\dot{m}_{f,r}$ (g/s)	$\dot{m}_{experiment,s}$	$\dot{m}_{experiment,r}$	$\frac{\dot{m}_{experimental,s}}{\dot{m}_{f,s}}$	$\frac{\dot{m}_{experimental,r}}{\dot{m}_{f,r}}$
G	2,5	4,46	0,675	0,726	0,27	0,17
E	0,76	1,35	0,663	0,76	0,87	0,57

where G stands for Gasoline, and E stands for Ethanol in the table and s and r stands for square and rectangle respectively.

For gasoline it can be seen that the theory of Gottuk [37] *et al* holds. If the alcohol results are only checked with Equation 4.2, the results will not fall into the expected range.
If Equation 4.2 is used;

$\dot{m}_f = \dot{m}_{max}$ D>0.2m

with necessary values from table 4.1., maximum burning rate for ethanol is calculated and presented in Table 4.3.

Table 4-3 Analytical and experimental results for mass loss rate

$\dot{m}_{max}$ = 0,015 (g/s)					
$\dot{m}_{max,square}$	1,345	$\dot{m}_{experiment,square}$	0,663	$\frac{\dot{m}_{experimental,square}}{\dot{m}_{max,square}}$	0,5
$\dot{m}_{max,rectangle}$	2,078	$\dot{m}_{experiment,rectangle}$	0,76	$\frac{\dot{m}_{experimental,rectangle}}{\dot{m}_{max,rectangle}}$	0,365

As it can be seen from Table 4.3, alcohol data for rectangle is close to the expected range however the square pan does not fall into the expected rangei.e., it is greater than the 20-30% of the pool data.

For 100ml fuel source, the rectangle pan geometry is a typical spill fire. However the square pan restricts the fuel to spread freely. This restriction may result a deviation in the behavior of the fire.

4.3.2. Effect of Tunnel

Experiments are conducted to investigate the effect of enclosure on the burning rate. The experiments are conducted without ventilation both in open and enclosure case. Main expectation is to see an enhancement in mass loss rate due to back radiation from walls of the tunnel. However the experimental results contradict with the expectations. As in Figure 4-6 and Figure 4-7 for all fuel sources the open fires show a greater MLR than tunnel fires for rectangle and square pan.

These results contradict with the study of Sugawa [14] who states that enclosure enhances burning rate. The main reason for this result can be due to tunnel geometry. In open fire the fuel source is fed by oxygen easily. However in the case of tunnel fire, if the soot created cannot be swept away, the soot may start to block both the back radiation of walls and oxygen supply. The tunnel geometry used has 90^{o} bends on both side of the exit which increases the head loss is high and makes it difficult for smoke to move out.

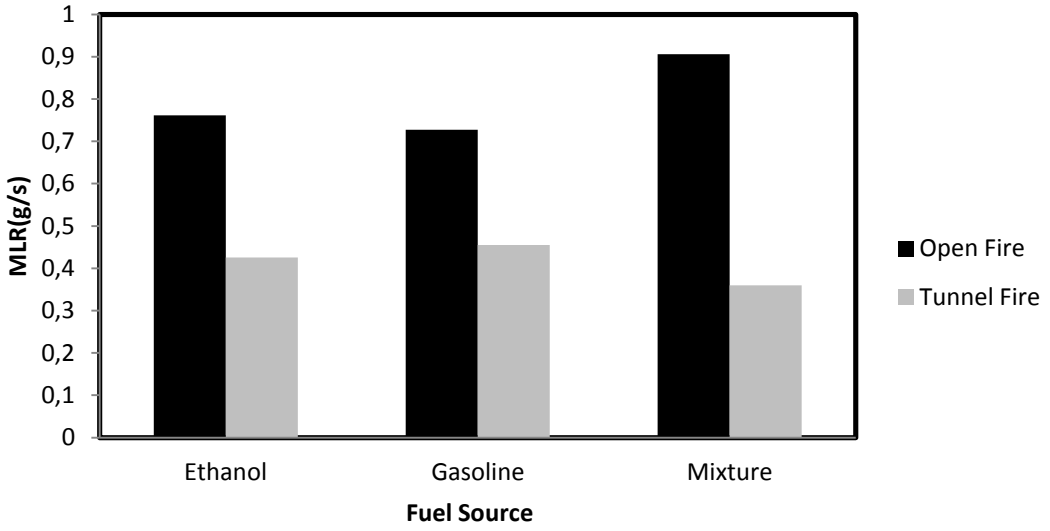

Figure 4-6 Average mass loss rate comparisons of open fire and tunnel fire for 100ml of fuel source in rectangle pan

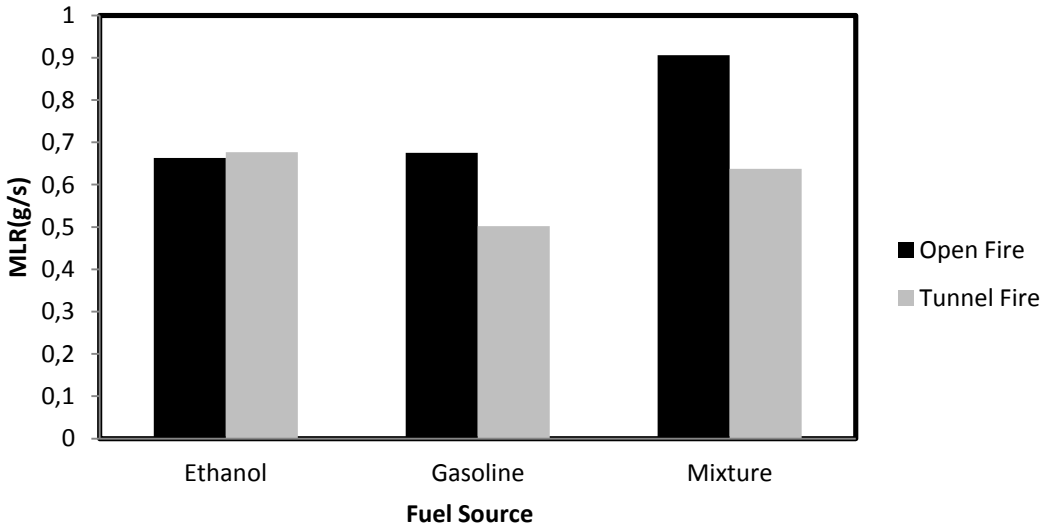

Figure 4-7 Average mass loss rate comparisons of open fire and tunnel fire for 100ml of fuel source in square pan

4.3.3. Effect of Ventilation Velocity on Mass Loss Rate and Heat Release Rate

The burning characteristics of Ethanol, Gasoline and a blend of two (70%Gasoline, 30%Ethanol) are studied under different ventilation conditions.

Ventilation may have three distinct effects on mass burning rates and heat release rates of the fuels. The first effect is the enhancement of both MLR and HRR due to increase in oxygen supply to fuel source. The second effect is the cooling effect. If the ventilation velocity is higher than a certain value, heat loss with convection dominates the fire characteristics and decreases the burning rate. These two cases are valid if the fire is ventilation controlled. The third case is that it may have no effect on the fire. If there is no effect of ventilation on fire, the fire is said to be fuel controlled.

There is no universally accepted result for enclosure fire dynamics for a pool fire. A meaningful example can be seen in the comparison of Saito et al [40] and Roh et al [10]. Saito et al studied the burning rates of methanol and n-heptane pool fires . the results showed that, the burning rates of both methanol and n-heptane pool fires decreased with increasing wind speed. However Roh et al found that the mass loss rate of methanol decreases with increasing ventilation velocity on the other hand for heptanes pool fires the mass loss rate increases with increasing ventilation velocity.

For 100ml ethanol experiments in square pan, the average burning rates and peak mass loss rates are presented in Figures 4-8 and 4-9 respectively. The main trend is that both average and peak mass loss rates decreases with increasing ventilation velocity. This means that the burning rates are affected from ventilation and the fire is ventilation controlled. Moreover the cooling effect of the ventilation dominates the oxygen enhancement effect.

When the pan geometry is changed to the rectangle one, the burning characteristics of 100ml ethanol also change. As in Figure 4-10 and Figure 4-11 the average mass loss rate and peak mass loss rates shows an increasing trend when the velocity is changed from 0 m/s to 0.5 m/s. From this velocity on, a decreasing trend in average and peak mass loss rate is observed. Hence the ventilation enhances the MLR till 0.5 m/s ventilation velocity; however it does not have a significant effect afterwards and fire may be called as a fuel controlled fire.

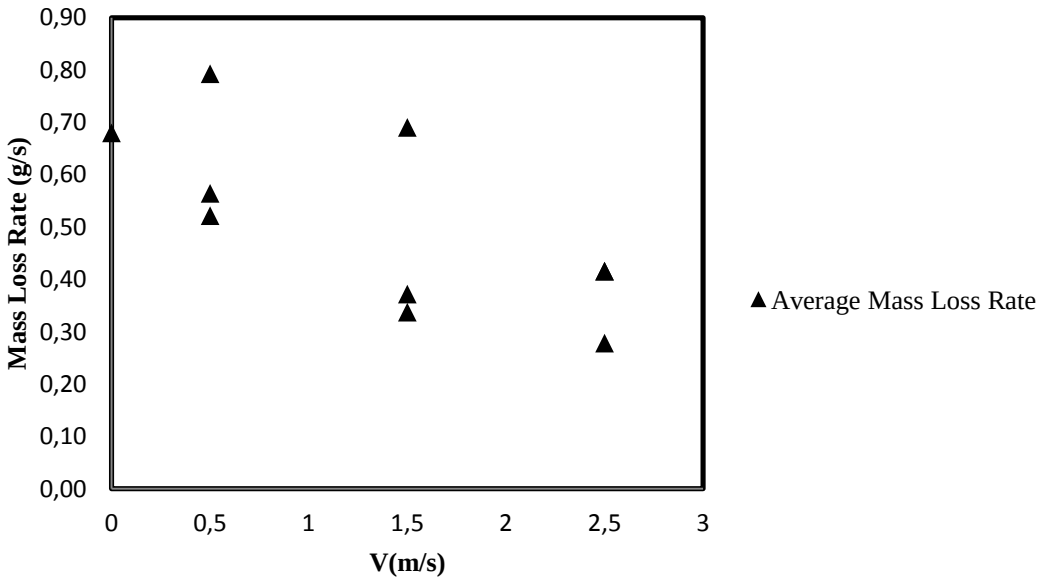

Figure 4-8 Average mass loss rate for 100ml ethanol for different velocities in square pan

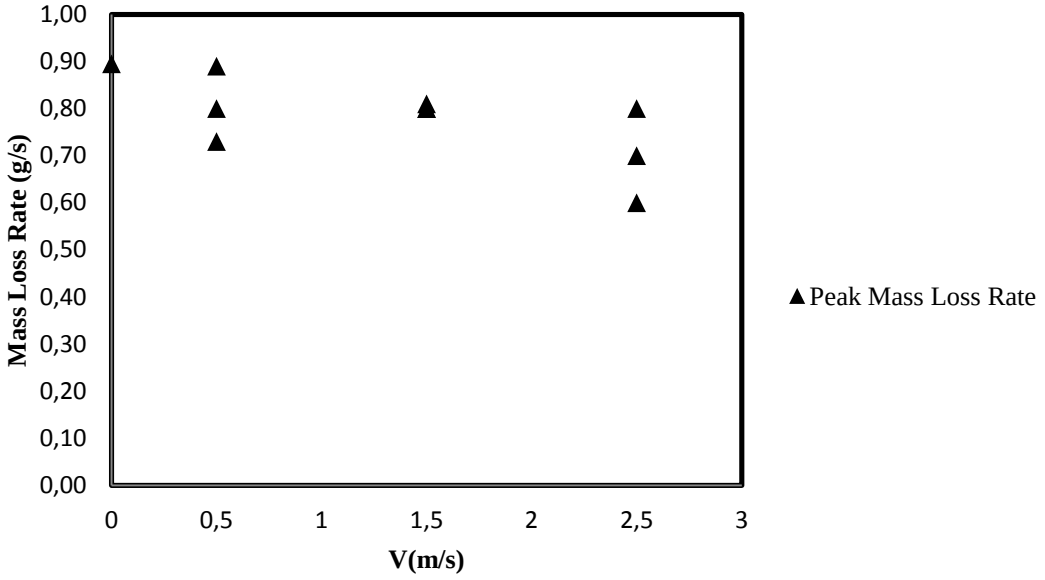

Figure 4-9 Peak mass loss rate for 100ml ethanol for different velocities in square pan

It should be noted that the ventilation velocities for this scaled experiments were 0 m/s, 0.5 m/s, 1.5m/s and 2.5m/s which would be 1.8m/s, 5.4m/s, 9m/s respectively due to Froude scaling that there is no study in the literature for this range of velocity for full scale.

In the rectangle pan the results are more stable for all fuel sources. One of the possible reasons for this may be due to smaller depth of the fuel source. Since the fuel source depth is below 1mm (0,6mm) most of the energy releasedfor all cases happen to increase the temperature of the pan. Another possible reason is the differences of the flame location under varying ventilation velocities.. When the flame is deflected with increasing velocity, the deflected flame runs over the pan which avoids the feeding of fuel source with the heat from the high temperature flames. This is more dramatic in square pan since the length in the flame deflection direction is 18cm smaller with respect to the rectangle pan. This makes rectangle

pan more advantageous about benefiting from the flame since the deflected flame will be still on pan for 18cm more compared to square one.

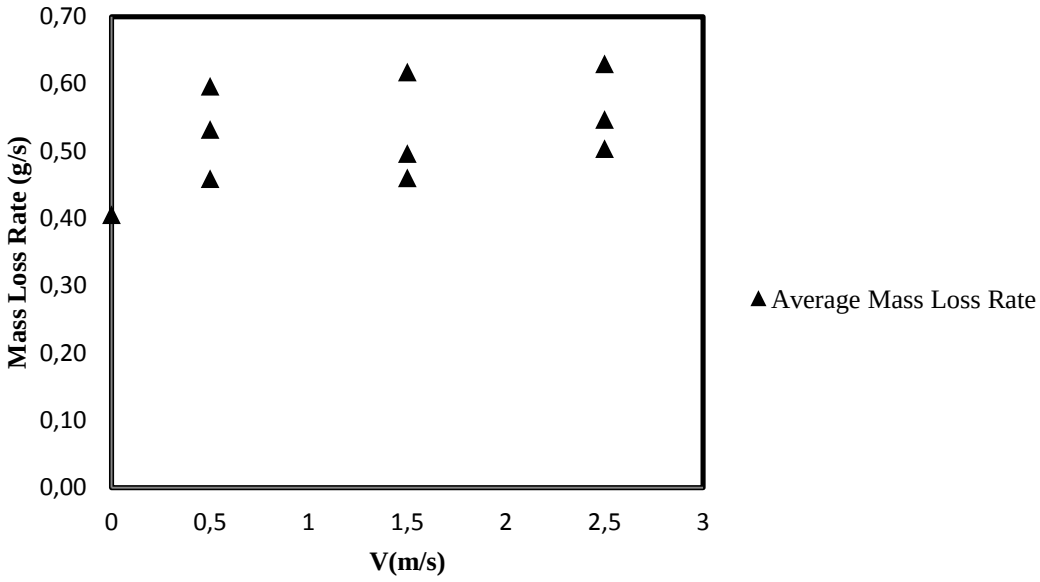

Figure 4-10 Average mass loss rate for 100ml ethanol for different velocities in rectangle pan

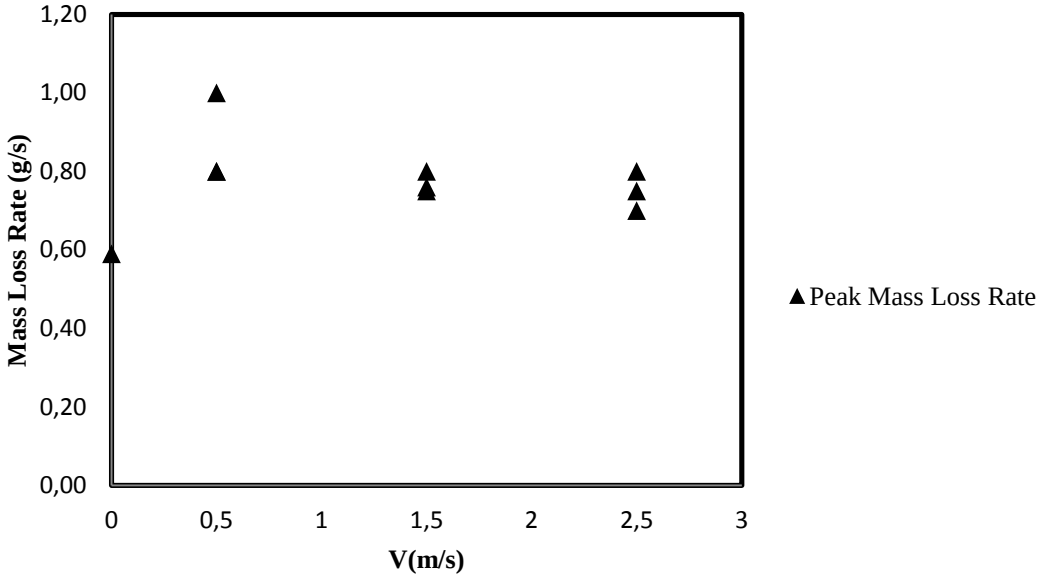

Figure 4-11 Peak mass loss rate for 100ml ethanol for different velocities in rectangle pan

When the amount of fuel source increases, the burning characteristics of fire change. The fires in these experiments are unsteady which means that there is no steady-state burning. Figure 4-12 and Figure 4-13 shows average and peak mass loss rate for 200 ml ethanol in square pan. It can be seen that the same decrease in average and peak mass loss rate after 0.5 m/s ventilation velocity can also be observed in 200ml square experiments. Hence the fire is still ventilation controlled in square pan.

However for 200ml rectangle pan experiments, it is not possible to observe the same trend of 100ml ethanol experiment in rectangular pan as in Figure 4-14 and Figure 4-15.

The decreasing mass loss rate trend with increasing ventilation velocity in square pans can also be observed in 300ml ethanol experiments as in Figure 4-16 and Figure 4-17. The burning behavior of 300ml ethanol in rectangle pan shows the same trend as in 100 ml and 200 ml ethanol experiments, i.e.; changes very slightly with increasing velocity as in Figure 4-18 and 4-19.

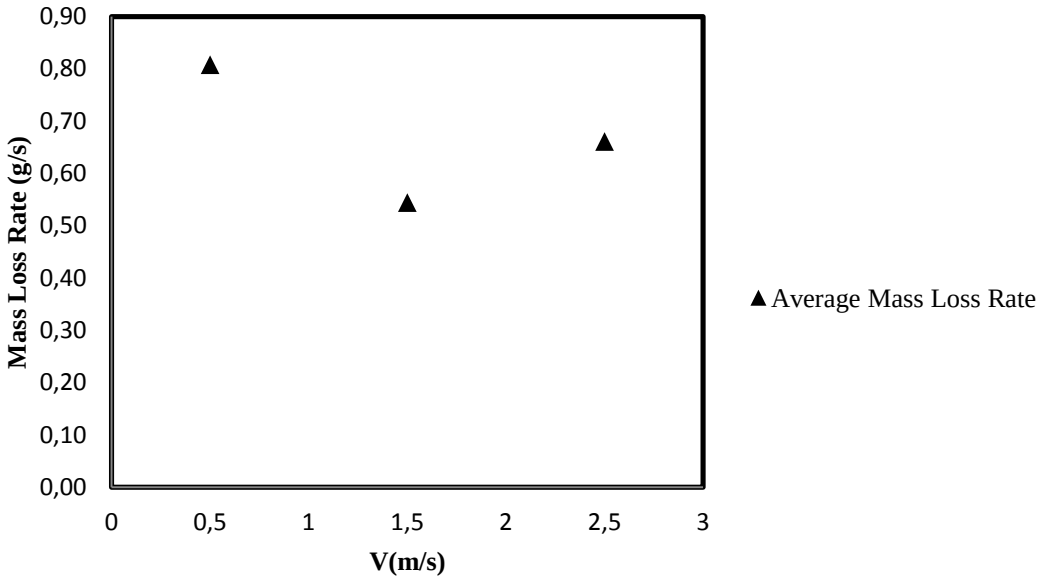

Figure 4-12 Average mass loss rate for 200ml ethanol for different velocities in square pan

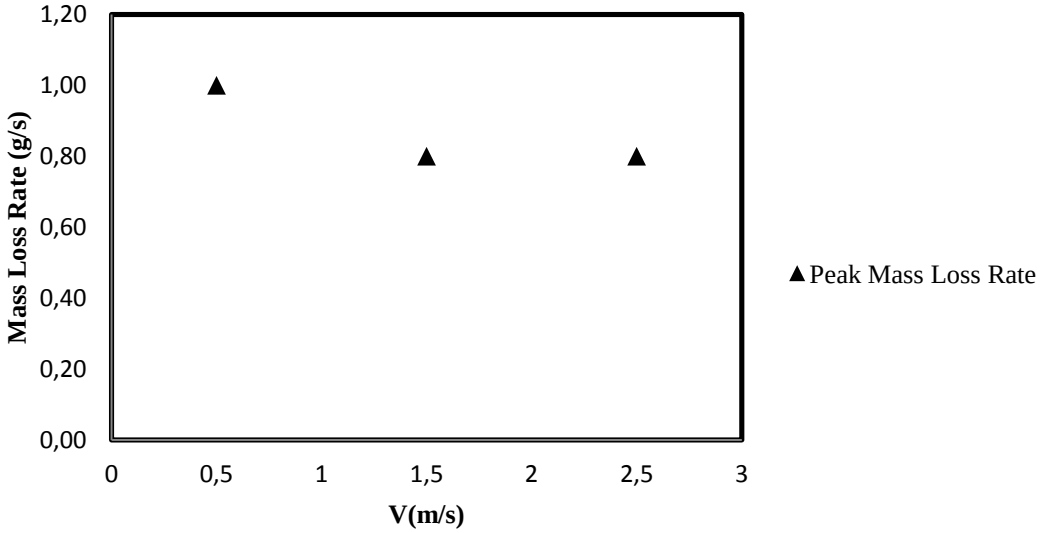

Figure 4-13 Peak mass loss rate for 200ml ethanol for different velocities in square pan

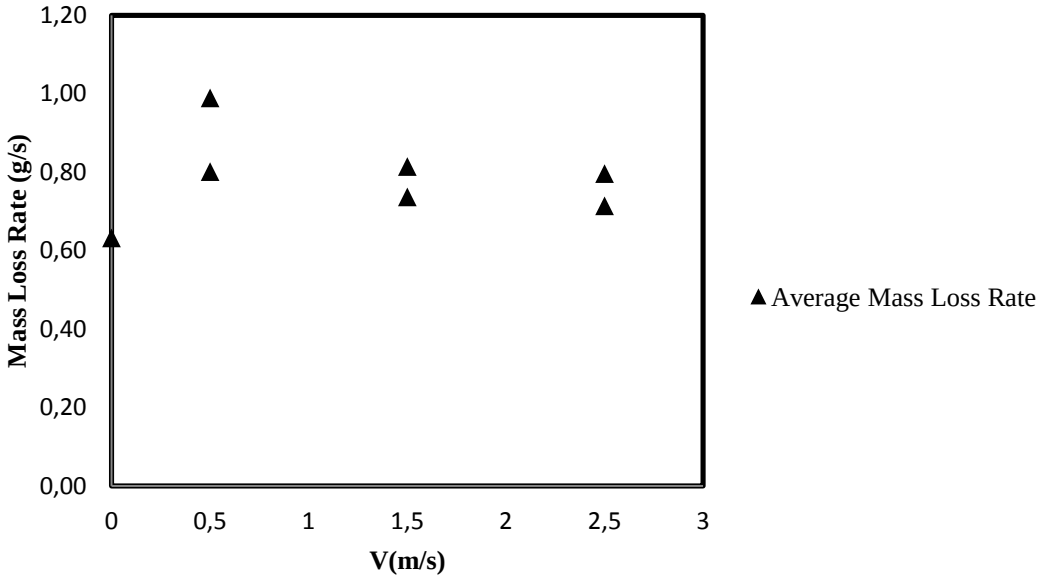

Figure 4-14 Average mass loss rate for 200ml ethanol for different velocities in rectangle pan

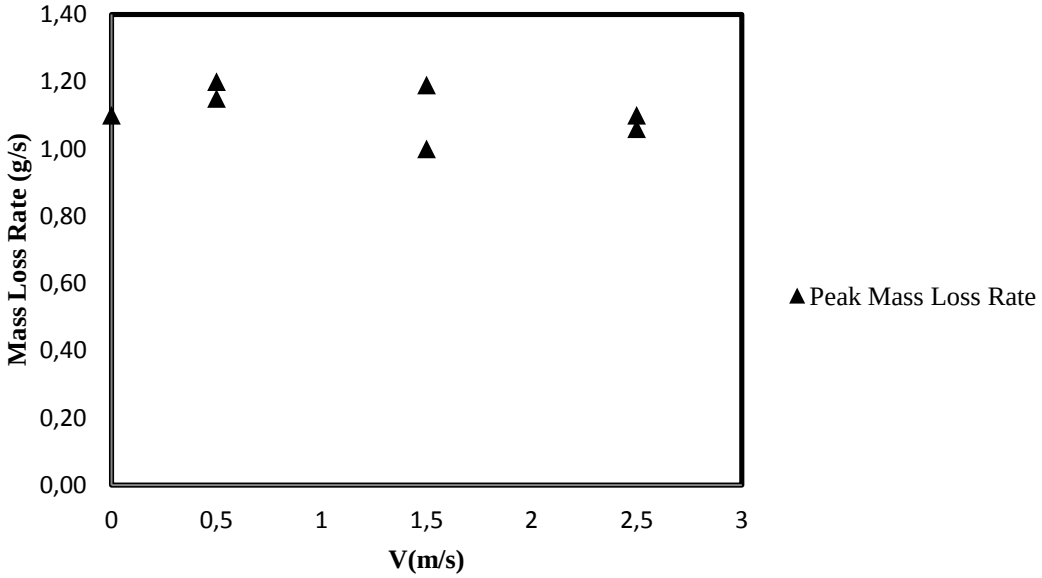

Figure 4-15 Peak mass loss rate for 200ml ethanol for different velocities in rectangle pan

What makes 0.5 m/s ventilation velocity critical in terms of mass loss rate in square pan is mostly related to physical effects of the ventilation on fire and flame. During the experiments, it is observed that at 0.5 m/s ventilation velocity, the flames of the fire are not deflected which enables those flames to heat the fuel source. However in 1.5 m/s and 2.5 m/s ventilation velocities, the flames are highly deflected and the heating and radiation effect is avoided. This is the most probable reason for the decreasing trends of mass loss rates in square pans. This reasoning also helps to explain why the same phenomenon is not observed in rectangular pans. When the flame is deflected in rectangular pan fire, the deflected flame is still mostly on the pan itself (at least 18cm longer than the square pan) which enables the rectangular pan to benefit from the deflected flame far more than square pan. Hence the same effect cannot be observed in rectangular pans.

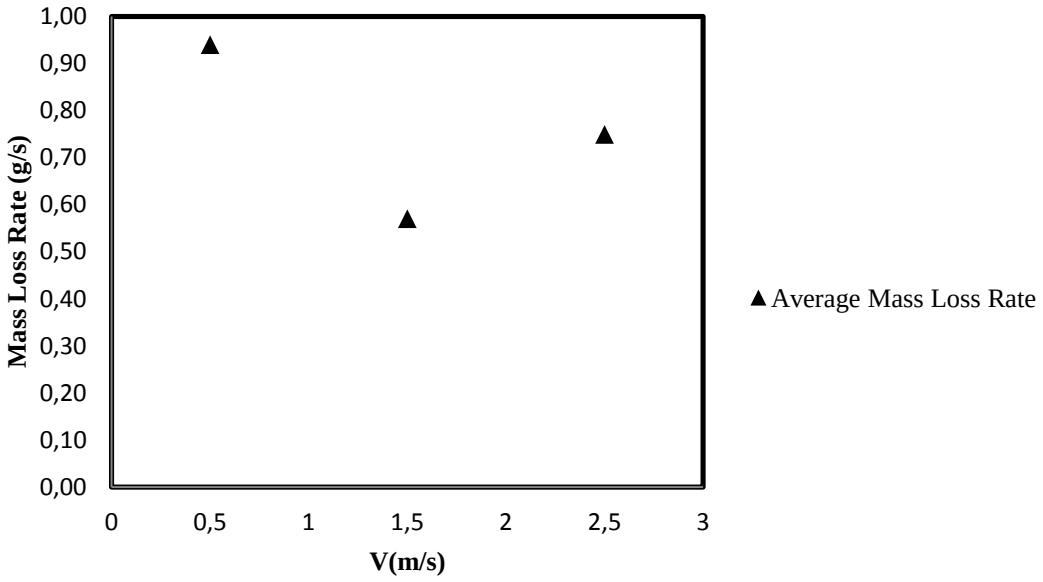

Figure 4-16 Average mass loss rate for 300ml ethanol for different velocities in square pan

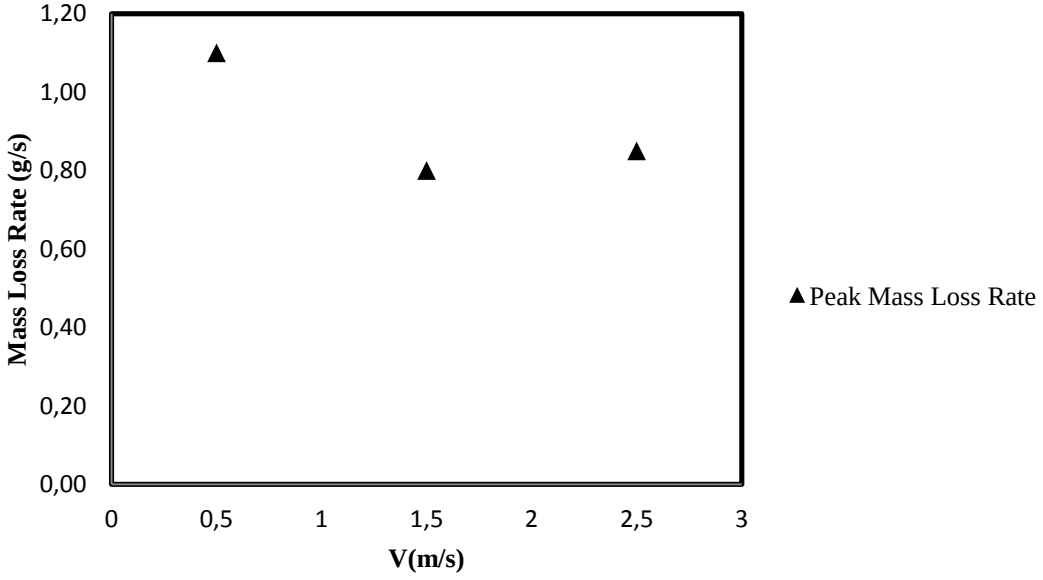

Figure 4-17 Peak mass loss rate for 300ml ethanol for different velocities in square pan

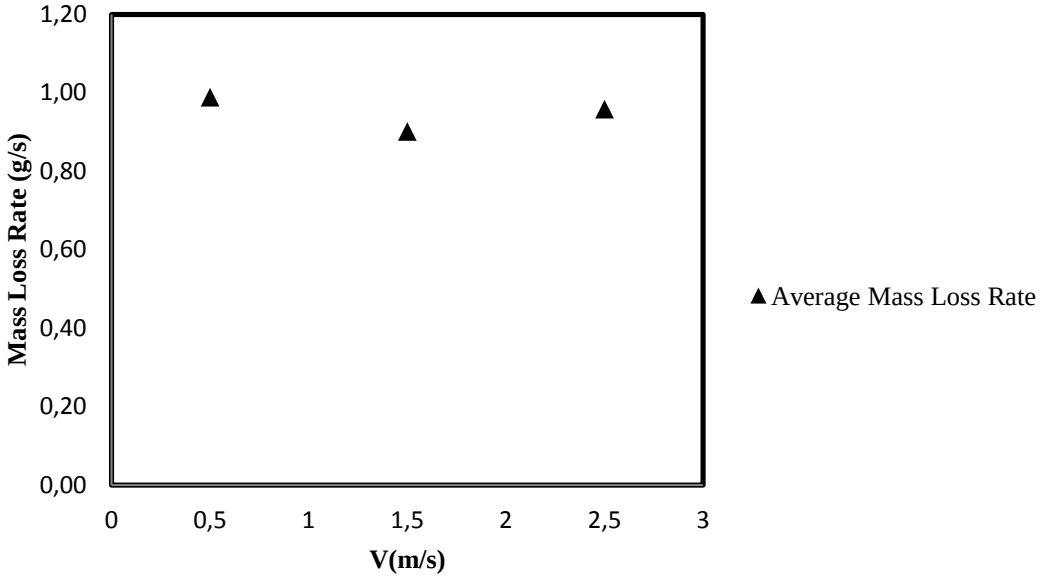

Figure 4-18 Average mass loss rate for 300ml ethanol for different velocities in rectangle pan

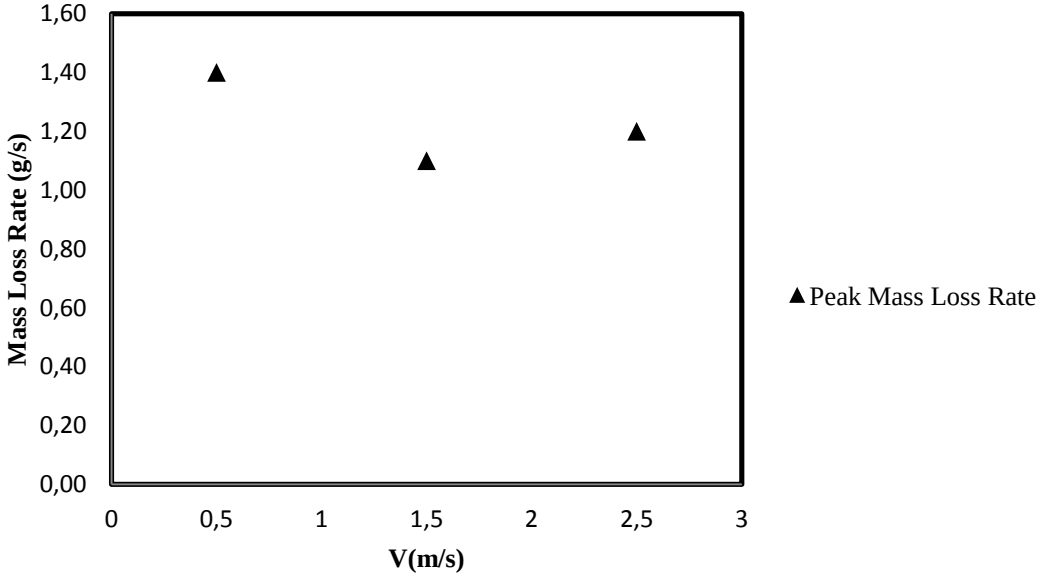

Figure 4-19 Peak mass loss rate for 300ml ethanol for different velocities in rectangle pan

The trends shows difference for the gasoline fires. For gasoline, the rectangle pan cannot avoid the decrease in mass loss rate as in Figure 4-20 and Figure 4-21 for square pan and Figure 4-22 and Figure 4-23 for rectangle pan for 200ml Gasoline.

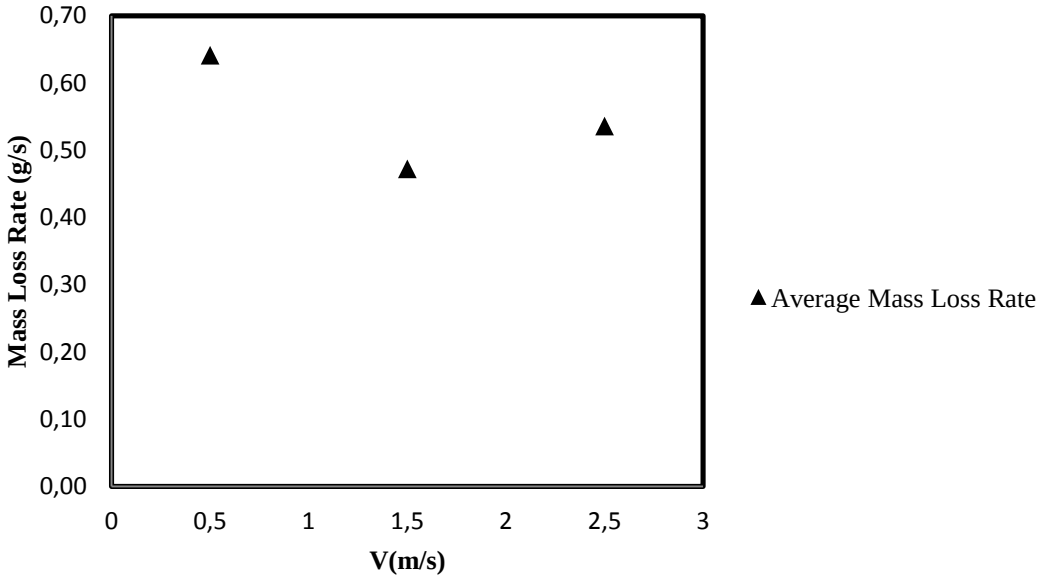

Figure 4-20 Average mass loss rate for 200ml gasoline for different velocities in square pan

As in the figures, the average and peak mass loss rates decrease after 0.5 m/s ventilation velocity in square pan as in ethanol. The main difference between these two fuel sources is observed in rectangle pan. For gasoline, the mass loss rate trend is the same with square pan which means that the mass loss rates decrease after 0.5 m/s ventilation velocity. This difference exists due to different flame characteristics of gasoline and ethanol. Ethanol has a non-luminous, low radiating flame whereas

gasoline has a luminous and highly radiating flame. Hence the flame deflection affects gasoline fire far more dramatically compared to ethanol.

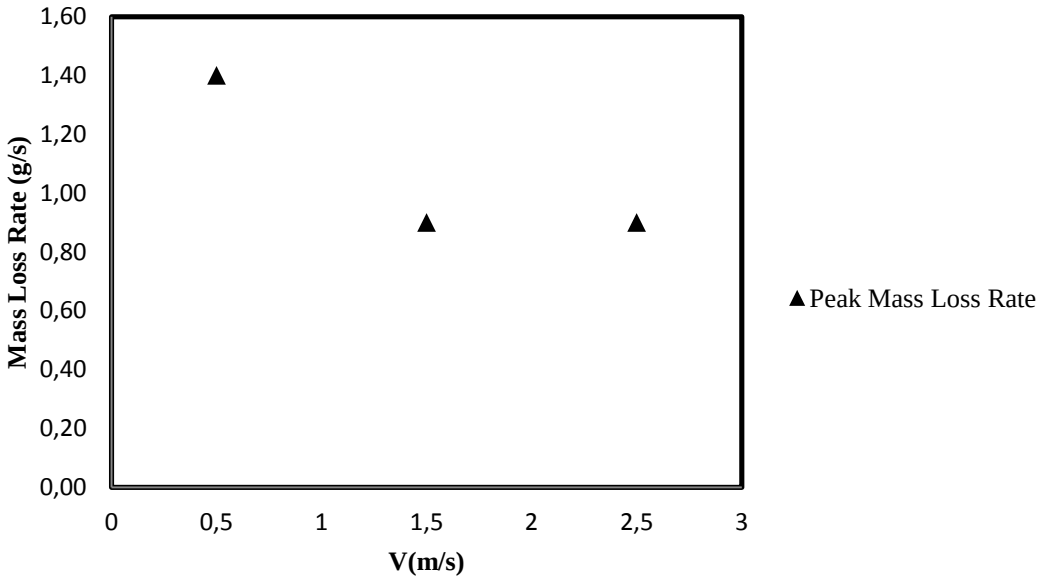

Figure 4-21 Peak mass loss rate for 200ml gasoline for different velocities in square pan

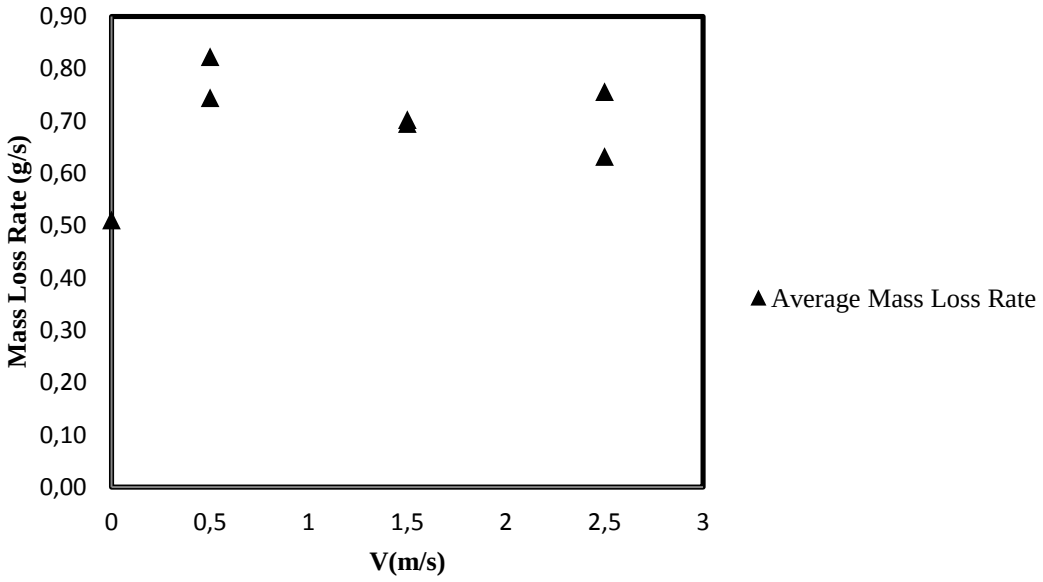

Figure 4-22 Average mass loss rate for 200ml gasoline for different velocities in rectangle pan

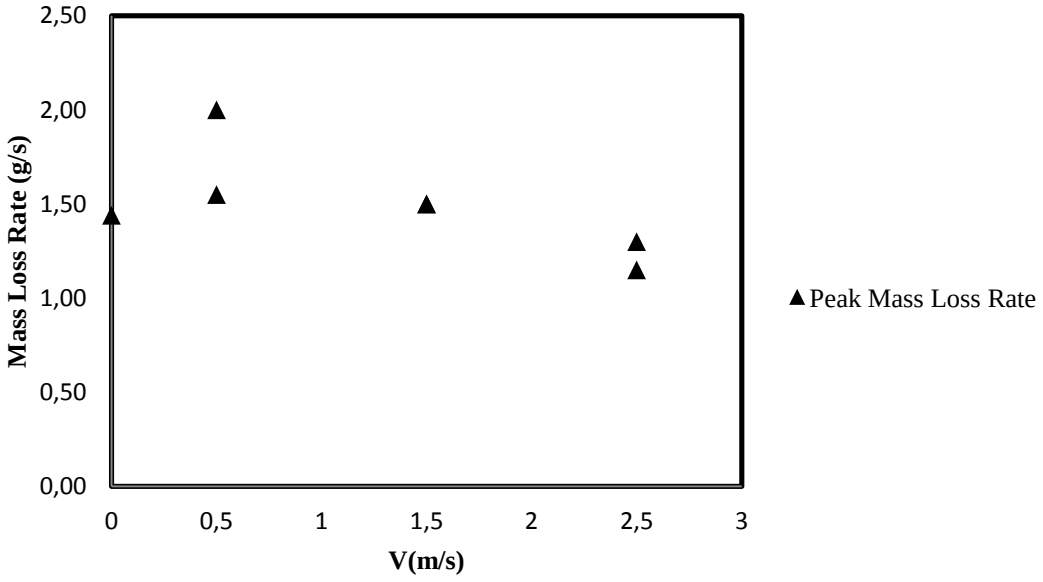

Figure 4-23 Peak mass loss rate for 200ml gasoline for different velocities in rectangle pan

The mixture is the blend of gasoline and ethanol so the burning characteristic of mixture is expected to be in between. The behavior of the blend for square and rectangular pans are shown in Figure 4-24, Figure 4-25, Figure 4-26 and Figure 4-27.

Figure 4-28 shows the effect of ventilation velocity on ethanol for different initial fuel depth in square pan. As shown in the figure, the heat release rate is nearly constant for different ventilation velocities. This means that in terms of peak heat release rate, the fire scenarios are fuel controlled. The same trend can be observed for rectangle pan as shown in Figure 4-29. The difference between the trends of mass loss rate and heat release rate may depend on the combustion efficiency of fire which means that all the fuels evaporated do not burn.

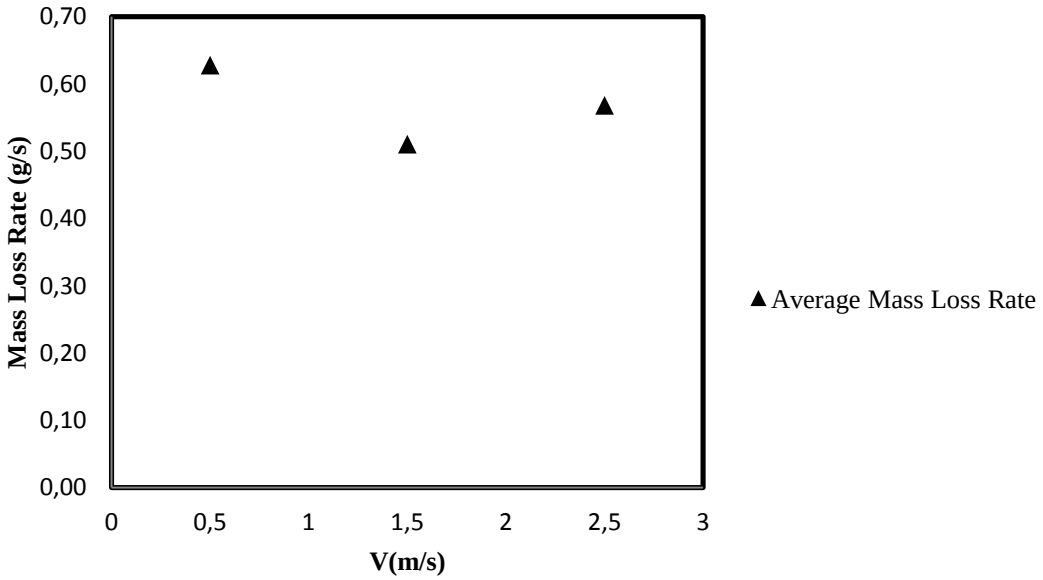

Figure 4-24 Average mass loss rate for 200ml mixture for different velocities in square pan

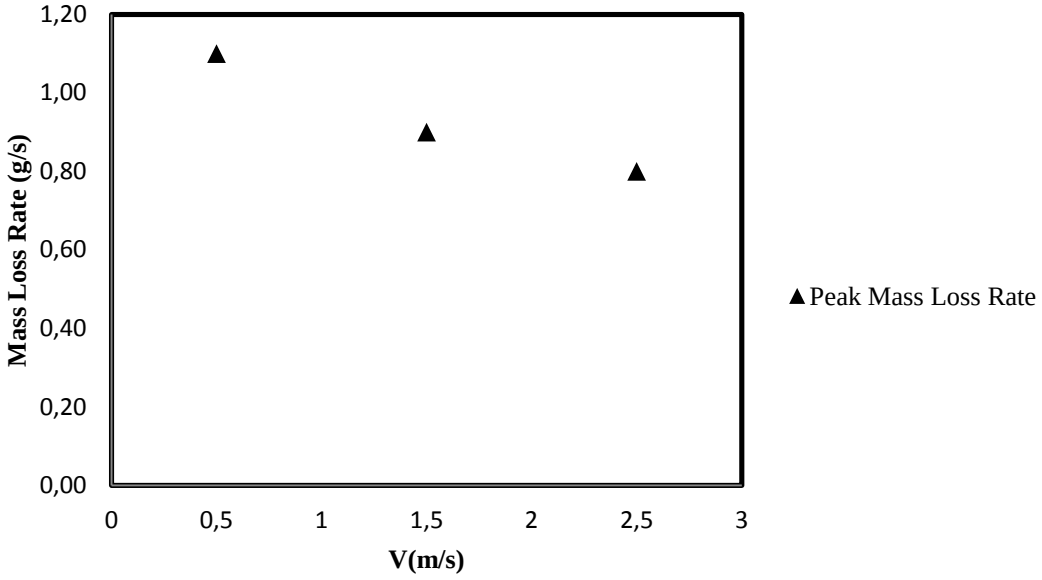

Figure 4-25 Peak mass loss rate for 200ml mixture for different velocities in square pan

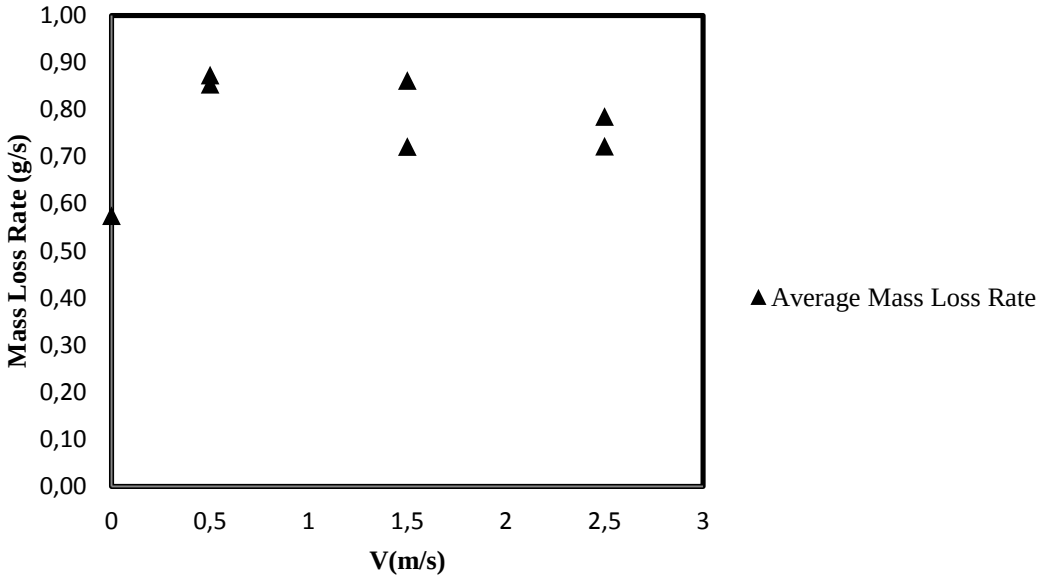

Figure 4-26 Average mass loss rate for 200ml mixture for different velocities in rectangle pan

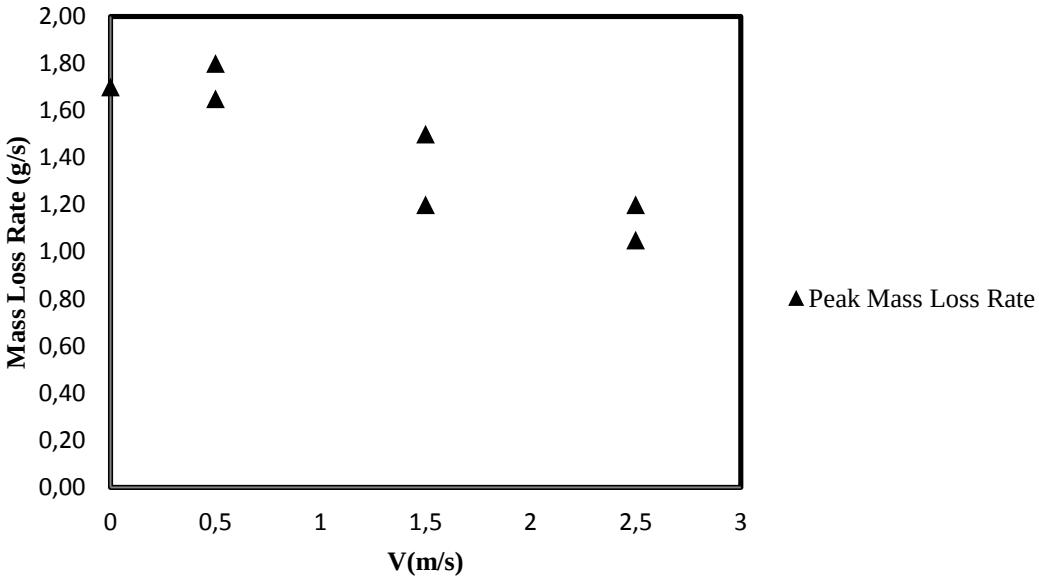

Figure 4-27 Peak mass loss rate for 200ml mixture for different velocities in rectangle pan

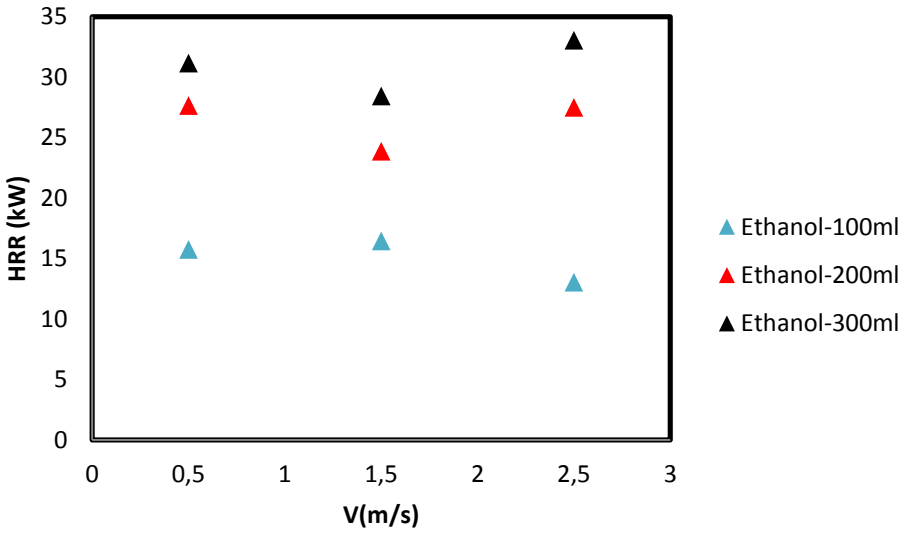

Figure 4-28 Peak heat release rate with different ventilation velocities and different amount of fuel source for ethanol in square pan

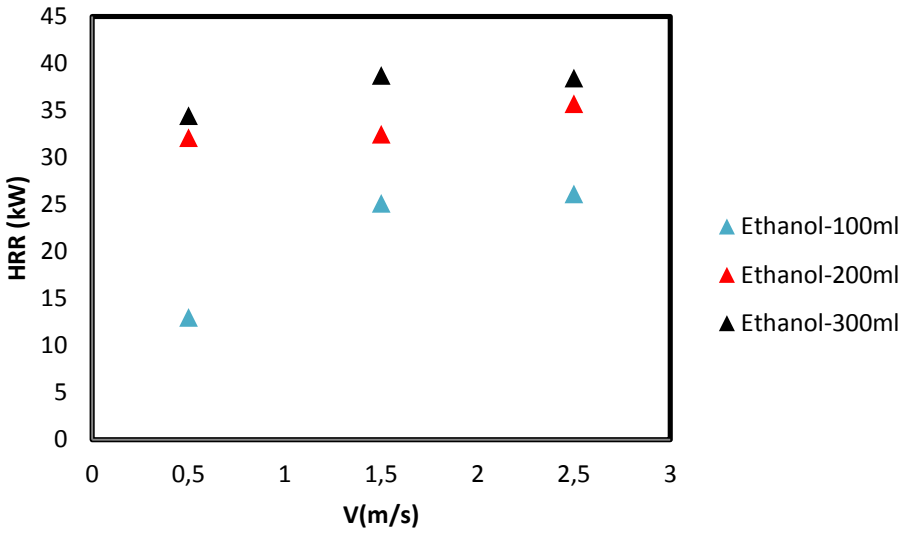

Figure 4-29 Peak heat release rate with different ventilation velocities and different amount of fuel source for ethanol in rectangle pan

4.3.4. Effect of Geometry on Mass Loss Rate and Heat Release Rate

Using the same fuel source of same initial amount for both square pan and rectangular pan for different velocities, it is observed that the mass loss flux (mass loss rate per unit area) of square pan is always greater than rectangular pan as shown in Figure 4-30 and Figure 4-31 and Figure 4-32.

As noted earlier, the confined geometry leads the square pan to have a larger depth, which would also create a more steady burning. The greater depth creates a better insulation, which leads a lower heat loss to the pan. This trend is same for all amounts of the fuels used in this study.

These results may seem to contradict with the work of Hu *et al* as in Figure 1-10. From these figures it can be concluded, that with same burning area and same initial fuel depth, the mass loss rate per unit area for rectangle and square pans do not

differ. However the burning areas in these experiments are not same i.e., 0,09 cm^2 for square pan and 0,144 $cm^2$for rectangle pan. The initial fuel depths are also different for the cases of this thesis.

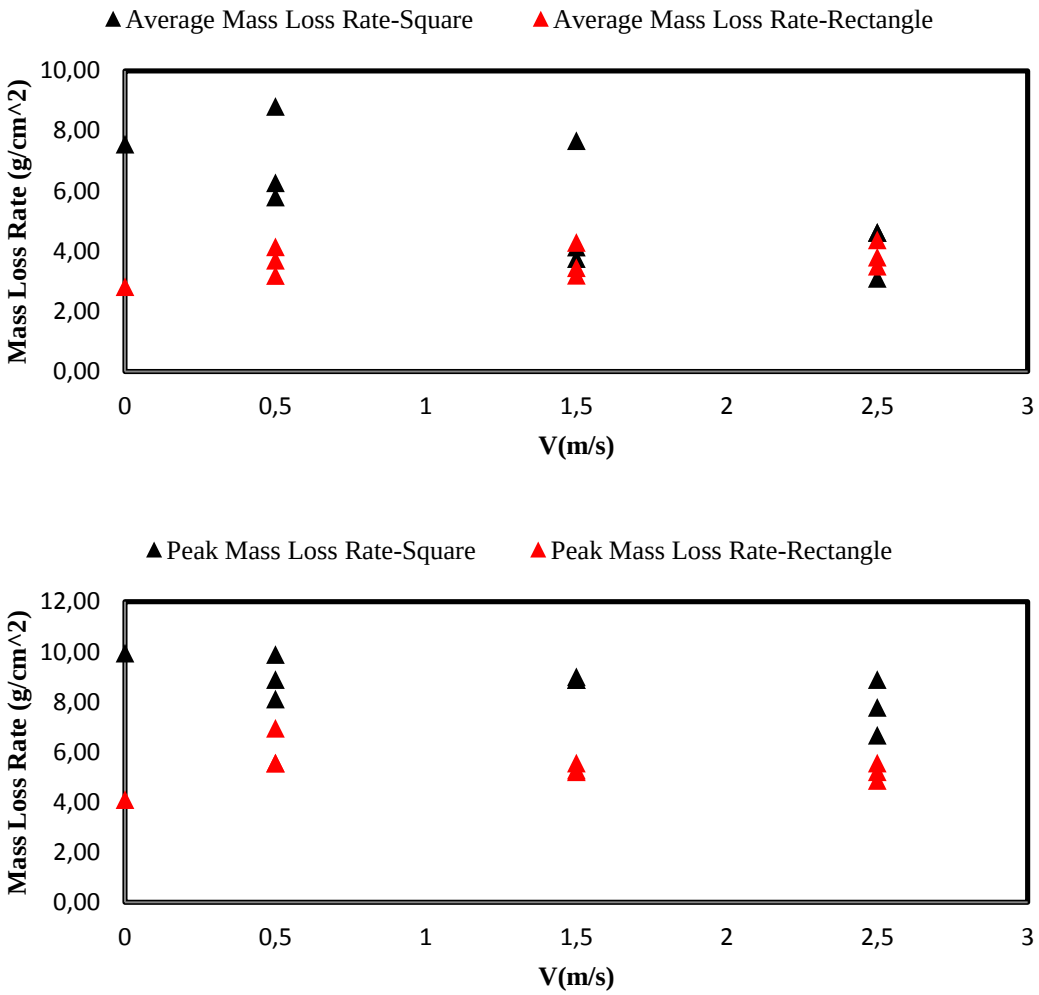

Figure 4-30 Comparison of average mass loss rate and peak mass loss rate for 100ml ethanol for square and rectangle pan.

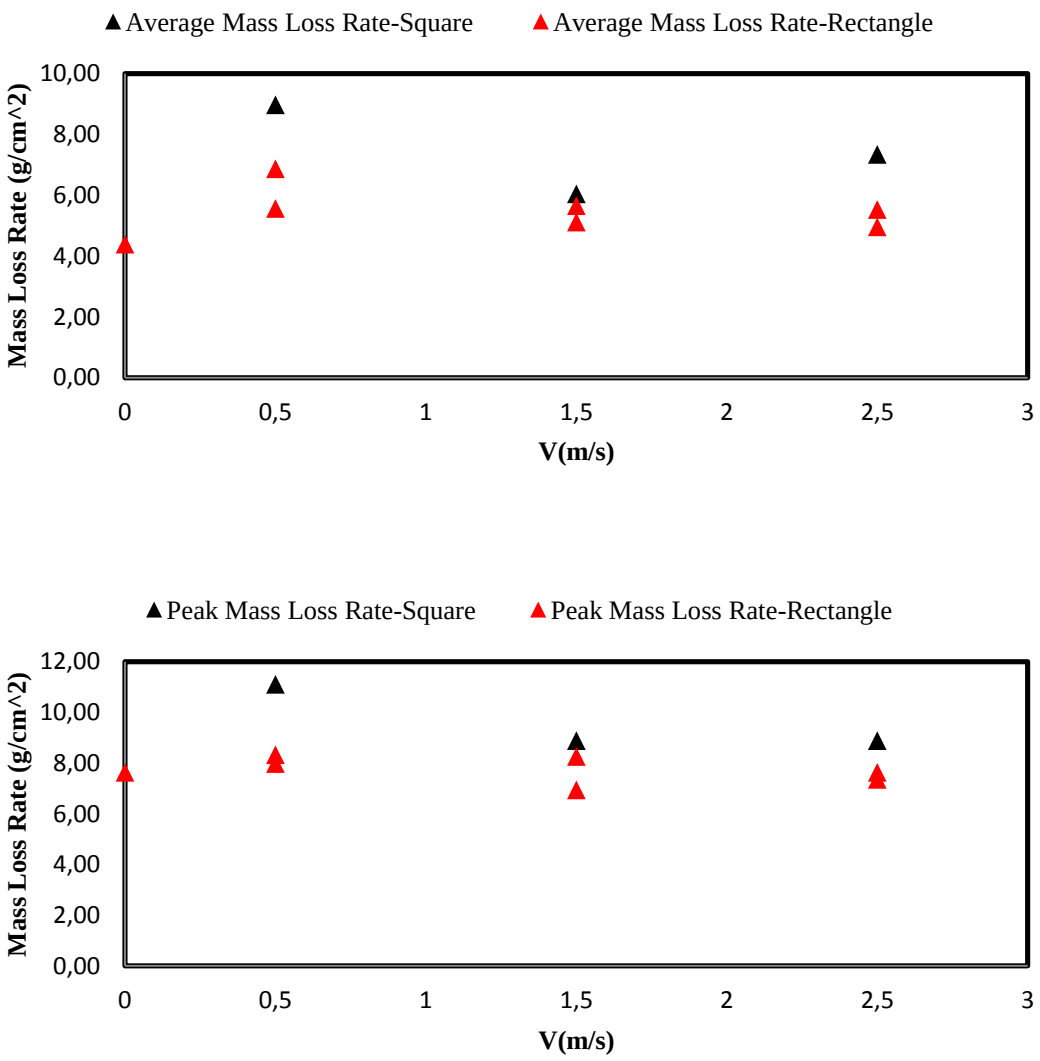

Figure 4-31 Comparison of average mass loss rate and peak mass loss rate for 200ml ethanol for square and rectangle pan.

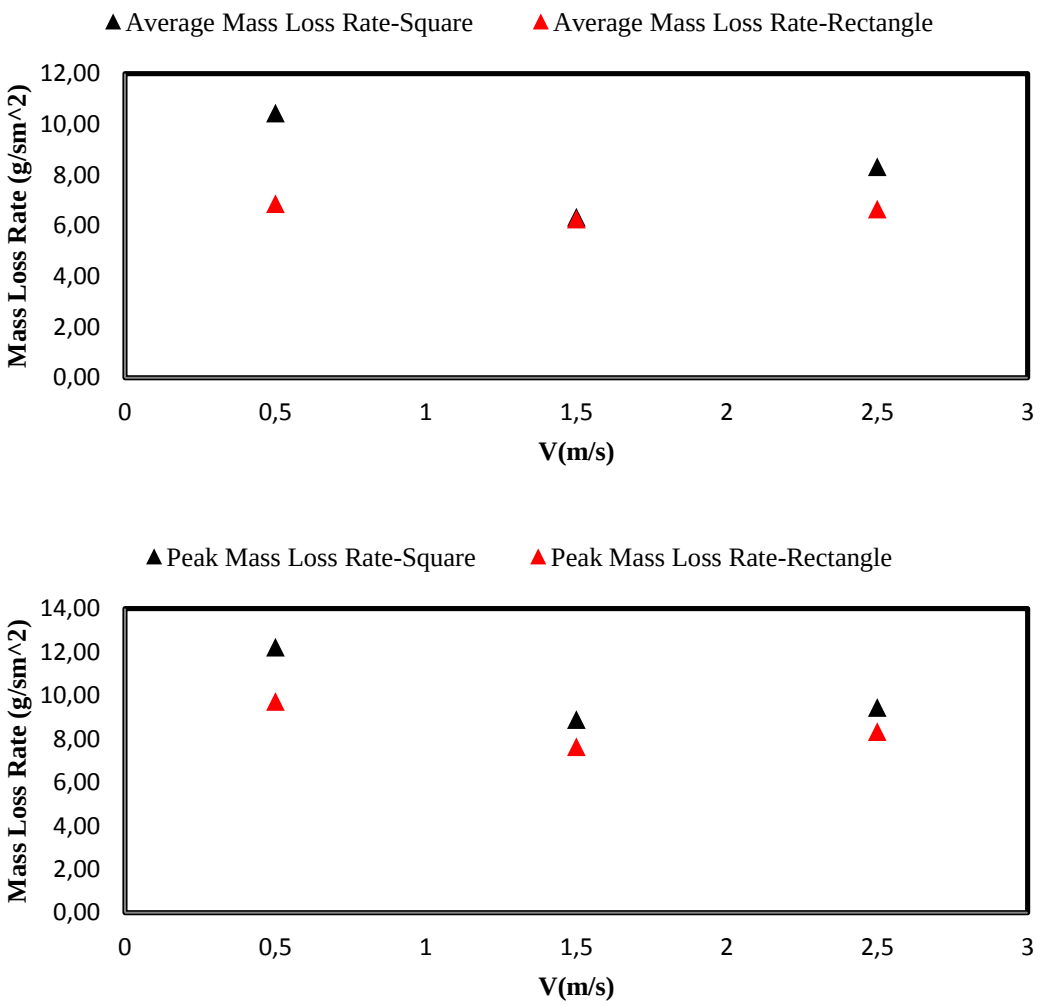

Figure 4-32 Comparison of average mass loss rate and peak mass loss rate for 300ml ethanol for square and rectangle pan.

In terms of heat release rate, the most important parameter is the peak heat release rate. Form this point of view, the rectangle has higher heat release rates since the fuel consumed per unit time is higher. However, if the heat fluxes are compared, the trends are similar to those of mass loss rate trends i.e., the heat release rate per unit area is higher in square pans as in Figure 4-33.

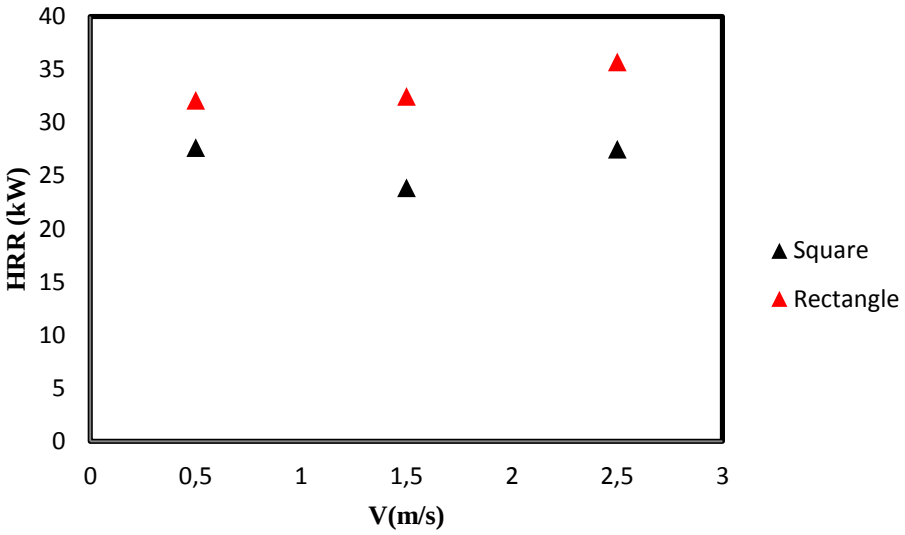

(a)

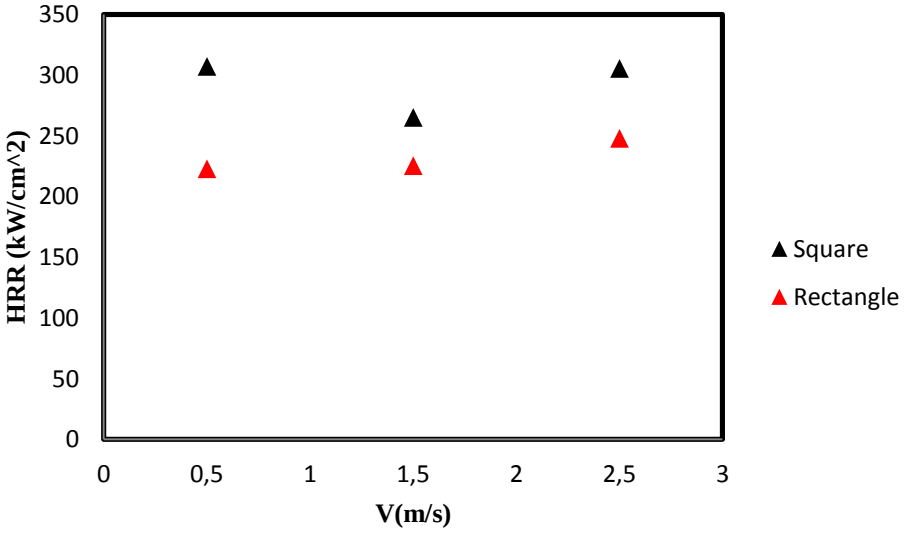

(b)

Figure 4-33 Comparison of (a) peak heat release rate (b) peak heat flux of 200 ml ethanol in square and rectangle pans for different values of ventilation velocity

4.3.5. Effect of Fuel Source on Mass Loss Rate and Heat Release Rate

Three different type of fuel is used in the experiments. These fuels are ethanol, gasoline and a mixture (70% gasoline + 30% ethanol) of these two fuels. Under different ventilation conditions the mass loss rate and heat release rate characteristics of these fuels are investigated.

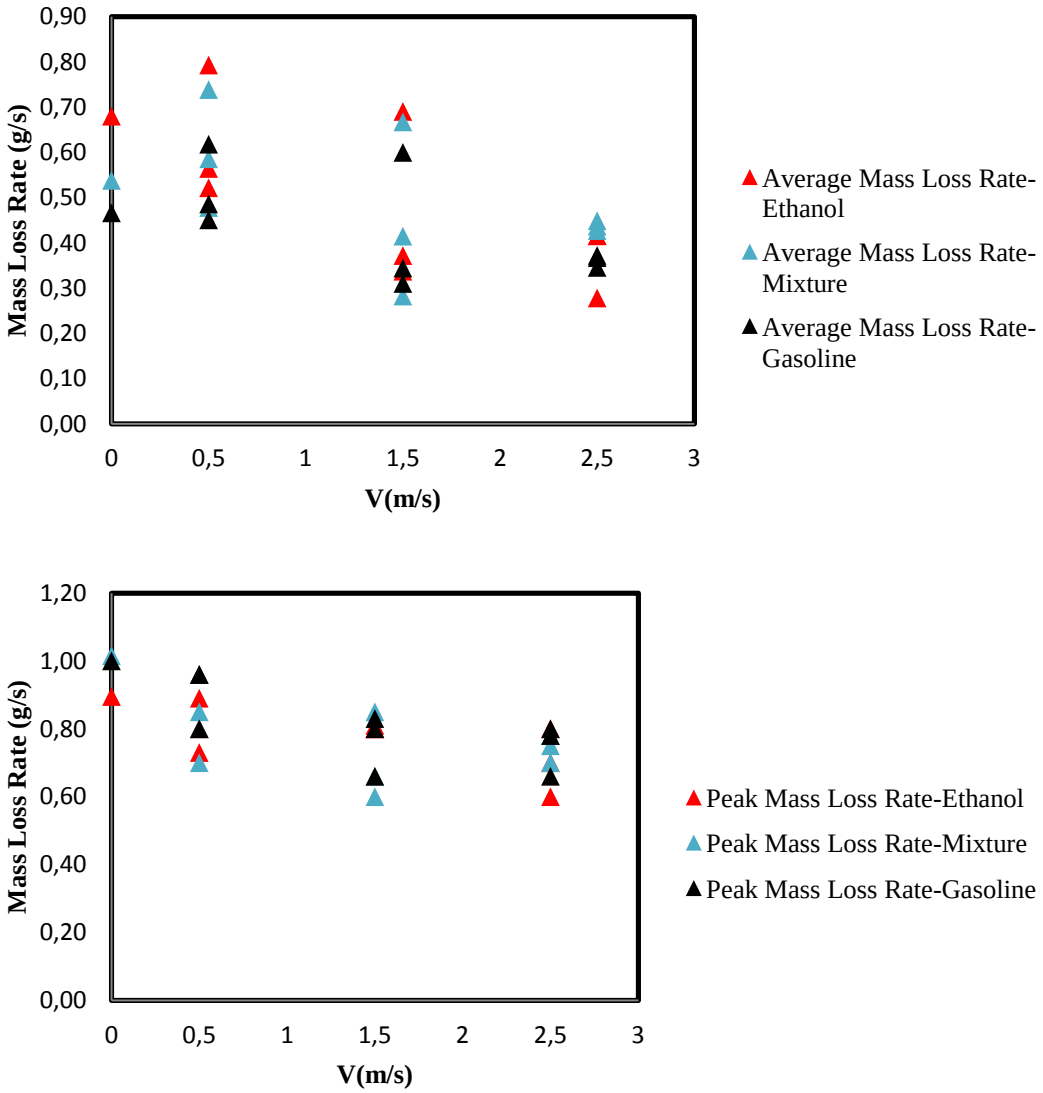

Figure 4-34 Average and peak mass loss rate for different 100ml fuel source for different ventilation velocities is square pan

As in Figure 4-34 for average mass loss rate values ethanol is the largest, whereas the trend of gasoline is the lowest with keeping the mixture in between. The trend is completely different in terms of peak mass loss rate where ethanol has the lowest peak mass loss rate values and gasoline with highest. These trends become clearer with increased fuel source as in Figure 4-35.

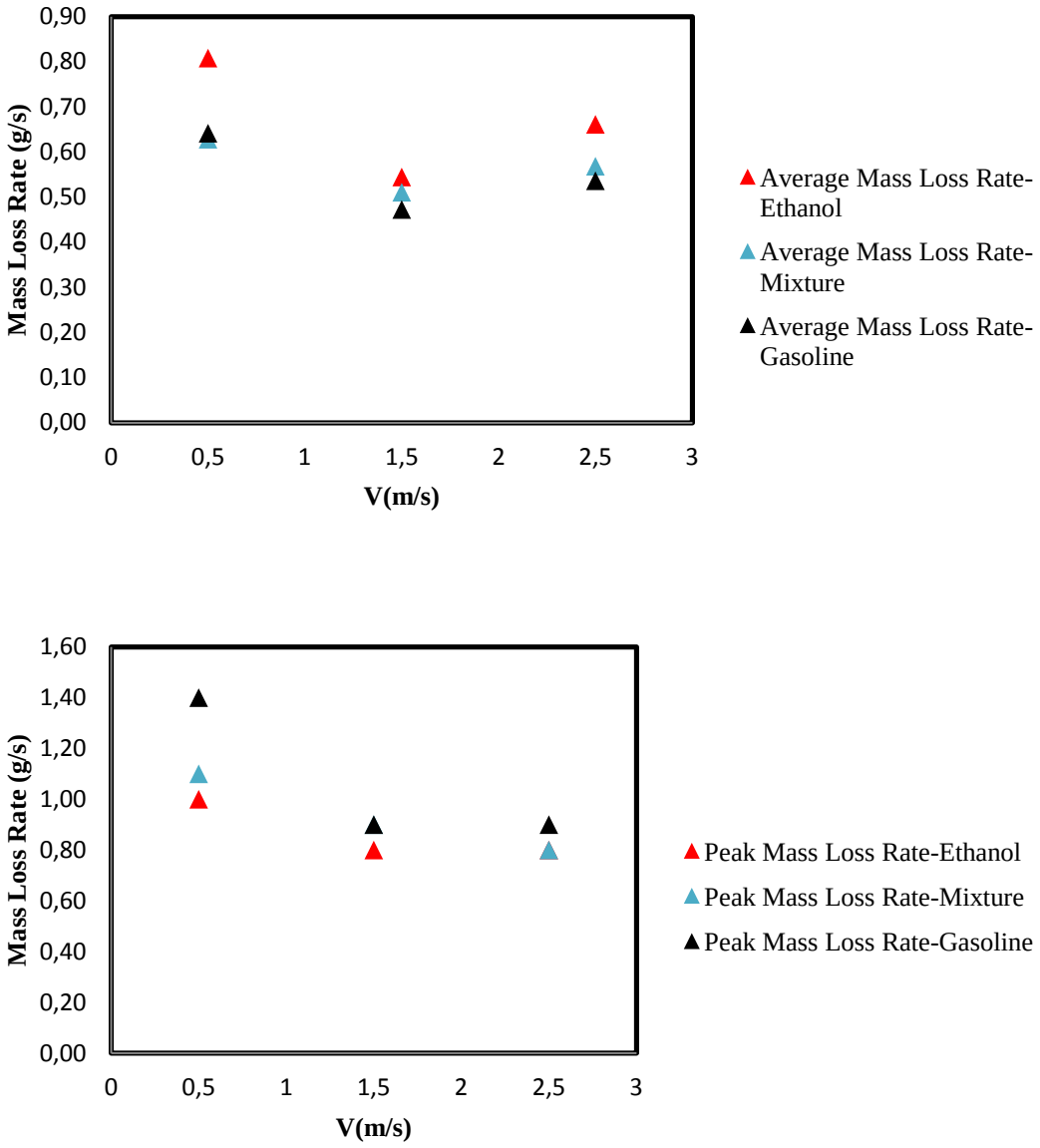

Figure 4-35 Average and peak mass loss rate for different 200ml fuel source for different ventilation velocities is square pan

Yet another important issue to be underlined is, although higher burning rates are expected for gasoline, the experimental results showed a different picture. The averaging methods are by dividing the burned fuel mass to consumed time for full combustion. Although gasoline has higher peak values for burning, ethanol has a steadier burning trend as seen in Figure 4-36.

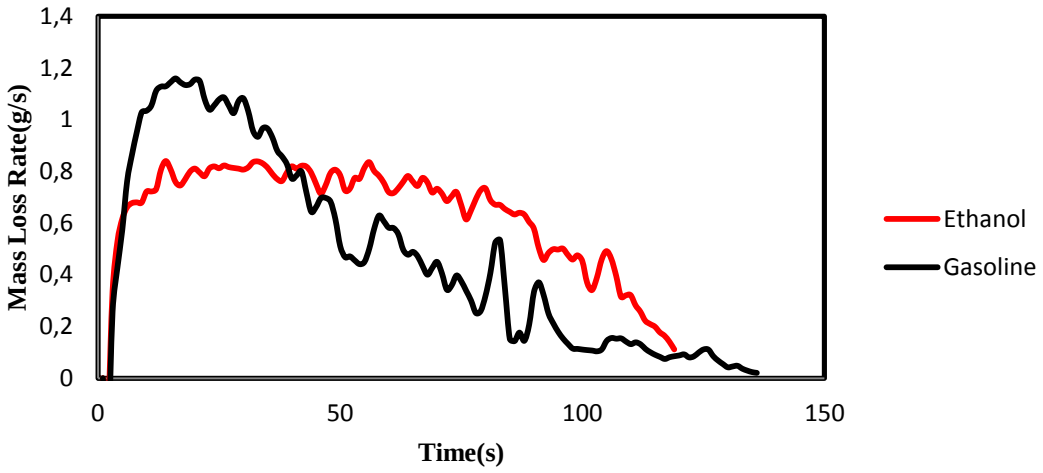

Figure 4-36 Time history of mass loss rate for ethanol and gasoline

The average and peak mass loss rate trends observed in square pans (Figure 4-34 and 4-35) does not change in rectangle pan as in Figure 4-37. This trend is mostly dominated with the heat of combustion of each fuel source. Since gasoline has the highest heat of combustion among other fuel sources with highly radiating flame, the feeding of the fuel source is more and the highest peak value is observed in gasoline. However in average ethanol has higher values since it burns more steadily in terms of mass loss rate as in Figure 4-36.

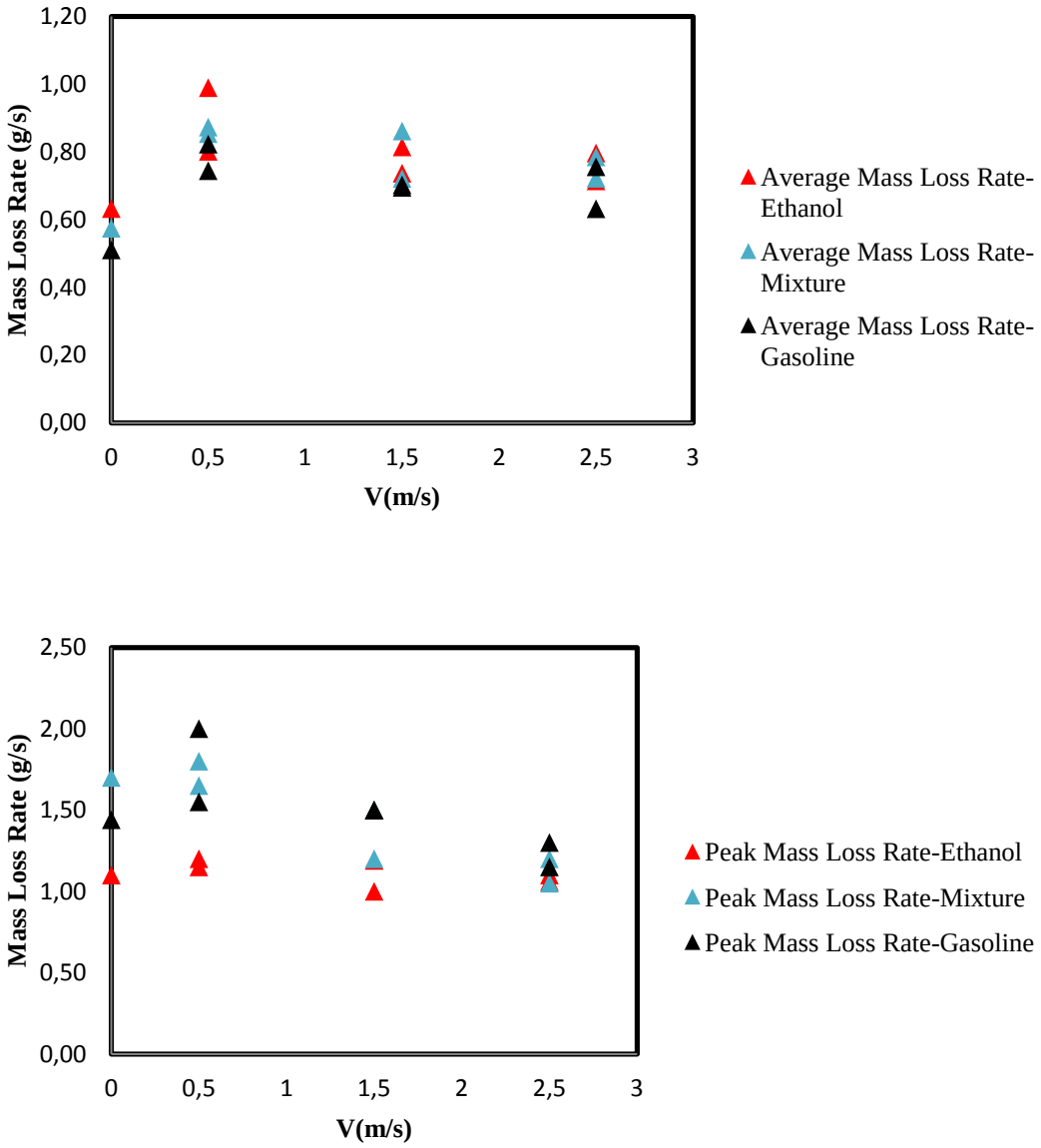

Figure 4-37 Average and peak mass loss rate for different 200ml fuel source for different ventilation velocities is rectangle pan

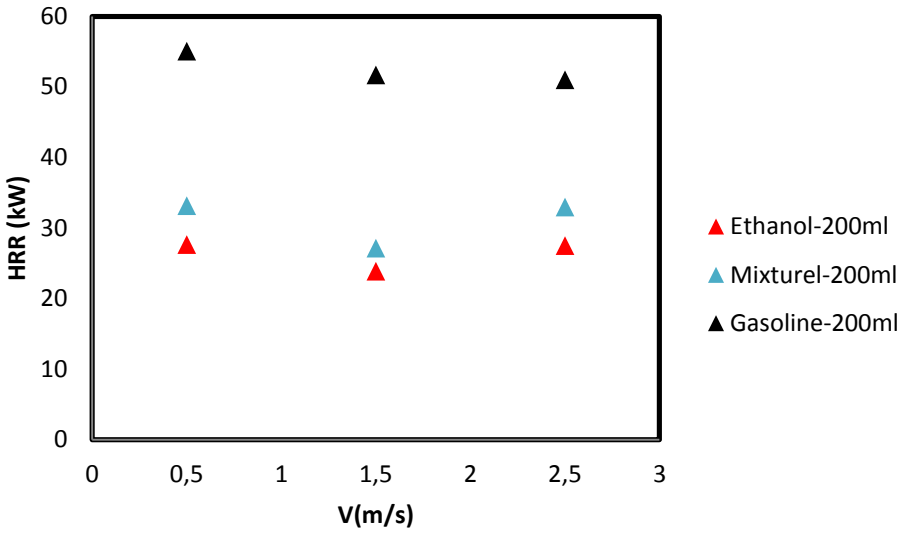

(a)

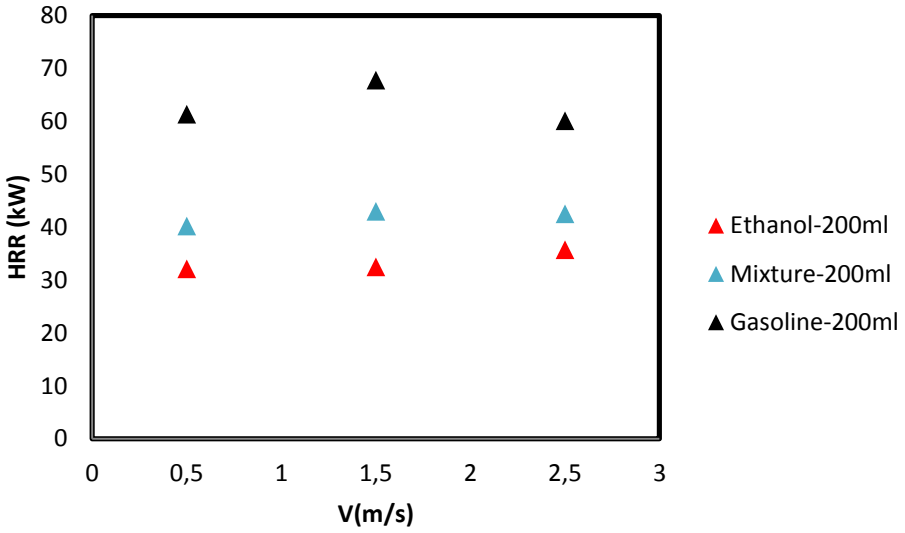

(b)

Figure 4-38 Peak heat release rate values for 200ml fuel source in (a) square (b) rectangle pan

4.3.6. Effect of Initial Fuel Source Amount on Mass Loss Rate and Heat Release Rate

In SFPE Handbook of Fire Protection Engineering, it is noted that having a deep fuel layer of a pool and hence keeping burning surface as far as possible from solid pan serves as a good insulator to the top fuel surface during burning. The main reason is because most of the solid materials would have an higher thermal conductivity (15.1 W/ mK for steel and 0.11 for gasoline at 300K [34])than the fuel, resulting in the fuel surface heating up more quickly, and in turn vaporizing and burning at a higher rate.

The increasing trend of average and peak mass loss rate for increased amount of initial fuel is observed in Figure 4-39 and 4-40. The same trend was also observed in the works of Benfer as shown in Figure 1-12 [39] and Garo *et al* [20] in Figure 1-11. The depth of the pool can only be increased up to a certain value in this study hence the discussion for the higher initial fuel depth in the work of Garo *et al* cannot be done here.

The effect of initial fuel amount on heat release rate under different ventilation conditions can be seen in Figure 4-28 and Figure 4-29. These results are consistent with mass loss rate values. Although the efficiency of combustion is not known, increasing the initial fuel volume increases the thermal insulation between fire and pan which creates a steadier burning.

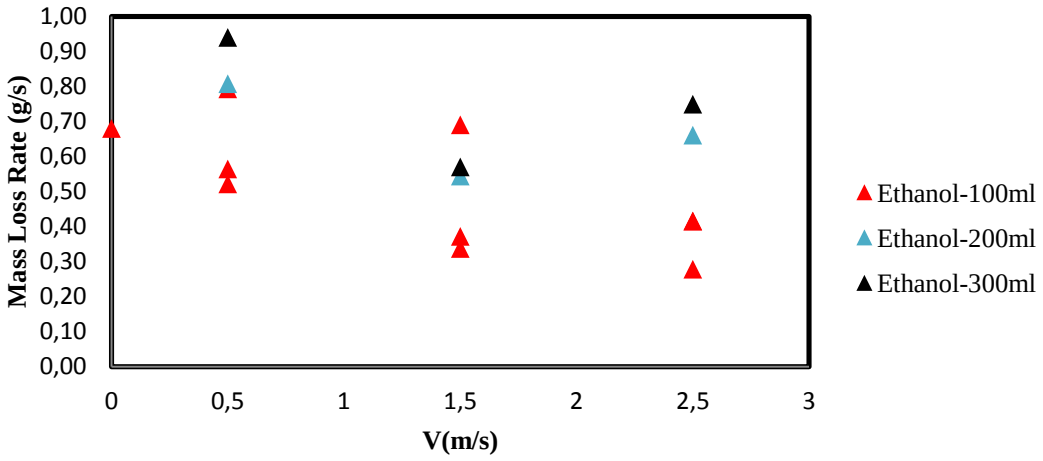

(a)

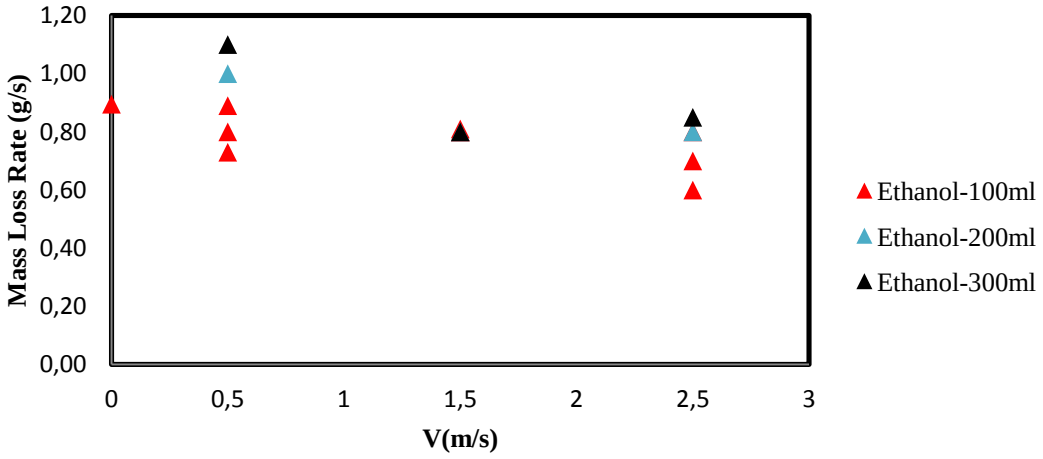

(b)

Figure 4-39 (a) Average and (b) peak mass loss rate for different velocities for different amount of ethanol sources in square pan

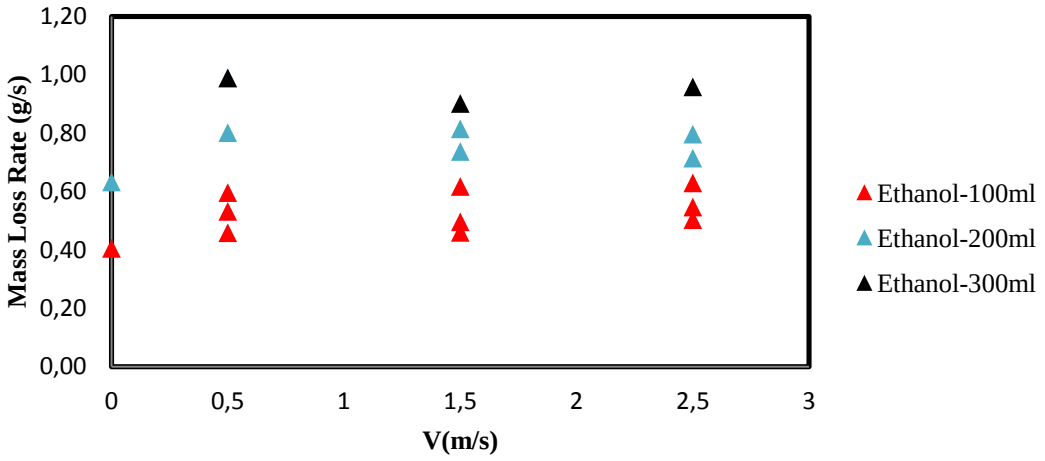

(a)

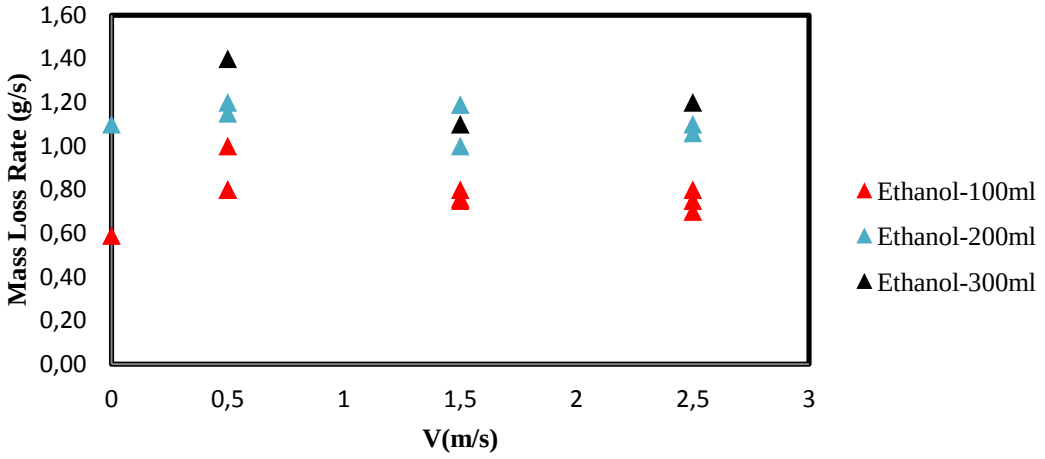

(b)

Figure 4-40 (a) Average and (b) peak mass loss rate for different velocities for different amount of ethanol sources in rectangle pan

CHAPTER 5

NUMERICAL MODELLING

Numerical modeling is done with FDS. The real tunnel geometry is not directly simulated in the FDS, since the code do not have a capability to create circular geometries. The tunnel is approximated as a rectangular cross –section.

For the tunnel pool fire simulations, the same tunnel geometry is used. The primary objective was to simulate the ethanol fire only and then to add gasoline to the fuel. Indeed the code writers of the FDS do not recommend using FDS to simulate the liquid pool fires. The simulation can be done by two ways. The first one is to use the liquid ethanol fuel definition in FDS. By this method the top surface of the pan is defined as the burner surface with ethanol. The volume, where it refers to the thickness for a fixed surface area, is defined. In the second method instead of defining a continuous medium for liquid, particles are defined. By injecting these particles with desired flow rate, the behavior of the liquid fire is simulated. In this method thermo physical and thermo chemical properties of the particles are defined by the user.

The tunnel geometry used in the simulations is shown in Figure 5-1. Nozzle or sprinklers are used to inject particles into tunnel. 204000 grid cells are used in the simulations which creates cubic cells with 1cm sides. Figure 5-2 shows the grids and 5-3 shows the particle injection to the pan. A typical fire simulation is shown in Figure 5-4.

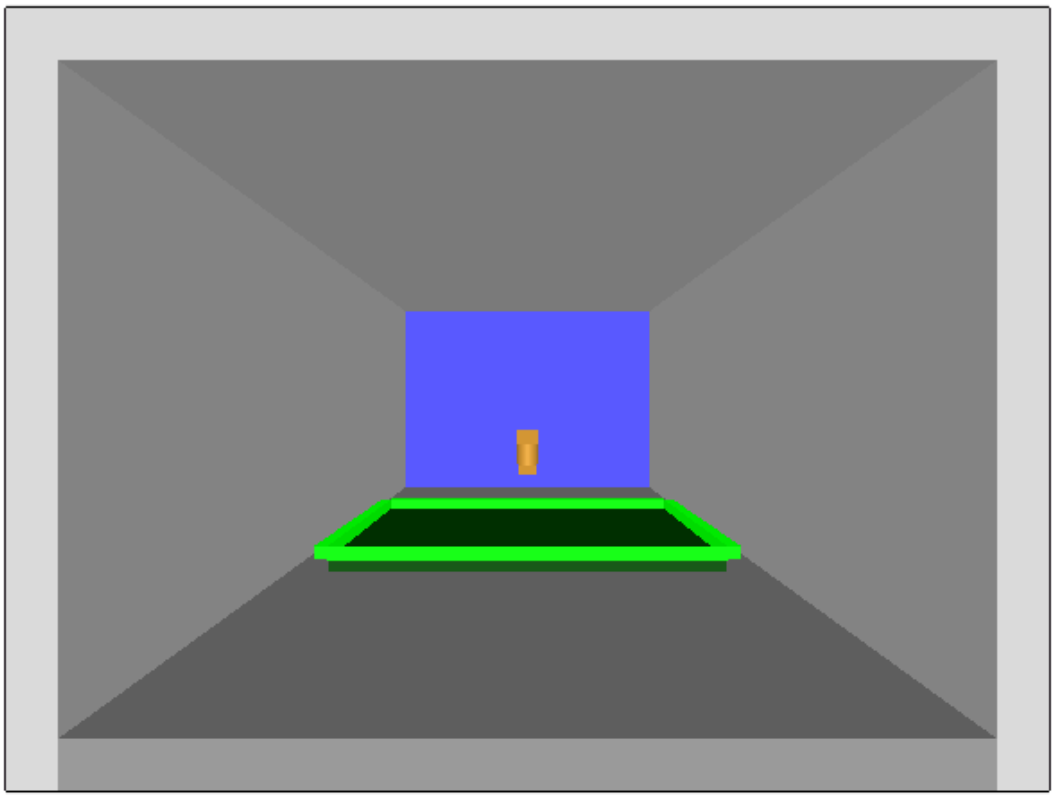

Figure 5-1 Tunnel Geometry and nozzle location for pool fire

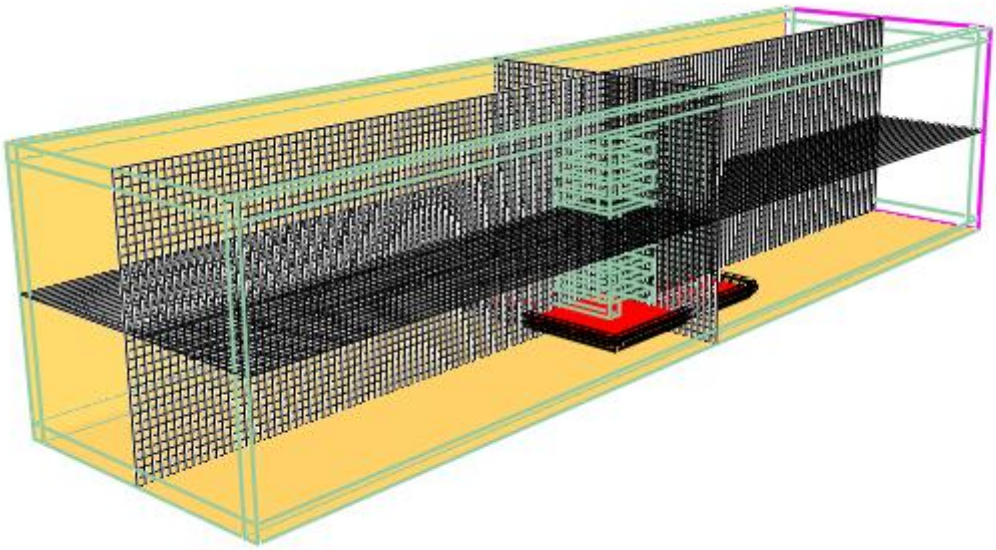

Figure 5-2 Tunnel Geometry with grids

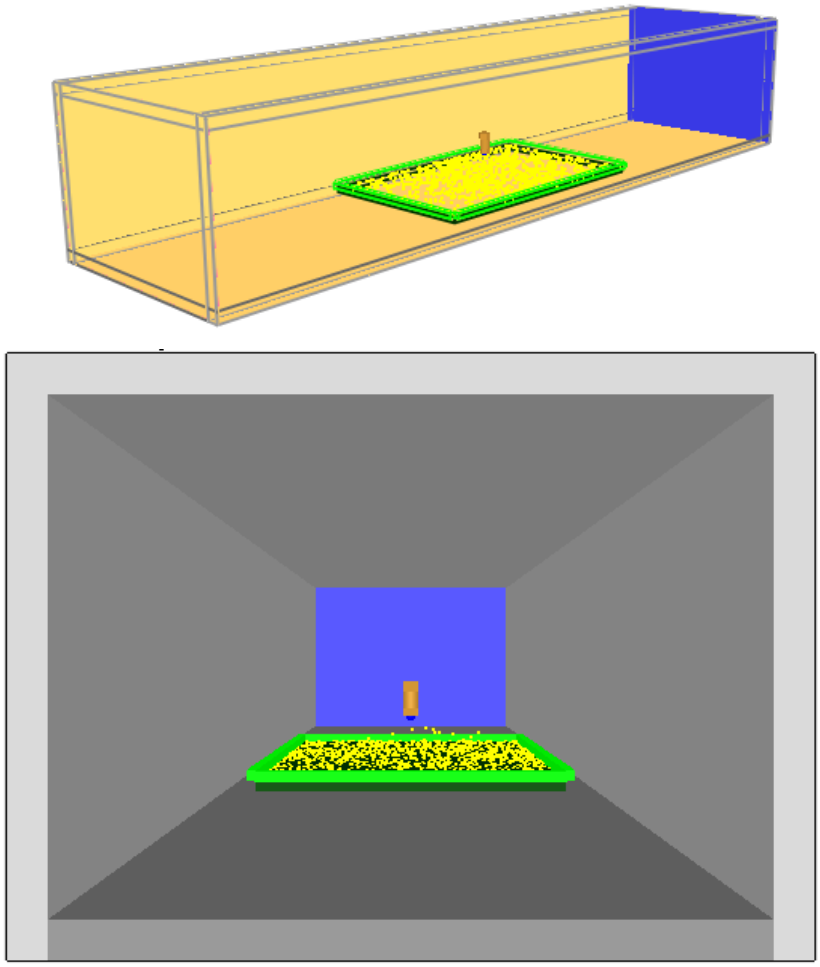

Figure 5-3 Particles injected by nozzle

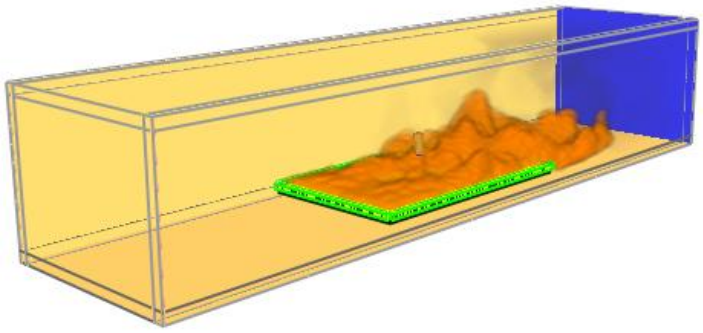

Figure 5-4 Visualization of flame and soot for 300ml ethanol with 2.5m/s ventilation velocity in a rectangle pan in FDS

Ethanol fires are chosen as case studies and FDS is used to simulate the experiments. Ethanol properties are defined in FDS library; hence the thermal properties are not modified.

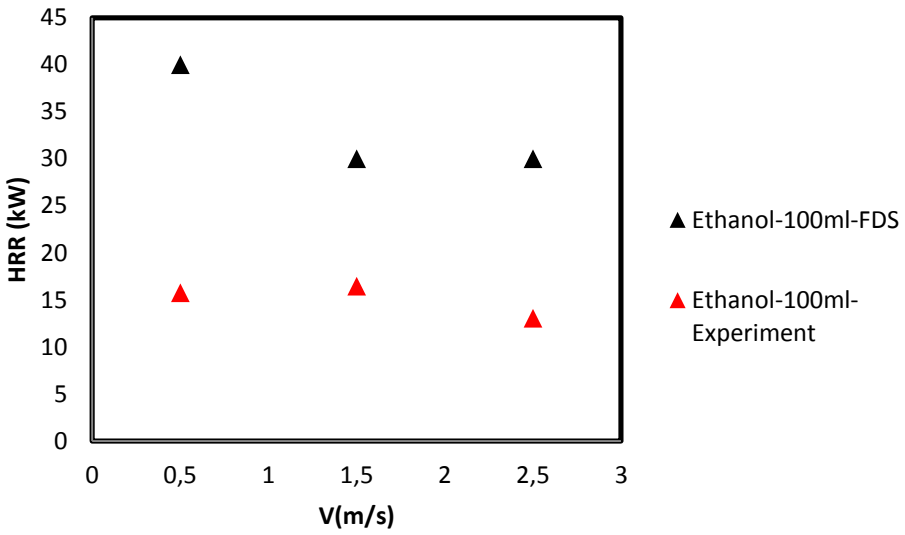

Figure 5-5 Comparison of peak heat release rate of FDS and Experiment for 100ml ethanol for varying velocities in square pan

One end of the tunnel is set to the atmospheric conditions and the other end is set to desired ventilation velocity. The tunnel walls are set to ambient temperature and defined as insulated which avoids heat transfer out of the tunnel.

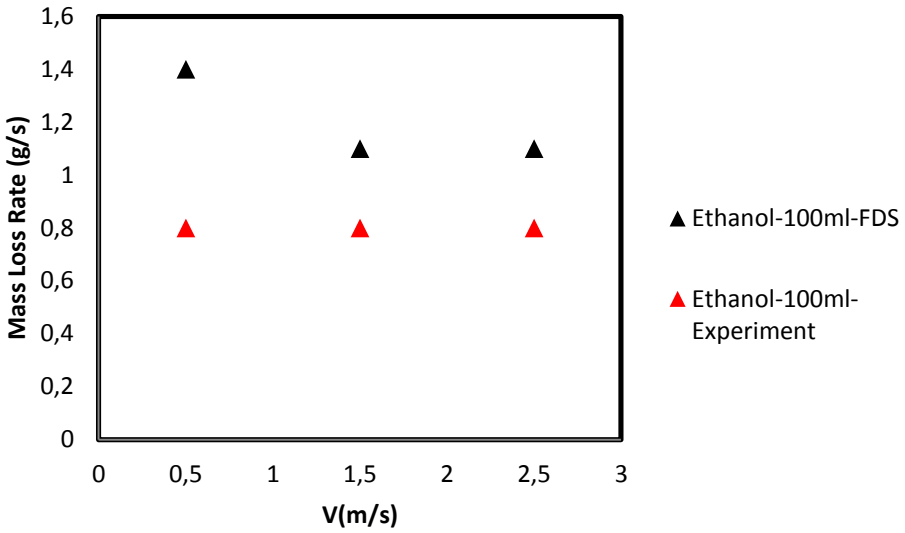

Figure 5-6 Comparison of peak mass loss rate of FDS and experiment for 100ml ethanol for varying velocities in square pan

As it is seen in Figure 5-5, Figure 5-6, Figure 5-7 and Figure 5-8 FDS is able to catch the trend of mass loss rate and HRR or 100ml ethanol square pan and 300ml ethanol in square pan however, there is a variation in the magnitude It should be noted that liquid pool fires are still under development for FDS. Both mass loss rate and HRR values cannot be simulated by FDS with high accuracy..

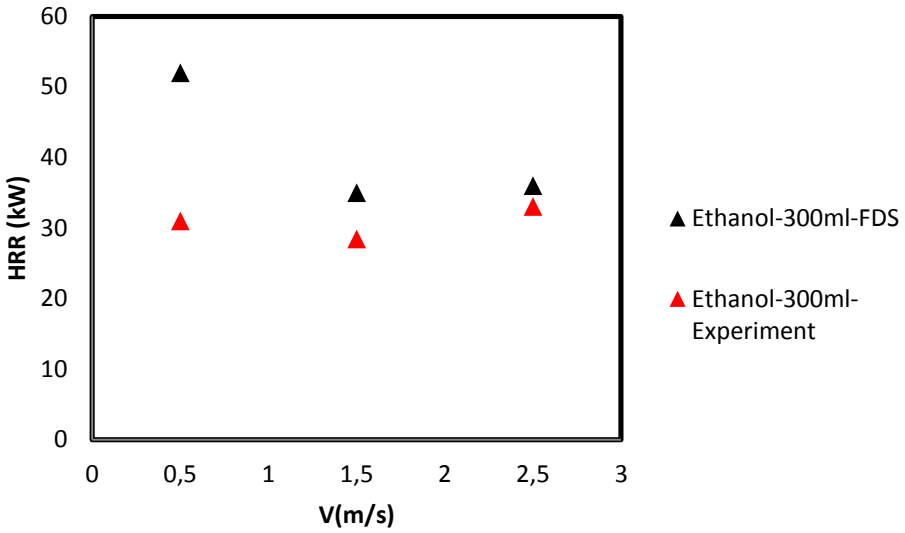

Figure 5-7 Comparison of peak heat release rate of FDS and experiment for 300ml ethanol for varying velocities in square pan

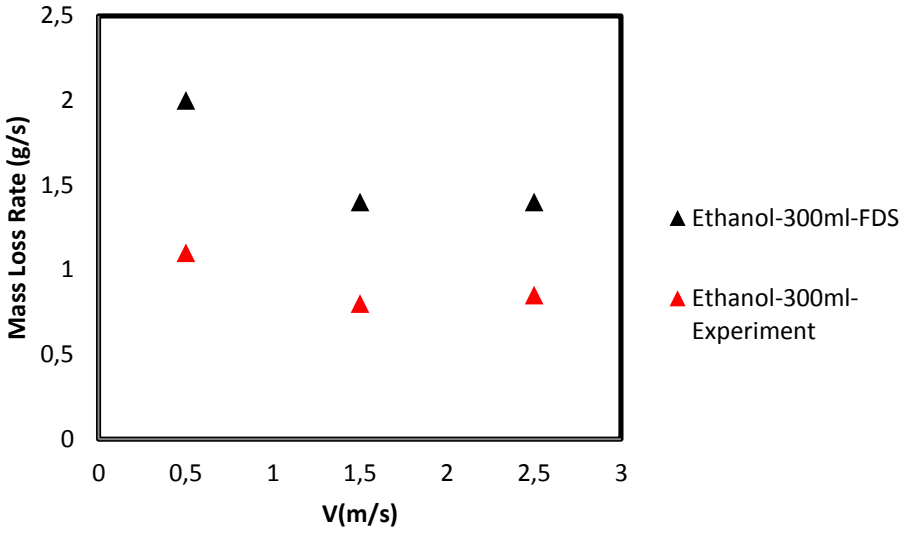

Figure 5-8 Comparison of peak mass loss rate of FDS and experiment for 300ml ethanol for varying velocities in square pan

In Figure 5-9 and Figure 5-10, 300 ml ethanol burning experiments in rectangle pan and its FDS simulation results are presented. It is clear that FDS is able to catch the trend of fire behavior under different ventilation conditions, however there is a variation in the magnitudes again.

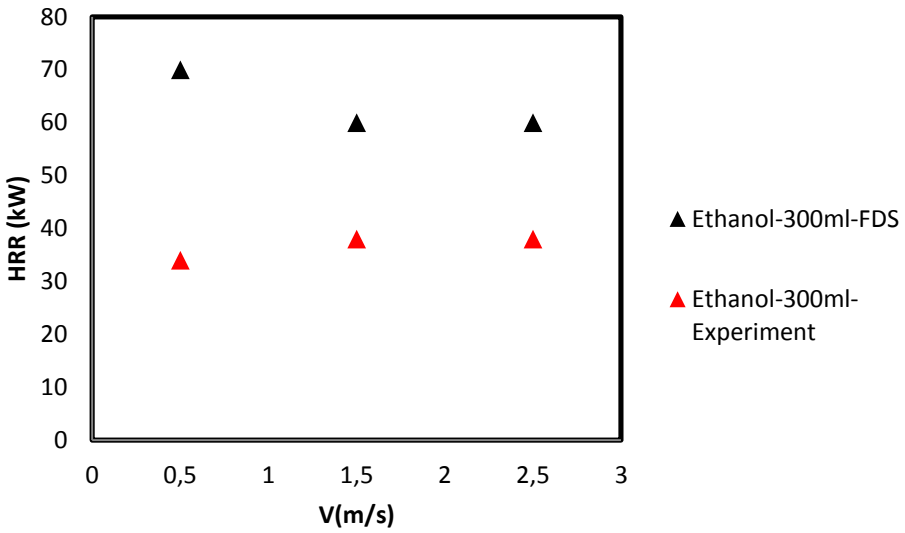

Figure 5-9 Comparison of peak heat release rate of FDS and experiment for 300ml ethanol for varying velocities in rectangle pan

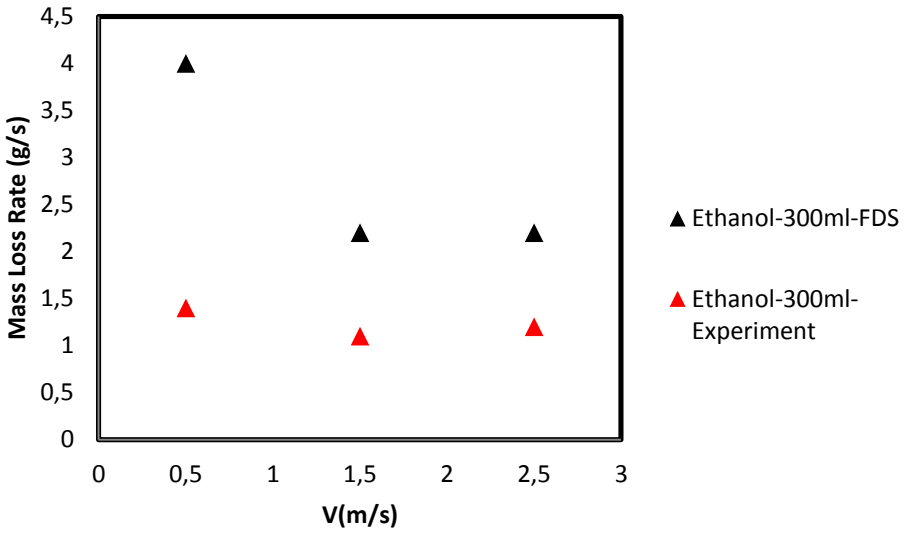

Figure 5-10 Comparison of peak mass loss rate of FDS and experiment for 300ml ethanol for varying velocities in rectangle

CHAPTER 6

CONCLUSION

In this study the burning behavior of three different liquid fuel sources are investigated in a scaled tunnel for varying conditions, i.e., ventilation velocity, fuel source, initial fuel amount and pan geometry. For velocity variation, 0.5m/s, 1.5m/s and 2.5m/s are used. Fuel amounts are 100ml, 200ml and 300ml. Two pan geometries are used; 30 cm x 30 cm and 30 cm x 48 cm for square and rectangle form respectively. For liquid pool fire source, ethanol, gasoline and mixture of ethanol and gasoline are chosen since ethanol and ethanol mixtures are being investigated as an alternative liquid fuel source. The experimental conditions studied in this thesis differ from literature in three ways. First of all the scale of burning area to tunnel cross section is too high in this study. Secondly the tunnel ventilation refers up to 9 m/s for full scale tunnel. Third difference is due to pan geometry which lead a pool fire since it is a confined geometry but behaves like spill fire since the depth of the liquid fuel is very small.

The results of experiments are investigated for their average mass loss rates, peak mass loss rates and heat release rates. The average mass loss rate behavior, especially for 100ml and 200ml is consistent with literature [37]. Increasing the amount of fuel leads an increase in average mass loss rate and the results approximate to that of literature pool fire results.

The HRR values show that in constant fuel sources the peak heat release rates stay constant for 1.5 m/s and 2.5m/s. It is seen that the fire is fuel controlled which means that increasing the oxygen do not lead an increase in peak HRR value. A decrease for peak heat release rate is observed for gasoline and mixture between 0.5 m/s and 1.5m/s. The main reason of this is the flame deflection. There is a big difference in flame motion between 0.5m/s and other ventilation velocities, i.e.; 1.5m/s and 2.5m/s. For 1.5 m/s and 2.5m/s the flame is deflected along the tunnel with a very low height and the radiation from flame and plume is lower than those of 0.5m/s where the flame height reaches to ceiling of the tunnel and the deflection of the flame is lower. For ethanol experiments this effect is lower since it is non-luminous and radiation effect is less important compared to gasoline and mixture. The behavior of ethanol is similar to methanol since they both have non-luminous flames. The experimental results are consistent with literature [15,19] where the burning behavior is fuel controlled. Hua et al. [19] reveals that the shape of the pan significantly changes the burning trend of gasoline. However generally after a certain velocity the burning rate is constant and this is a similar trend observed in this study.

For liquid pool fire, 100ml and 300ml square and 300ml rectangle ethanol fuel is simulated using FDS. The burning behavior trend agrees well with the experimental trends. However the value of both peak mass loss rates and peak HRR overshoots the results. In the literature [30,41] it is reported that FDS has problems in simulating HRR and MLR values for liquid fires, even for the ethanol reactions defined in FDS. Using particles injected by a nozzle is one of the most accurate ways to simulate burning behavior of ethanol. However there exist too many parameters to control the burning. Hence an extensive research should be done for a better fit of the numeric model and the experimental values.

REFERENCES

[1] Quintere, James G. *Fundemantals of Fire Phenomena.* ,John Wiley & Sons LTD, 2006.

[2] Lacroix, D.*Facts and Lessons International Tunnel Fire & Safety Conference.* Roterdam, Netherlands : 1999. p. 9.

[3] Pucher, K. and Pucher, R. Roterdam *Fire in the Tauern Tunnel.*, Netherlands : 1999. 9.

[4] Allison, R. London, *Inquiry into the fire on heavy good vehicles shuttle.* : 1996.

[5] Quintiere, James G. *Enclosure Fire Dynamics,* CRB Press, 2000.

[6] Beard, Alan and Carvel, Richard. *The Handboook of Tunnel Fire Safety* , 2004.

[7] Apte, V. B. and Kett, J. H. Boston ,*Pool Fire Plume Flow in a Large- Scale Wind Tunnel.* Procedings of the 3rd Internatinal Symposium on Fire Safety Science, 1991.

[8] Carvel, R. O. and Beard, A. N.,*The influence of longitudinal ventilation systems in tunnels.,* Tunnel and Underground Space Technology, 2001.

[9] Burgess, D. S., Strasser, A. and Grumer, J.,*Diffusive burning of liquid fules on open trays.* 3, Fire Research Abstract Review, 1961, Vol. 3.

[10] Roh, J. S., et al.,*An experimental study on the effect of the ventilation velocity on burning rate in tunnel fires -heptane pool fire case.* 43, Building and Enviroment, 2008, Vol. 1.

[11] Lee, S. R. and Ryou, H.,*An experimental study of the effect of the aspect ratio on critical velocity in longitudinal ventilation tunnel fires,* Journal of Fire Sciences, 2005.

[12] Chen, B. et al.,*Inıtial fuel temperature effects on burning rate of pool fire* ,Journal of Hazardous Materials, 2011.

[13] Hamins, Antony ve Kashiwagi, Takashi., *Characteristics of pool fire burning.* Building and Fire Research Laboratory, National Instıtute of Standards and Technology, 1996.

[14] Sugawa, Osami, et al., *Experimental study on gasoline pool fire using a full scale service station model and 1/15 reduced scale model.* Tokyo : Center for Fire Science and Technology, University of Tokyo.

[15] Woods, Joshua A.R., Fleck, Brian A. and Kostiuk, Larry W.,*Effects of transverse air flow on burning rates of rectangular methanol pool fires,* Combustion and Flame, 2006.

[16] Parag, Shintre and Raghavan, Vasudevan ,*Experimental invstigation of burning rates of pure ethanol and ethanol blended fuels,*Combustion and Flame, 2009.

[17] Kang, Quan Sheng, Lu, Shou Xiang and Chen, Bing ,*Experimental study on burning rate of small scale heptane pool fires,* Chinese Science Bulletin, 2010, Vol. 55.

[18] Chatris, J. M., et al. *Experimental study on burning rate in hydrocarbon pool fires.* Barcelona, Spain : Centre d'Estudis del Risc Tecnolo'gic (CERCET), Universitat Polite'cnica de Catalunya.

[19] Hua, L. H., Liu, S. ve Peng, W.,*Experimental study on burning rates of square/rectangular gasoline and methanol pool fires under longitudinal airflow in a wind tunnel,* Journal of Hazardous Materials, 2009.

[20] Garo, Jean-Pierre, et al.,*Combustion of liquid fuels floating on water.* Thermal Science, 2007, Vol. 11.

[21] Hayasaka, H.,*Unsteady burning of small pool fires ,* Fire Safety Science, Vol. 5.

[22] Cheong, M. K., Fleischmann, C. M. and Spearpint, M. J.,*Calibrating FDS simulation of good vehicle fire growth in a tunnel using the Runehamar fire experiment,* Journal of Fire Protection Engineering, 2009, Vol. 19.

[23] Cheong, M. K., Fleischmann, C. M. and Spearpint, M. J. *A comparison of a statistical and computational fluid dynamics approach to estiamte heat release rate in road tunnel fires* ,Fire Technology Journal , 2010, Vol. 46.

[24] Saber, H. H, et al. *A numerical study on the effects of ventilation on fire development in a medium-sized residential room.*, Institute for Resarch in Construction, 2008.

[25] Hwang, C. C. Edwards, J. C.,*The cirtical ventialtion velocity in tunnel fires - a computer simulation.*, 2005.

[26] Xin, Y., et al.*Fire dynamics simulation of a one-meter methane fire.* Combustion and Flame, 2008.

[27] Wen, J. X., et al.*Validaiton of FDS for the prediciton for the medium-scale pool fires,* Fire Safety Journal, 2007.

[28] Allison, M., *Simulating the fuel mass loss rate in fire dynamics simulator using a new furniture caloriemter database,* Faculty of Graduate School of the University of Maryland College Park, 2010.

[29] McGill, Jason Michaels., *Simulation of Vaporization of combustion of a large scale cyrogenic liquid methane pool,* : University of Maryland College Park, 2006.

[30] Overholt, Kristopher. https://docs.google.com/Doc?id=ajfdr2fw6926_28dpdrsq. [Online]

[31] Kayılı, Serkan. *Effect of vehicles blockage ratio on heat release rate in cae of a tunnel fire,* Middle East Technical University, 2009.

[32] McGrattan, K. *Fire Dynamics Simulator (Verison 5) User Guide, NIST Special Publicaitons ,1019-5,* NIST, 2009.

[33]*Fire Dynamics Simulator (Version 5) Tecnical Reference Guide, NIST Special Publicaiton, 1018-5,* NIST, 2009.

[34] DiNenno, Philip J., et al. *SFPE Handbook of Fire Protection Engineering.* Massachussetts : National Fire Protection Assocation Inc , Society of Fire Protection Engineers, 2002.

[35] Blinov, V. and Khodydiko, G. N. *Diffusion burning of liquid,* Moscow, 1961.

[36] Babrauskas, Vytenis. *Estimating large pool fire burning rates.,*Center for Fire Research , National Bureau of Standards, 1983.

[37] Gottuk, D., et al. *Optical Fire Detection for Mİlitary Aircraft Hangars : Final Report on OFD Performance to Fuel Spill Fires and Optical Stresses.*, Naval Research Laboratory, 2001. NRL/MR/6180-00-8457.

[38] Hamins, A., Fischer, S.J. and Kashiwagi,*Heat Feedback to the Fuel Surface in Pool Fires.* T. 1-3, 1994, Combustion Science and Technology, Vol. 97, pp. 37-62.

[39] Benfer, Matthew E. *Spill and Burning Behavior of flammable liquids,* Faculty of the Graduate School of the University of Maryland, College Park, 2010.

[40] Saito, N., et al.,*Experimental study on fire behavior in a wind tunnel with a reduced scale model.* Granada, Spain : Proceedings of the 2nd International Conference on Safety in Road and Rail Tunnels, 1995. pp. 303-310.

[41] Smardz, Piotr., *Validation of Fire Dynamics Simulator (FDS) for forced and natural convection flows* , University of Ulster, 2006.

[42] Quintiere, James G. Fundamentals of Fire Phenomena ,John Wıley & Sons, LTD, 2006, p. 2.

APPENDIX A

EXPERIMENTAL RESULTS

Table A-1 Experimental Results

E #	Velocity (m/s)	Fuel Source	Fuel Amount	Pan G.	A. MLR(g/s)	P. MLR(g/s)	HRR(kW)	FDS HRR (kW)	FDS P.MLR (g/s)
1	Open Fire	Ethanol	100ml	S	0,65	0,71	NA		
2	0	Ethanol	100ml	S	0,68	0,90	NA		
3	0,5	Ethanol	100ml	S	0,52	0,80	15,75	40,00	1,40
4	0,5	Ethanol	100ml	S	0,56	0,73	NA		
5	0,5	Ethanol	100ml	S	0,79	0,89	NA		
6	0,5	Ethanol	200ml	S	0,81	1,00	27,65	42,00	1,80
7	0,5	Ethanol	300ml	S	0,94	1,10	31,16	52,00	2,00
8	1,5	Ethanol	100ml	S	0,34	0,80	16,45	30,00	1,10
9	1,5	Ethanol	100ml	S	0,37	0,80	NA		
10	1,5	Ethanol	100ml	S	0,69	0,81	NA		
11	1,5	Ethanol	200ml	S	0,54	0,80	23,87	50,00	1,80
12	1,5	Ethanol	300ml	S	0,57	0,80	28,44	35,00	1,40
13	2,5	Ethanol	100ml	S	0,42	0,80	13,04	30,00	1,10
14	2,5	Ethanol	100ml	S	0,28	0,60	NA		
15	2,5	Ethanol	100ml	S	0,42	0,70	NA		
16	2,5	Ethanol	200ml	S	0,66	0,80	27,5	35,00	1,40
17	2,5	Ethanol	300ml	S	0,75	0,85	33,05	36,00	1,40

Table A-1 Cont'd Experimental Results

E #	Velocity (m/s)	Fuel	Fuel Amount	Pan G.	A.MLR(g/s)	P. MLR(g/s)	HRR(kW)	FDS HRR (kW)	FDS P.MLR (g/s)
18	Open Fire	Ethanol	100ml	R	0,73	0,79	NA		
19	0	Ethanol	100ml	R	0,41	0,59	NA		
20	0	Ethanol	200ml	R	0,63	1,10	NA		
21	0,5	Ethanol	100ml	R	0,60	0,80	12,99		
22	0,5	Ethanol	100ml	R	0,46	1,00	NA		
23	0,5	Ethanol	100ml	R	0,53	0,80	NA		
24	0,5	Ethanol	200ml	R	0,99	1,20	32,1		
25	0,5	Ethanol	200ml	R	0,80	1,15	NA		
26	0,5	Ethanol	300ml	R	0,99	1,40	34,44	70,00	4,00
27	1,5	Ethanol	100ml	R	0,62	0,75	25,12		
28	1,5	Ethanol	100ml	R	0,50	0,80	NA		
29	1,5	Ethanol	100ml	R	0,46	0,76	NA		
30	1,5	Ethanol	200ml	R	0,74	1,00	32,47		
31	1,5	Ethanol	200ml	R	0,81	1,19	NA		
32	1,5	Ethanol	300ml	R	0,90	1,10	38,72	60,00	2,20
33	2,5	Ethanol	100ml	R	0,63	0,80	26,12		
34	2,5	Ethanol	100ml	R	0,50	0,70	NA		
35	2,5	Ethanol	100ml	R	0,55	0,75	NA		
36	2,5	Ethanol	200ml	R	0,71	1,10	35,71		
37	2,5	Ethanol	200ml	R	0,80	1,06	NA		
38	2,5	Ethanol	300ml	R	0,96	1,20	38,44	60,00	2,20

Table A-1 Cont'd Experimental Results

E #	Velocity (m/s)	Fuel	Fuel Amount	Pan G.	A.MLR(g/s)	P. MLR(g/s)	HRR(kW)
39	Open Fire	Mixture	100ml	S	0,73	1,08	NA
40	0	Mixture	100ml	S	0,54	1,02	NA
41	0,5	Mixture	100ml	S	0,48	0,70	20,08
42	0,5	Mixture	100ml	S	0,59	0,80	NA
43	0,5	Mixture	100ml	S	0,74	0,85	NA
44	0,5	Mixture	200ml	S	0,63	1,10	33,16
45	0,5	Mixture	300ml	S	0,68	1,40	54,2
46	1,5	Mixture	100ml	S	0,28	0,60	20,2
47	1,5	Mixture	100ml	S	0,41	0,66	NA
48	1,5	Mixture	100ml	S	0,67	0,85	NA
49	1,5	Mixture	200ml	S	0,51	0,90	27,14
50	1,5	Mixture	300ml	S	0,60	1,00	36,49
51	2,5	Mixture	100ml	S	0,44	0,70	26,14
52	2,5	Mixture	100ml	S	0,45	0,75	NA
53	2,5	Mixture	100ml	S	0,43	0,78	NA
54	2,5	Mixture	200ml	S	0,57	0,80	32,97
55	2,5	Mixture	300ml	S	0,57	1,00	37,06

Table A-1 Cont'd Experimental Results

E #	Velocity (m/s)	Fuel	Fuel Amount	Pan G.	A.MLR(g/s)	P. MLR(g/s)	HRR(kW)
56	Open Fire	Mixture	100ml	R	0,75	1,10	NA
57	0	Mixture	100ml	R	0,32	0,72	NA
58	0	Mixture	200ml	R	0,57	1,70	NA
59	0,5	Mixture	100ml	R	0,56	1,30	21,16
60	0,5	Mixture	100ml	R	0,59	0,95	NA
61	0,5	Mixture	100ml	R	0,59	1,10	NA
62	0,5	Mixture	200ml	R	0,85	1,80	40,19
63	0,5	Mixture	200ml	R	0,87	1,65	NA
64	0,5	Mixture	300ml	R	1,26	1,85	50
65	1,5	Mixture	100ml	R	0,46	0,80	34,07
66	1,5	Mixture	100ml	R	0,57	0,96	NA
67	1,5	Mixture	100ml	R	0,50	0,88	NA
68	1,5	Mixture	200ml	R	0,72	1,20	42,97
69	1,5	Mixture	200ml	R	0,86	1,50	NA
70	1,5	Mixture	300ml	R	0,94	1,40	54,63
71	2,5	Mixture	100ml	R	0,49	0,80	36,19
72	2,5	Mixture	100ml	R	0,52	0,85	NA
73	2,5	Mixture	100ml	R	0,50	0,82	NA
74	2,5	Mixture	200ml	R	0,72	1,05	42,5
75	2,5	Mixture	200ml	R	0,79	1,20	NA
76	2,5	Mixture	300ml	R	0,90	1,20	50,65

Table A-1 Cont'd Experimental Results

E #	Velocity (m/s)	Fuel	Fuel Amount	Pan G.	A.MLR(g/s)	P. MLR(g/s)	HRR(kW)
77	Open Fire	Gasoline	100ml	S	0,59	0,94	NA
78	0	Gasoline	100ml	S	0,47	1,00	NA
79	0,5	Gasoline	100ml	S	0,45	0,80	23,75
80	0,5	Gasoline	100ml	S	0,49	0,96	NA
81	0,5	Gasoline	100ml	S	0,62	0,96	NA
82	0,5	Gasoline	200ml	S	0,64	1,40	55,07
83	0,5	Gasoline	300ml	S	0,69	1,50	90,09
84	1,5	Gasoline	100ml	S	0,34	0,80	37,07
85	1,5	Gasoline	100ml	S	0,31	0,66	NA
86	1,5	Gasoline	100ml	S	0,60	0,83	NA
87	1,5	Gasoline	200ml	S	0,47	0,90	51,7
88	1,5	Gasoline	300ml	S	0,67	1,25	63,81
89	2,5	Gasoline	100ml	S	0,37	0,80	42,93
90	2,5	Gasoline	100ml	S	0,35	0,66	NA
91	2,5	Gasoline	100ml	S	0,37	0,78	NA
92	2,5	Gasoline	200ml	S	0,54	0,90	51,01
93	2,5	Gasoline	300ml	S	0,67	1,25	67,78

Table A-1 Cont'd Experimental Results

E #	Velocity (m/s)	Fuel	Fuel Amount	Pan G.	A.MLR(g/s)	P. MLR(g/s)	HRR(kW)
94	Open Fire	Gasoline	100ml	R	0,56	1,10	NA
95	0	Gasoline	100ml	R	0,44	0,95	NA
96	0	Gasoline	200ml	R	0,51	1,44	NA
97	0	Gasoline	300ml	R	0,96	2,38	NA
98	0,5	Gasoline	100ml	R	0,46	1,40	30,92
99	0,5	Gasoline	100ml	R	0,49	0,94	NA
100	0,5	Gasoline	100ml	R	0,35	0,79	NA
101	0,5	Gasoline	200ml	R	0,82	2,00	61,33
102	0,5	Gasoline	200ml	R	0,74	1,55	NA
103	0,5	Gasoline	300ml	R	1,21	2,50	84,09
104	0,5	Gasoline	300ml	R	1,05	2,20	NA
105	1,5	Gasoline	100ml	R	0,37	0,95	46,19
106	1,5	Gasoline	100ml	R	0,57	0,92	NA
107	1,5	Gasoline	100ml	R	0,40	0,95	NA
108	1,5	Gasoline	200ml	R	0,70	1,50	67,77
109	1,5	Gasoline	200ml	R	0,70	1,50	NA
110	1,5	Gasoline	300ml	R	0,94	1,65	81,69
111	1,5	Gasoline	300ml	R	1,02	1,95	NA
112	2,5	Gasoline	100ml	R	0,35	0,80	45,24
113	2,5	Gasoline	100ml	R	0,52	0,72	NA
114	2,5	Gasoline	100ml	R	0,50	0,75	NA
115	2,5	Gasoline	200ml	R	0,76	1,30	60,09
116	2,5	Gasoline	200ml	R	0,63	1,15	NA
117	2,5	Gasoline	300ml	R	0,94	1,60	72
118	2,5	Gasoline	300ml	R	0,87	1,50	NA

APPENDIX B

FDS Input File Examples

```
E300_05_R.fds
Generated by PyroSim - Version 2010.1.0928
02-Sep-2011 16:18:40

&HEAD CHID='E300_05_R'/
&TIME T_END=300.00, WALL_INCREMENT=1/
&DUMP RENDER_FILE='E300_05_R.ge1', DT_RESTART=300.00/
&MISC HUMIDITY=30.00, TMPA=26.00/
&RADI RADIATIVE_FRACTION=0.00/

&MESH ID='MESH', IJK=40,150,30, XB=0.00,0.4000,-0.60,0.90,0.00,0.3000/

&PART ID='ethanol drops',
     FUEL=.TRUE.,
     SAMPLING_FACTOR=5,
     QUANTITIES='DROPLET TEMPERATURE','DROPLET DIAMETER',
     DENSITY=787.00,


     SPECIFIC_HEAT=2.45,
     VAPORIZATION_TEMPERATURE=76.00,
     HEAT_OF_VAPORIZATION=880.00,
     HEAT_OF_COMBUSTION=2.6780000E004/

&REAC ID='ETHANOL VAPOR',
     FYI='VU Ethanol Pan Fire FDS5 Validation',
     C=2.00,
     H=6.00,
     O=1.00,
     N=0.00,
     SOOT_YIELD=8.0000000E-003/

&MATL ID='STEEL',
     FYI='Drysdale, Intro to Fire Dynamics - ATF NIST Multi-Floor Validation',
     SPECIFIC_HEAT=0.4600,
```

```
    CONDUCTIVITY=45.80,
    DENSITY=7.8500000E003,
    EMISSIVITY=0.95/


&SURF ID='duvar',
    RGB=146,202,166,
    BACKING='INSULATED',
    MATL_ID(1,1)='STEEL',
    MATL_MASS_FRACTION(1,1)=1.00,
    THICKNESS(1)=0.0100/

&SURF ID='duvar2',
    RGB=146,202,166,
    BACKING='EXPOSED',
    MATL_ID(1,1)='STEEL',
    MATL_MASS_FRACTION(1,1)=1.00,
    THICKNESS(1)=0.0100/

&SURF ID='Hava',
    RGB=51,51,204,
    VEL=0.50,
    NO_SLIP=.TRUE.,
    POROUS=.TRUE./

&PROP ID='Fuel Spray',
    PART_ID='ethanol drops',
    FLOW_RATE=1.50,


    FLOW_RAMP='Fuel Spray_FLOW_RAMP',
    DROPLET_VELOCITY=2.00/



&RAMP ID='Fuel Spray_FLOW_RAMP', T=0.00, F=0.00/
&RAMP ID='Fuel Spray_FLOW_RAMP', T=1.00, F=1.00/
&RAMP ID='Fuel Spray_FLOW_RAMP', T=11.00, F=1.00/
&RAMP ID='Fuel Spray_FLOW_RAMP', T=12.00, F=0.00/

&DEVC ID='noz_1', PROP_ID='Fuel Spray', XYZ=0.2000,0.1500,0.0800,
QUANTITY='TIME', SETPOINT=0.00/
&OBST XB=0.00,0.0200,-0.60,0.90,0.00,0.3000, COLOR='GRAY 60',
SURF_ID='duvar'/ duvar1
&OBST XB=0.3800,0.4000,-0.60,0.90,0.00,0.3000, COLOR='GRAY 60',
SURF_ID='duvar'/ duvar6
```

```
&OBST XB=0.00,0.4000,-0.60,0.90,0.00,0.0200, COLOR='GRAY 40',
SURF_ID='duvar'/ taban
&OBST XB=0.00,0.4000,-0.60,0.90,0.2800,0.3000, COLOR='GRAY 60',
SURF_ID='duvar'/ tavan
&OBST XB=0.0500,0.3500,-0.0900,0.3900,0.0200,0.0300, RGB=0,51,0,
SURF_ID='duvar2'/ Obstruction
&OBST XB=0.0500,0.3500,-0.1000,-0.0900,0.0300,0.0400, COLOR='GREEN',

SURF_ID='duvar2'/ yan
&OBST XB=0.0500,0.3500,0.3900,0.4000,0.0300,0.0400, COLOR='GREEN',
SURF_ID='duvar2'/ yan
&OBST XB=0.0400,0.0500,-0.0900,0.3900,0.0300,0.0400, COLOR='GREEN',
SURF_ID='duvar2'/ yan
&OBST XB=0.3500,0.3600,-0.0900,0.3900,0.0300,0.0400, COLOR='GREEN',
SURF_ID='duvar2'/ yan

&VENT SURF_ID='Hava', XB=0.00,0.4000,0.90,0.90,0.00,0.3000, IOR=-2/ hava
&VENT SURF_ID='OPEN', XB=0.00,0.4000,-0.60,-0.60,0.00,0.3000/ acik

&BNDF QUANTITY='BURNING RATE'/
&BNDF QUANTITY='WALL TEMPERATURE'/

&SLCF QUANTITY='MIXTURE FRACTION', VECTOR=.TRUE., PBX=0.2000/
&SLCF QUANTITY='TEMPERATURE', VECTOR=.TRUE., PBX=0.2000/
&SLCF QUANTITY='MIXTURE FRACTION', VECTOR=.TRUE., PBY=0.1500/
&SLCF QUANTITY='TEMPERATURE', VECTOR=.TRUE., PBY=0.1500/

&TAIL /
```